UNIVERSITY OF OKLAHOMA

Evolution and Stability of Ultra-Wide Trans-Neptunian Binaries

A DISSERTATION

SUBMITTED TO THE GRADUATE FACULTY

in partial fulfillment of the requirements for the

Degree of

Doctor of Philosophy

by

Hunter Campbell

Norman, Oklahoma

2023

Evolution and Stability of Ultra-Wide

Trans-Neptunian Binaries

A DISSERTATION APPROVED FOR THE

HOMER L. DODGE DEPARTMENT OF PHYSICS AND

ASTRONOMY

BY THE COMMITTEE CONSISTING OF

Dr. Nathan Kaib, Chair

Dr. Mukremin Kilic

Dr. Kuver Sinha

Dr. John Wisniewski

Dr. Peter Barker

Contents

Acknowledgements

This PhD Dissertation would not have been possible without the assistance and advice of my advisor, Dr. Nathan Kaib, who set me off on this project and steered me on the right path with excellent support and direction on what it means to be a researcher. The computing for this project was performed at the OU Supercomputing Center for Education & Research (OSCER) at the University of Oklahoma (OU). I would also like to thank Lukas Stone for providing much of the groundwork showing that this project was feasible and Kalee Anderson for providing invaluable data on the evolution of the Kuiper Belt.

I would like to thank my fellow OU graduate students for their camaraderie and support during our classwork, qualifying exam study, and all the times in between. I would also like to thank all of the OU Physics and Astrophysics faculty for their teaching and insight as I navigated through coursework and research. I especially thank Dr. Doerte Blume for teaching me about the Hamiltonian, Dr. Kieran Mullen for teaching me invaluable mathmetics skills, and Dr. John Wisniewski for teaching me about observation and methods of applied astronomy.

Lastly, I would like to thank my family: my parents, Frank Campbell and Julie Still, for raising me to always shoot for the stars, my sister, Grace Campbell, for helping proofread my emails, and my wife, Nurul, for her support and enduring my long talks about Kuiper Belt binaries.

Abstract

This research is focused around the longevity and formation of a class of binaries in the Kuiper Belt called Ultra-Wide Trans-Neptunian Binaries (Ultra-Wide TNBs). The presence of these seemingly fragile binary systems has been used to constrain various properties in both the modern Kuiper Belt and its primordial origins. By studying the evolution and potential formation of these binaries, even more can be learned and some things can be reassessed.

Using the SWIFT Regularized Mixed Variable Symplectic (RMVS) n-body integrator, we simulate the evolution of a number of binary systems perturbed by both collisions and gravitational perturbations. We show that Ultra-Wide TNBs like 2001 QW_{322} and 2000 CF_{105}, which had previously been seen as stable, are unlikely to have formed in the primordial Kuiper Belt and remain intact into the modern day. We also show that these same binaries can be formed by the gradual widening of initially tighter binaries under the same perturbations. These widened binaries bear properties consistent with observations and are produced efficiently enough to explain their present day population size.

If some Ultra-Wide TNBs are not primordial, then metrics using their survival to constrain the Size Frequency Distribution (SFD) of the Kuiper Belt are not effective. If Ultra-Wide TNBs are primarily formed through widening, their population size can be used to constrain this SFD, and the mass of the initial Kuiper Belt. In addition, the presence and formation of blue Ultra-Wide TNBs in the Cold Classical Belt can indicate the nature of Neptune's migration in the early Solar System.

Chapter 1

Introduction

1.1 The Trans-Neptunian Region

In 1930, American astronomer Clyde Tombaugh made history when he observed the distant icy body named Pluto. Though he thought he had discovered a planet the size of Earth, this would in fact be the first known body of the Kuiper Belt. In 1992, more than 60 years later, the second independent member of this emerging family of bodies, now called 15760 Albion, would be discovered (Jewitt & Luu, 1993). Many more would join it, culminating in the gradual discovery of a disc, far larger than the Asteroid Belt, surrounding the Solar System beyond the orbit of Neptune.

We now know the Kuiper Belt to be a vast and complex region of the Solar System just beyond the orbit of Neptune, largely located between 30 and 50 AU or 30 and 50 times further out than the Earth is from the Sun. It is composed of bodies called Trans-Neptunian Objects (TNOs) that may have formed planets if they had been in different parts of the Solar System but remain isolated today. However, at least some of the Kuiper Belt's members, in their relative isolation, have at least one companion (Noll et al., 2008, 2020). Charon was the first to be discovered. As a fairly large satellite of Pluto, it was relatively easy to spot. Following this, a second binary, 1998

WW$_{31}$ (Veillet et al., 2002) was discovered. And with the discovery of many more (Grundy et al., 2019), trends can be seen in the nature of these systems.

The Kuiper Belt, never having coalesced into a single body, serves as a time capsule into the conditions of the early Solar System. Both its formation and the formation and evolution of the planets have left their marks here. Orbits, colors, the properties or perhaps the absence of their binaries across the many populations of the Kuiper Belt tell a story about the Solar System's history.

1.2 Populations of the Kuiper Belt

From examining the orbital properties of Kuiper Belt bodies, we can neatly divide them into four populations, as modeled by Abedin et al. (2021) and proposed by Gladman et al. (2008). These are the Resonance population, the Scattering population, the Classical population, and the Outer/Detached population.

The Resonance population is composed of bodies that occupy mean motion orbital resonances with Neptune. This means that the orbital periods of these bodies have integer ratios with the orbit of Neptune. It can additionally be subdivided by the order of resonance each body has with Neptune. Pluto for instance, exists in a 3:2 resonance with Neptune, orbiting twice for every three times Neptune does, and is thus in the Resonance population (Gladman et al., 2008). The Resonance population can be further divided into three subpopulations:

- Inner Resonance: Subpopulation encompassing the N4:3 and N3:2 resonances.

- Main Resonance: N5:3 and N7:4.

- Outer Resonance: N2:1, N7:3, and N5:2.

These groups by no means represent the entire Resonant Population. There are other resonance groups further out than the outer group, and some among these three groups have not been included. The unnamed resonance groups, however, are far less populated.

The Scattering population is composed of bodies that have had an encounter with Neptune within the past 10 million years. This placed them in orbits of high eccentricity and inclination, with perihelia close to 30 AU. These bodies are very likely to have subsequent encounters with Neptune that will further alter their orbits. Thus, though each body in this population is ephemeral, the number of bodies here is sustained by Neptune's consistent influence.

The Classical population consists of bodies that neither occupy a mean motion resonance with Neptune, nor have perihelia close enough to Neptune's orbit for a recent interaction to have occurred. They can largely be thought of as exceptions to the previously mentioned KBO populations. They can also be further divided into three subpopulations on the basis of semi major axis. These boundaries are defined by the locations of resonance orbits with Neptune, with the 3:2 resonance being at roughly 39 AU and the 2:1 resonance being at roughly 47 AU.

- Inner Classical: Classical bodies with $a < 39$ AU.

- Main Classical: 39 AU $< a < 47$ AU

- Outer Classical: $a > 47$ AU

For reasons that are discussed later in this section, we prefer to group the Outer Classical Belt with the Detached Belt, rather than the other portions of the Classical Belt as defined by Gladman et al. (2008).

Another way to divide the the Classical Belt is via inclination. The high inclination and low inclination distinction becomes more convenient as many physical properties of these two subpopulations are also distinct. These different properties are discussed in more detail in Section 1.4. Consequently, we choose to divide the Classical Belt into the following two subpopulations:

- Cold Classical Belt (CCB): Classical bodies with solar inclinations lower than 5°.

- Hot Classical Belt (HCB): Classical bodies with solar inclinations greater than 5°

These populations are distinct, but part of a bimodal distribution. Indeed, they occupy the same semi-major axis space in the Kuiper Belt. An inclination distinction of 5°, however, is the usual convention to classify the two as follows.

Some additional orbital distinctions exist between the two. Cold Classical Belt (CCB) bodies with solar semi major axes less than 42.4 AU tend to be absent (Kavelaars et al., 2008) with perihelia rarely extending below 39 AU. Hot Classical Belt (HCB) bodies tend to have semi major axes down to 40 AU with perihelia extending as low as 35 AU (Petit et al., 2011). However, inclination is the primary way to distinguish these two populations.
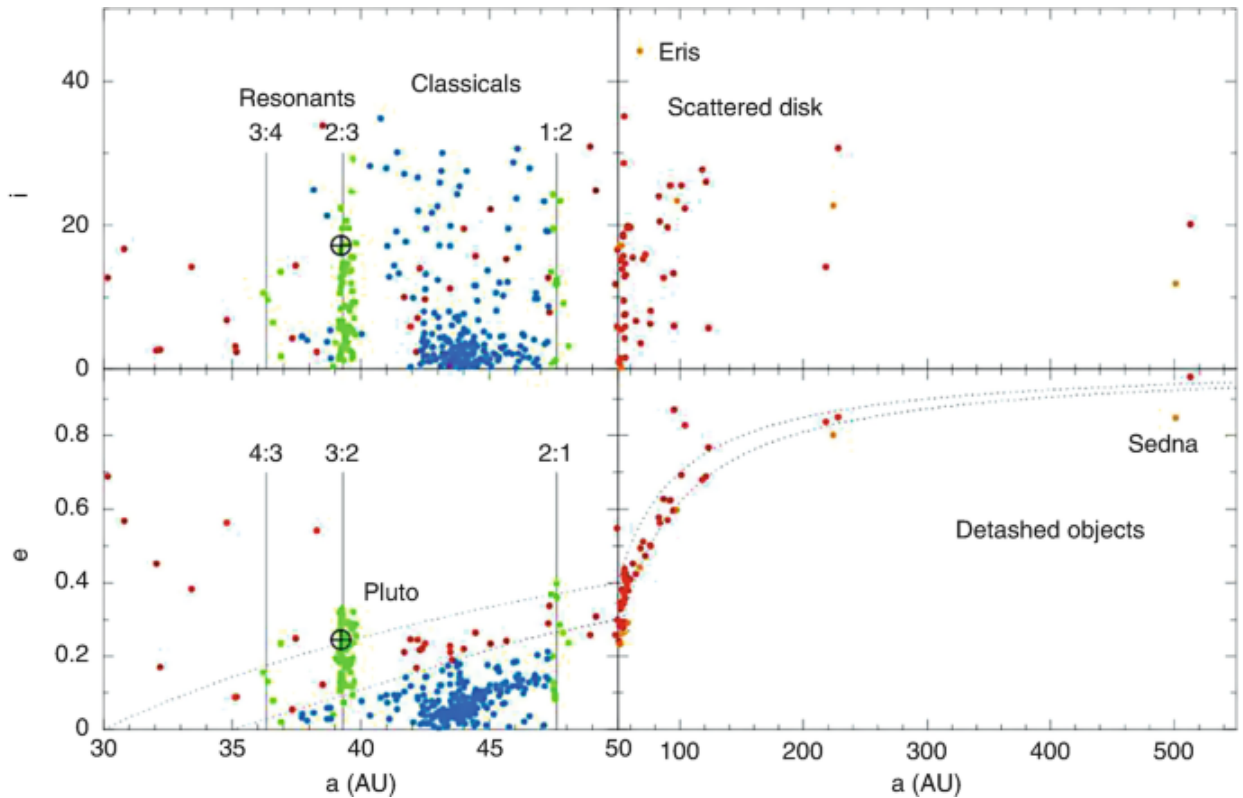
Figure 1.1: The varying populations of the Kuiper Belt, Figure 1 from Barucci (2015). The resonant bodies are shown in green and occupy very narrow ranges of specific semi major axes. The Classical bodies are shown in blue, occupying a large range of semi major axes with lower eccentricities. The Scattering bodies (scattered disk) shown in red and Detached bodies "detashed" in the image) shown in yellow tend to exist over very wide ranging semi major axes but are distinguished by whether or not their perihelion comes close to Neptune at 30 AU.

The Outer Classical/Detached population consists of bodies that similarly have little influence from Neptune but have semi major axes in excess of 47 AU. In principle, all KBOs in orbits beyond Neptune's influence could be thought of as "Classical" but

Gladman et al. (2008) make the case that lumping very distant eccentric bodies like Sedna in with bodies with circular orbits at 44 AU is not useful. Sedna's orbit takes it as close as 76 AU but its semi major axis is a far out as 480 AU meaning it has a comet like eccentricity of over 0.8 (Brown et al., 2004). Abedin et al. (2021) further merge the previously defined Outer Classical Population with the Detached population. This forms an Outer Classical/Detached population defined as bodies that have not had an interaction with Neptune within the last 10 million years and have a semi major axis beyond 47 AU. We find the grouping defined by Abedin et al. (2021) to be most useful. Hence, we refer to this population simply as the Detached population.

1.3 Early Migration

The structure of the Kuiper Belt and the orbital nature of each population is shaped by its formation history. The many diverse populations of Kuiper Belt bodies as well as their differing orbital and physical elements suggest that the modern belt is not the same as it was in the distant past (Morbidelli & Nesvorný, 2020). In the very early history of the Solar System, the arrangement of the planets may not have been the same as today. Indeed, the number of planets may not have been the same (Nesvorný, 2011). The theoretical framework behind this change has been termed the Nice model (Gomes et al., 2005; Tsiganis, K. et al., 2005; Levison et al., 2008).
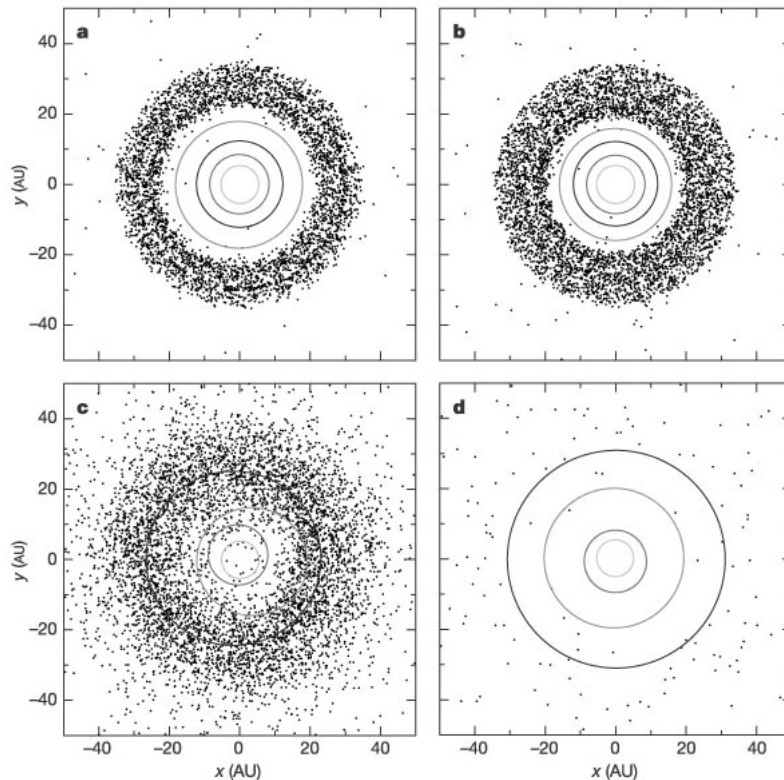
Figure 1.2: A rough visual overview of the Nice model, Figure 7 from Morbidelli et al. (2008). Panel (a) shows the primordial densely clustered Solar System with a very substantial debris disk at around 20 AU. Panel (b) is a snapshot of the disk just before beginning of instability; panel (c) shows shortly after the instability, and panel (d) shows the conclusion of instability and migration, where the planets occupy, for the most part, their present day orbits. The initially massive debris disk greatly decreases in density over time and migrates into the present day Kuiper Belt.

Initially, the outer Solar System is believed to have consisted of a far more compact set of gas giants in a roughly resonant configuration (Morbidelli & Crida, 2007). Beyond the giants is a disk of material, far denser than the present Kuiper Belt and beginning just beyond the orbit of the most distant gas giant, which was then at around 20 AU. The ice giants and Saturn principally interact with the disk by causing bodies to be scattered inward, sapping their orbital momentum, and resulting in the planets gradually migrating outward. Jupiter on the other hand, primarily interacts by scattering bodies outward, resulting in Jupiter gradually migrating inward (Fernandez & Ip, 1984; Malhotra, 1993). This gradual migration eventually results in Jupiter and Saturn reaching a 2:1 resonance, undermining the stability of the other gas giants. Uranus and Neptune, migrate deep into the primordial belt they had been feeding from. This journey may perhaps feature a third or even fourth ice giant that is ejected from the Solar System (Nesvorný & Morbidelli, 2012). The migration is partially modeled in Figure 2.

The primordial disk is then mostly ejected from the Solar System, with the remaining bodies migrating outward as well into the semi major axis space of the modern Kuiper Belt. These remaining bodies provide dynamical friction to lower the eccentricity of Neptune and feed Neptune's further gradual migration outward into its present orbit, yielding a Solar System resembling the one we have today (Gomes et al., 2005; Tsiganis, K. et al., 2005; Levison et al., 2008). This process of planetary instability has been used to explain the apparent late heavy bombardment on the Moon's surface and the relative lack of material in our Kuiper Belt compared to the sometimes monstrous outer belts of other Solar Systems (Wyatt, 2020), like that of Tau Ceti or Fomalhaut (Greaves et al., 2004; Kalas et al., 2005).

The bodies that migrate outward join those that were already there. The travelers, having had close encounters with one of the migrating ice giants, are left with

more excited inclinations, while the indigenous bodies are largely unaffected (Levison et al., 2008). This distinction is most apparent in the Classical Population, where, as discussed in the previous section, a bimodal split exists between the HCB and CCB. Additionally, as will be mentioned in the following section, the physical characteristics of the two populations further imply distinct formation and migration histories.

Two different populations of bodies in the newly formed Kuiper Belt remain, those that formed interior to Neptune's present orbit and have migrated, and those that have largely formed in situ. As migrations may have left excited inclinations (Petit et al., 2011), it is believed that the present day low inclination CCB and some low inclination 2:1 members are the primordial population of TNOs that have not migrated, while the remaining Kuiper Belt is thought to descend from that migrating population (Levison et al., 2008; Parker & Kavelaars, 2010; Nesvorný, 2018). This leaves us a further metric for dividing the Kuiper Belt based on formation history. The CCB and these 2:1 resonance members can be grouped into the Cold Kuiper Belt (CKB) while the remainder of the TNOs can be grouped into the Kinetic Kuiper Belt (KKB).

1.4 Physical Characteristics of each Population

A major distinction that is readily apparent between populations is that the CCB has a very different color distribution than any other scrutinized population. The contrast is particularly noteworthy in the HCB. Despite the two occupying the same semi-major axis space, the two populations divided by inclination are also divided by visible color. The CCB is dominated by objects that have an apparent red coloration, while the bodies of the HCB seem to have much greater color diversity (Doressoundiram et al., 2002; Petit et al., 2011; Fraser et al., 2014). This distinction has traditionally been thought to have been caused by one of two methods. Either these two populations have formed in different parts of the Solar System and thus have very different formation histories (Fraser & Brown, 2012; Fraser et al., 2017), or different environmental conditions cause one population to more preferentially experience resurfacing events (Fraser et al., 2017), altering their colors. It is perhaps true that a combination of these effects is at play.

This population distinction is further seen in the color distributions of dynamically hot TNOs as well. A clear trend of bodies with lower solar inclination having more red coloration was first spotted in the Centaur population(Tegler et al., 2016). Centaurs are bodies whose perihelion sits among the Solar System's gas giants, and because they are principally supplied by bodies straying from the Kuiper Belt, this trend was thought to be representative of the red hot Kuiper Belt bodies. This hypothesis would later be confirmed by the Col-OSSOS survey (Fraser et al., 2021), showing that this trend exists in the KKB as well. This cannot be the result of preferential resurfacing events, as impact frequency and velocity are far more related to a body's eccentricity than its inclination; and no such color eccentricity trend has been observed (Marsset et al., 2019).

However, these TNOs are merely small lights of determined brightness unless we

can determine an important parameter. The albedo of a body is the fraction of visible sunlight falling on its surface that is reflected back into space. Once this parameter is known, it is possible to learn how large a TNO is, even if it cannot be physically resolved by a telescope. Bodies with measured albedos tend to be found among Centaurs. Being much closer to the Sun, they are easier to observe, and in time, this trend would then be observed in the Kuiper Belt itself. Thus, the Kuiper Belt can again be divided into two categories, the darker KKB, and the red CKB (Lacerda et al., 2014; Farkas-Takács et al., 2020).

While the known albedo of the Kuiper Belt varies between 0.04 and 0.16, the distribution of these albedos is very clearly bimodal (Fraser et al., 2014). The lighter population, corresponding well with the CKB, has far redder surfaces with estimated mean albedos of approximately 0.14 to 0.15 (Lacerda et al., 2014; Vilenius et al., 2014). However, a slightly different answer would come following the flyby of the New Horizons probe through the Kuiper Belt, the first and maybe only close up measurements of a Kuiper Belt body. This direct measurement of the CCB body 486958 Arrokoth gave an R band albedo of 0.21 (Hofgartner et al., 2021). Regardless, the albedo of this population is far different than its darker alternative. The albedos of the darker population of the Kuiper Belt, on the other hand, tend towards 0.05 and feature grayer surface coloration (Lacerda et al., 2014).

Most relevant to this thesis, however, is the vast difference in the fraction and nature of binary systems in each population. The CCB and HCB, despite the two's coexistence in the same semi major axis space, exemplify this difference. The CCB boasts a binary to single fraction of 30%, while the HCB has a binary fraction of only 10% (Noll et al., 2008). The binary systems of the CCB also tend to be composed of equal sized bodies, as well as having much larger separations on average than the rest of the Kuiper Belt, sometimes considerably so (Noll et al., 2008, 2020). The HCB lacks

any significant fraction of systems with equally sized binary components (Nesvorný & Vokrouhlický, 2019). The vast difference in the CCB binary fraction is also likely to stem from its different history.

It should be noted that there are biases here. Any Kuiper Belt body sample being examined is inevitably going to be biased towards brighter objects, simply because these are the objects that are more likely to be seen. And because binary objects are inherently brighter than single objects, simply because two bodies are brighter than one, binary systems are likely to be overrepresented in any sample; especially if the system is composed of two equal mass components. This, coupled with the fact that the Size Frequency Distribution (or SFD, see Section 2.2) of the CCB is steeper than the HCB (from which much of this sample is drawn), makes the binary fraction of the CKB likely to be inflated. However, this high fraction holds for even the highest magnitudes of CCB bodies observed. Even here, at H > 6.15 mag, the ratio hovers around 20% (Noll et al., 2020), still much higher than 10% of the HCB (Noll et al., 2008; Fraser et al., 2017).

1.5 Ultra-Wide Trans-Neptunian Binaries

Within the Cold Classical region of the Kuiper Belt, there exist a number of binary systems with very unusual properties. Unlike the HCB and much of the rest of the Solar System, CCB binaries very often consist of two near equally sized bodies, rather than a small body orbiting a larger one as is common elsewhere in the Solar System (Noll et al., 2008, 2020). But what makes them most unusual is their incredibly wide separations. These Ultra-Wide Trans-Neptunian Binaries (Ultra-Wide TNBs) are some of the more extreme objects in the Solar System. 2001 QW$_{322}$ is the binary with the widest known separation of approximately 102,100 km, despite neither of the pair being larger than 130 km in diameter (Kavelaars et al., 2001; Petit et al., 2008; Grundy et al., 2019). Though 2001 QW$_{322}$ is the most widely separated of the known Ultra-Wide TNBs, several other systems are known to have similar extremities (Parker et al., 2011).

Because these binaries can have wildly different masses, it is not useful to talk about their separation in terms of physical distance. The more massive 2001 QW$_{322}$ (2×10^{18} kg) will be more tightly bound than the less massive 2000 CF$_{105}$ at equal physical separations (Parker et al., 2011). Thus, it becomes much more useful to talk about a binary's separation in terms of percent of a Hill radius. The Hill radius is the maximum separation that a binary can have before the gravity of an outside body (the Sun in this case) necessarily disassociates it. This point for circular orbits is defined as,

$$R_H \approx a \sqrt[3]{\frac{m_b}{M_\odot}} \tag{1.1}$$

where a is the solar semimajor axis of the binary, m_b is the binary mass, and $M_\odot$ is the mass of the Sun. To better compare different binaries in terms of stability, we

typically use this parameter to measure separation.

Among these very widely separated binaries are 2005 EO$_{304}$ with a separation of 7×10^4 km corresponding to a Hill radii separation of 0.15 R$_H$. A good comparison would be our own Earth-Moon binary system, which has a Hill radius separation of 0.25 R$_H$. However, while the Earth and the Moon are the most massive bodies in their region of the Solar System by far, these Kuiper Belt binaries have to share their orbits with millions of other bodies of comparable size and mass. Collisions with similarly sized bodies would likely not be uncommon, and close passages of bodies with significantly more mass than the entire system may occur frequently. Hence, these objects have been of particular interest to this study and many prior ones (Petit & Mousis, 2004; Parker et al., 2011; Brunini & Zanardi, 2015; Nesvorný et al., 2021).

The exact definition of Ultra-Wide ranges from being greater than 5% Hill radius (Grundy et al., 2019) to being substantially greater than 5% (Parker et al., 2011). For the purposes of this research, we use the definition of tight binaries as having separations less than 5% R$_H$ while Ultra-Wide binaries have separations greater than 7% R$_H$. This is the de facto standard adopted by (Parker et al., 2011) as well. Through this definition, there are 9 known Ultra-Wide binaries, with some possessing separations far greater than this. The widest, 2001 QW$_{322}$, has a separation of 22.2% R$_H$. These 9 known Ultra-Wide TNBs are detailed in Table 1 (Grundy et al., 2019).

Ultra-Wide binaries likely make up at least 1.5% of the of all CCB bodies (Lin et al., 2010), which considering the already present binary fraction, means that Ultra-Wide binaries make 5% of all binaries there (Lin et al., 2010; Parker et al., 2011).

The mutual orbital properties of Ultra-Wide TNBs do not match well with their tight counterparts. The Ultra-Wide inclination distribution is substantially more planar, lacking any bodies with mutual inclinations between 55° and 125°. As seen in Table 1, 3 of the 9 known systems have retrograde orbits (inclinations greater than

Name	System Mass kg	$a_\odot$ AU	sep_m km (R_H)	ecc_m	inc_m deg
2002 PD$_{149}$	5.43×10^{17}	43.0	26000 (0.099)	0.588	21.9
Mors–Somnus	7.75×10^{17}	39.5	20990 (0.096)	0.1494	24.3
2006 JZ$_{81}$	1.183×10^{18}	44.8	33000 (0.090)	0.85	11.0
2000 CF$_{105}$	1.85×10^{17}	43.8	34300 (0.165)	0.33	167.9
2001 QW$_{322}$	2.15×10^{18}	44.1	102100 (0.223)	0.464	152.8
2003 UN$_{284}$	1.312×10^{18}	42.7	54000 (0.145)	0.38	23.0
2005 EO$_{304}$	2.103×10^{18}	45.7	70000 (0.154)	0.22	15.9
2006 BR$_{284}$	5.70×10^{17}	43.9	25400 (0.088)	0.275	54.1
2006 CH$_{69}$	8.30×10^{17}	45.8	27000 (0.081)	0.856	132.5

Table 1.1: The parameters of all 9 known Ultra-Wide TNBs from Grundy et al. (2019) and Parker et al. (2011). Listed are the binaries' names, total system mass, solar semi major axis, mutual separation, mutual eccentricity, and mutual inclination.

90°) in comparison to the less than 15% of tight binaries (Grundy et al., 2019). Ultra-Wide TNBs additionally have far more eccentric mutual orbits, with none having an eccentricity below 0.2, while almost half of all tight binaries have an eccentricity less than that. It should be noted that the small sample of Ultra-Wide binaries can make it difficult to make definitive statements about their orbital distributions.

One final physical property about these binaries makes implications about their formation history. Unlike most other bodies in the CCB, CCB binaries are blue, rather than red (Fraser et al., 2017). Blue non-binary "singles" make up only 2% of the CCB bodies with known color. (Fraser et al., 2021). This implies that these binaries were implanted into the CCB from closer to the Sun though in a manner distinct from the implantation of the HCB to account for their low solar inclination.

1.5.1 Formation

Due to the unique properties of these Ultra-Wide binaries, some formation mechanisms that otherwise apply to many binary systems in and out of the Kuiper Belt do not work here. The accretion of a collision derived debris disk is capable of forming binary components of unequal size like those of Pluto and Eris, but not equal size binaries like those in the CCB (Brown et al., 2007).

In the early Solar System, conditions may have been suitable for the formation of equal mass binary systems by capture. In essence, for such an event to occur, two bodies must pass sufficiently close to each other and then have enough of their relative energies reduced such that they become bound to each other. Various mechanisms for energy loss have been proposed, ranging from the interactions of an unattached third body (Goldreich et al., 2002), the loss of a smaller binary formed via accretion after collision (Funato et al., 2004), to temporary chaos assisted capture made stable by disk processes (Astakhov et al., 2005). The loss of another binary component is probably how the likely former TNO Triton was captured into Neptune's orbit (Agnor & Hamilton, 2006).

These mechanisms, detailed by Nesvorný et al. (2010) vary in their ability to explain the observed properties of the equal mass binaries that we see, as well as in their apparent efficiency. For instance, it seems the interference of a third body forms equal mass binaries more efficiently than trading a collisionally formed low mass companion (Goldreich et al., 2002). Additionally, this collision-based formation tends to produce binaries with far higher eccentricity distributions than we currently observe. Even the three body capture mechanisms seem to be far more likely to produce retrograde binaries than prograde ones, which as mentioned in the previous section, does not match the apparent inclination distribution we see. And no mechanism is likely to be able to explain the apparent trend in identical surface color and composition between

binary components (Schlichting & Sari, 2008). Despite a wide diversity of colors in the Kuiper Belt, even within individual populations, these wide binary systems appear to match each other (Benecchi et al., 2009). The best way to explain this would be for these binary components to have formed together, perhaps already being part of a binary as they accrete material.

Another proposed formation mechanism is excess angular momentum during accretion, termed, streaming instability. As material accretes into a system, excess angular momentum prevents all of the material from accumulating onto a single body, instead forming two (Youdin & Goodman, 2005; Nesvorný et al., 2010; Nesvorny et al., 2019). This process has also been proposed to explain binary star formation and black hole disk scattering (Kratter et al., 2008; Alexander et al., 2008). In the Kuiper Belt, the conditions necessary to form clumps of material like this could have occurred frequently, largely independent of the initial conditions of the disk (Li et al., 2019). While efficient formation is possible, the distinct blue coloration of these binaries implies that they have not formed in the CCB but have instead been implanted there. This implantation must have occurred differently to that of the HCB to account for their low solar inclination, however. A possible mechanism for such migration is the slowly outwardly receding 2:1 Neptune resonance orbits. Binaries and indeed single bodies may be caught in this resonance and be slowly pushed outward without ever having a close passage with the planet itself. A close encounter would more than likely result in a binary's destruction (Parker & Kavelaars, 2010; Stone & Kaib, 2021). If Neptune's migration becomes abrupt at 28 AU, then the previously caught blue bodies are released in the CCB (Nesvorný, 2015).

These mechanisms are perfectly capable of forming wide blue equal mass binaries in the CCB without excessive fine tuning of initial conditions. The resulting binaries have orbital properties consistent with our known sample, neither having excessively high

eccentricities, nor excessively retrograde orbits. The fraction of wide binaries formed may even be greater than the fraction we observe (Nesvorný et al., 2010). Therefore, with a formation model as efficient as this, the presence of Ultra-Wide TNBs may not be unusual, as long as their dynamical stability does not pose an issue to their long term survival.

1.5.2 Survivability

Kuiper Belt binaries exist in a dynamic environment and are likely to undergo many encounters with other passing bodies, ranging from distant flybys to direct hits. If a binary like 2001 QW$_{322}$ is not bound tightly enough, then it is possible that these encounters would preclude it from being able to survive into the present day if it had formed in the primordial Kuiper Belt (Petit & Mousis, 2004).

The first study to thoroughly examine the long term stability of Ultra-Wide TNBs is Petit & Mousis (2004). They studied three mechanisms in which an Ultra-Wide TNB may become disassociated and each mechanism's associated timescale, disassociation through collisions with passing bodies, disassociation through gravitational perturbation of passing bodies, and the complete destruction of one of the binary components in an especially energetic collision. The three mechanisms are illustrated in Figure 3.
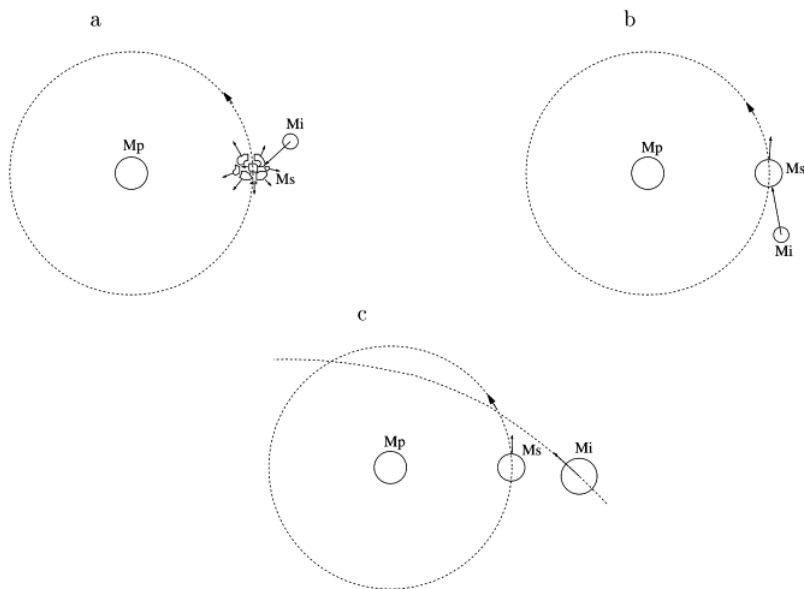
Figure 1.3: A visualization of the three different tested possibilities for binary disassociation. Taken from Petit & Mousis (2004) Figure 1. Panel (a) depicts the complete destruction of a binary component through a collision with a passing body. Panel (b) depicts a similar collision but with only enough energy to unbind the binary. Panel (c) depicts a passing body unbinding the binary entirely through its perturbing gravity, rather than a collision.

Petit & Mousis (2004)'s study was an analytic one. Their methodology was to determine the size an interacting TNO would need to have in order to disassociate a given binary, assuming a constant impact velocity of 0.5 and 1.5 km/s. For instance, it was determined how large a colliding body would need to be to dislodge one of the binary components, or how large would a passing body need to be for its gravity to do the same? Assuming this size, an assumed SFD, and the probability of collision, the average time between binary destruction events can be determined.

Petit & Mousis (2004) concluded that non-destructive collisional disassociation (panel (b) of Figure 3) was the most relevant option in the breaking of TNBs, collisions large enough to completely break up a binary component are obviously less common than collisions that can disassociate a system. A binary like 2001 QW$_{322}$ has an average lifetime in a collisionally interactive regime of 1.9 Gyrs as opposed to a lifetime of 3.4 Gyrs in a perturbative interaction regime, assuming an average TNO mass density of 1 g cm^{-3} (more on this in Section 2.2). Though the exact figures are obtained using an older Kuiper Belt SFD, they do illustrate that collisional interactions seem to be more influential than gravitational perturbative ones. This result has had a major influence on subsequent studies into the nature of TNB stability.

Newer studies investigate the evolution of binaries almost exclusively with the assumption that collisional interactions are their major driving force. Parker & Kavelaars (2011) is one such study. Using a better constrained SFD, they seek to recreate the original study done by Petit & Mousis (2004) but with two major methodological differences. They only consider collisional interactions, and they allow a binary to experience multiple collisions and evolve over time. Due to the power law nature of the Kuiper Belt's SFD (Petit et al., 2011; Lawler et al., 2018; Kavelaars et al., 2021), there are significantly more small bodies than large ones; thus, a binary is far more likely to be struck many times by smaller bodies than to be disassociated by a single

large one. Instead of merely calculating the average time between collisions that would dislodge a binary in a single event, they instead simulate billions of years of Kuiper Belt interactions and record the aggregate effects of many collisions. Included in their methodology is the potential mass loss that occurs during collisions. In measuring the average lifetime of a binary in a given Kuiper Belt, Parker & Kavelaars (2011) find that the ratio between Petit & Mousis (2004)'s analytical calculation and their own simulation is as follows:

$$\frac{\tau_{sim}}{\tau_a} = 0.007 \times 3.12^q + 1 \qquad (1.2)$$

where q is the exponent of the given Kuiper Belt SFD (assuming a single power law model). This indicates that the analytical analysis done by Petit & Mousis (2004) will slightly overestimate the lifetimes of TNBs. This overestimation is highly dependent on the assumed SFD. Given a reasonable q value of 3 (more on this in Section 2.2), an analytical calculation would be off by a factor of 1.3. Even with this factor included, given the revised SFD proposed by Parker & Kavelaars (2011), they now find that even the least bound Ultra-Wide TNBs may survive into the modern Kuiper Belt.

A more recent study conducted by Nesvorný et al. (2021) replicated the multiple collision nature of Parker & Kavelaars (2011)'s work but incorporated a more sophisticated mass loss and accretion model. Most importantly, they subject their simulated binaries to a time dependent evolving Kuiper Belt, accounting for the vast difference in Kuiper Belt population density in the past. This diachronic model contrasts with the static monochronic model used by Parker & Kavelaars (2011) which only simulated the Kuiper Belt as it exists now.

Nesvorný et al. (2021)'s results, however, are fairly consistent with those of Parker & Kavelaars (2011). All currently observed binaries have a good chance ($\gg 50\%$) of surviving into the present day Solar System. Survival is in fact likely at far wider

separations than any binary yet observed, with separations up to 50% R_H remaining stable. This is a far different result than that of Petit & Mousis (2004), which despite the iterative collision model and the far greater number of collisions brought on by an evolving Kuiper Belt, still yielded much shorter binary lifetimes, due to their far shallower SFD. Figure 4 from Nesvorný et al. (2021) illustrates these results.

Though Ultra-Wide TNBs are often discussed in the context of the CCB, their long term stability if formed in the KKB has also been studied. If such binaries can form in the CCB, they may also form elsewhere. The KKB, however, has had a more tumultuous history of migration than the CCB. Most components have likely undergone a close encounter with one or more of the giant planets during the early Nice Model instability (Nesvorný & Vokrouhlický, 2019), and Scattering Belt bodies have likely had one or more additional encounters since then (Gladman et al., 2008). These encounters, far more so than those of other KBOs, are very efficient at dissasociating wider binaries (Stone & Kaib, 2021).

A key takeaway from these results is that despite the incredibly wide separation of some Ultra-Wide TNBs in the CCB, it indeed appears possible for them to be survivors from the primordial Kuiper Belt. Thus, their existence can be fully explained by their formation via gravitational instability in the early days of the Solar System. Assuming the effects that these binaries are subjected to are dominated entirely by collisions with other TNOs, they may be primordial and require no additional explanation.
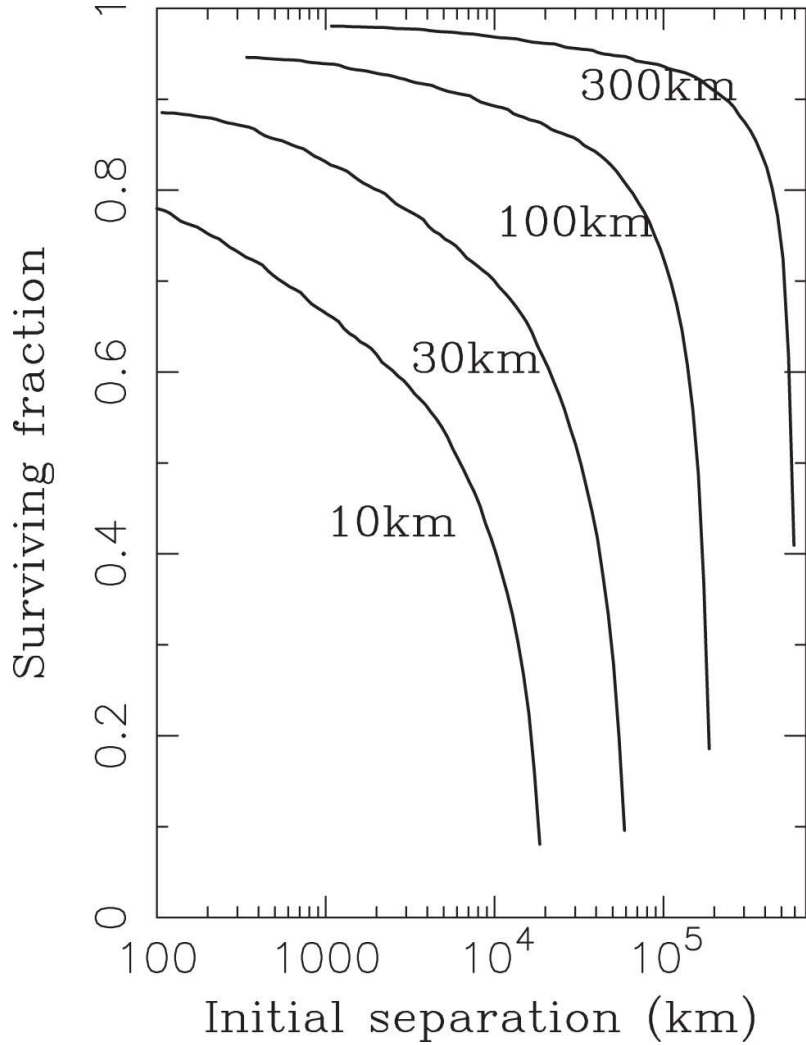
Figure 1.4: The surviving fraction of binaries into the present day as a function of their primordial mutual orbital properties. Figure 18 from Nesvorný et al. (2021). Each curve corresponds to the combined radius ($R_1 + R_2$) of the binary. For comparison, 2001 QW$_{322}$ has a combined radius of $\approx$ 120 km and a separation of $\approx 10^5$ km.

1.5.3 Evolution

While Petit & Mousis (2004) determines the average time between individual binary destroying events, Parker & Kavelaars (2011) and subsequent studies allow for a binary to evolve over time. These newer studies account for the effects of many different

collisions, rather than a single one. If multiple collision events are allowed to happen, then a binary will evolve over time. If this evolution causes a binary to widen, over time, it will become less stable. As observed by Parker & Kavelaars (2011), allowing a binary to evolve inevitably leads to lower stability over time. But if a binary can change over time, collisions may have an observable effect on the orbital elements of binaries that are not disassociated.

A hypothesis tested by Parker & Kavelaars (2011) is that the Ultra-Wide binaries like 2001 QW$_{322}$ or 2000 CF$_{105}$ might in part be evolved systems that began with much tighter separations. In testing this, they are readily able to produce Ultra-Wide TNBs from such tight populations but find that they cannot account for inconsistencies in the inclination distributions of tight and wide binaries. Because Ultra-Wide TNBs tend to have very planar orbits and, at the time of Parker & Kavelaars (2011), were thought to have had a near equal ratio of prograde to retrograde orbits, one cannot simply be a widened population of the other. For wide binaries to come from tight ones, some mechanism must be able to change their inclination distribution. Parker & Kavelaars (2011) find that even allowing for evolution from many different impacts, this distribution does not significantly change. Additionally, in their estimation, prograde orbits do not flip to retrograde sufficiently often and do not become more planar to any significant degree, as shown in Figure 5. Thus, they conclude that the known Ultra-Wide TNBs cannot simply be tight binaries widened through collisions alone.

Parker & Kavelaars (2011) additionally have trouble replicating the observed eccentricity distinctions between wide and tight binaries. In binaries widened by collisions, they observe that the emerging eccentricity distribution is far higher than actually observed in the Kuiper Belt. Orbital velocities, completely randomized in three-dimensional space, yield an eccentricity distribution termed a thermalized distribution and defined as,

$$f(e) = 2e \tag{1.3}$$

Over a multitude of perturbations, an eccentricity distribution naturally assumes this distribution (Jeans, 1919), which is much higher than what is observed among Ultra-Wide TNBs.
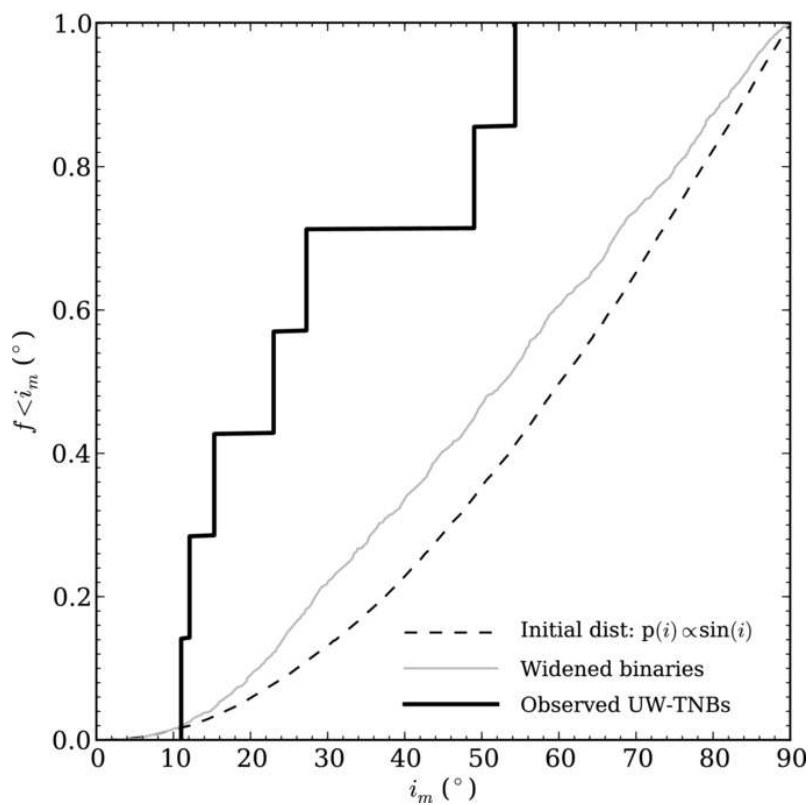

Figure 1.5: Comparison of the final inclination distribution of collisionally widened binaries versus the known sample, taken from Parker & Kavelaars (2011) Figure 9. The initial inclination distribution (dotted line) resembles the known tight binary distribution. The widened distribution and the known wide distribution are represented by the gray and black lines, respectively.

Other studies have looked into the effects of Kozai-Lidov oscillations and tidal friction (Kozai, 1962; Perets & Naoz, 2009; Porter & Grundy, 2012; Brunini & Zanardi, 2015). In this context, Kozai-Lidov oscillations are the periodic changes in a system's eccentricity and inclination caused by an outside perturbing force, which in this case is the Sun. In effect, an orbit's eccentricity and its inclination can exchange amplitude. An eccentric orbit loses its eccentricity but gains inclination, and vice versa, cyclically. These oscillations preserve a binary's semi major axis and the vertical component of the orbit's angular momentum relative to the Sun as the argument of perihelion librates. The timescales over which Kozai mechanisms operate can be approximated by,

$$T_K \approx \frac{P_b^2}{P_S}(1 - e_S^2)^{3/2} \tag{1.4}$$

where P_b is a binary's mutual orbital period, P_S is a binary's solar orbital period, and e_S is the binary's solar eccentricity. This time scale for the typical wide Kuiper Belt binary is on the scale of tens of thousands of years. Parker & Kavelaars (2011) does not account for this effect as their simulations do not include the Sun.

Kozai oscillations are cyclical, however. On their own, they cannot alter a binary's mutual semi major axis, only cause its eccentricity and inclination to oscillate. This oscillation additionally does not affect a binary's mutual separation and only becomes significant for bodies of already high initial inclination if their orbit is initially circular (Porter & Grundy, 2012). Binaries with circular orbits require an inclination of 39°, for this to occur(Kozai, 1962). But for binaries with high inclinations, like what is seen among the tight or initially tight population of CCB binaries, Kozai oscillations may be a mechanism to transfer this inclination elsewhere for another effect, such as tidal friction, to take over.

Tidal friction is a force that can act between two bodies orbiting each other eccen-

trically. Gravitational stresses upon the structure of each binary component work to induce an eccentric orbit to reduce its separation and become more circular (Perets & Naoz, 2009; Porter & Grundy, 2012). This eccentricity reduction is not cyclical and occurs throughout the entire lifetime of the binary. Brunini & Zanardi (2015) details that this, in combination with Kozai oscillations, can cause an overall reduction in a binary system's inclination. Because the Kozai effect can cause a binary's inclination and eccentricity to oscillate, and eccentricity is constantly being lost to tidal forces, inclination, in effect, would also be lost, potentially leaving a lasting mark on the mutual inclination distribution of modern day Kuiper Belt binaries. Wide binaries are more susceptible to this effect, potentially explaining how their inclination distribution can be so different without a mechanism being apparent from impact based evolution to change them. Brunini & Zanardi (2015) accounts for both of these effects, while Parker & Kavelaars (2011) and Nesvorný et al. (2021) do not.

It has also been noted by Grundy et al. (2019) that a binary with a large Kozai-acquired eccentricity may also be more likely to become retrograde. A sufficiently wide binary at the height of its apoapsis is more sensitive to gravitational perturbation and can be more easily flipped into a retrograde orientation. As unplanar inclination and high eccentricity are gradually leached away by tidal friction, a population of planar and comparatively more retrograde wide binaries may be formed, in contrast to the tight population that is not as affected by Kozai oscillations (Grundy et al., 2019).

However, the impact of tidal friction is reliant on knowledge about the internal structure of the bodies that it affects, summed up as a body's tidal Love number (Love, 1909). This parameter essentially measures the rigidity of a body and the degree to which it can be affected by tidal friction. Brunini & Zanardi (2015) assume different possible extremes in terms of Kuiper Belt body structure; from homogeneous ice to a differentiated mix of both rock and ice. No other studies attempt to simulate

this effect. As our knowledge of Kuiper Belt internal structure improves, the full effect of tidal processes on binary evolution will become clearer. But as of now, it does help address the problems of binary widening encountered by Parker & Kavelaars (2011).

1.6   Objective

Ultra-Wide TNBs that are stable, despite existing in a perturbative environment, can be a good indicator as to what the conditions in the Kuiper Belt must be. A very dense Kuiper Belt full of massive bodies will likely have eroded these binaries, so we can place an upper limit on this population. And if binaries like 2001 QW_{322} are assumed to be primordial, existing since the formation of the Kuiper Belt, then we can make inferences on the belt's structure and evolution across its entire history.

Our hypothesis is that because the initial study done by Petit & Mousis (2004) is only analytical and did not account for the possibility that many smaller encounters can affect a binary's evolution, they did not fully account for the influence that gravitational perturbations can have on a binary. We suspect that the gradual widening of binaries observed by Parker & Kavelaars (2011) from collisional evolution may be comparably significant, if not more significant, for gravitational perturbations. Thus, we wish to test the stability of the widest binaries under the influence of specifically gravitational perturbations and compare this to their stability under impacts. Under reasonably assumed Kuiper Belt parameters, we also wish to learn the likelihood that these binaries could have survived into the modern day or if some other mechanism must be at play to explain their presence.

If these binaries are not primordial, then they must have formed sometime in the comparatively more recent past. As observed by Parker & Kavelaars (2011), wide binaries can be formed from the repeated impacts of passing bodies on initially tight stable binaries, though with perhaps aberrant orbital properties. We wish to see if gravitational perturbations can also gradually widen and maintain a steady population of wide binaries from an initially tight population. The fraction of Ultra-Wide TNBs predicted by Lin et al. (2010) is 5%. If binary widening sustains a population this size while keeping up with binary decay, it will show that gravitational perturba-

tion is a possible mechanism for the continued existence of wide binaries today. Prior studies have used specific distributions of initial separations for tight binaries; we wish to determine which initial conditions a binary may have for it to become Ultra-Wide. Additionally, we wish to determine whether these binaries will have properties consistent with the wide binaries we observe today. Parker & Kavelaars (2011) claim that collisionally widened binaries do not have inclinations resembling the known sample, we wish to see if gravitationally widened ones do.

Finally, we will fully simulate the effects of both gravitational perturbation and impacts on the evolution of a binary. Though prior research may have overemphasized the role of collisions over perturbation, both are very likely to play an important role. The results of Petit & Mousis (2004) can be re-evaluated in the context of a dynamic changing Kuiper Belt while allowing for a binary to evolve over time from many iterative interactions. If the widest binaries have low stability in such regimes, then it can be shown that they indeed cannot be primordial. As per Parker & Kavelaars (2011)'s results, a sufficiently large population of Ultra-Wide binaries can be sustained through collisional encounters, though their inclination distributions are incompatible with observations. With both effects in play at once, we wish to see if we can keep this high population of wide binaries but with properties consistent with what we observe.

The following chapter details our methodology used throughout the remainder of the thesis, while Chapter 3 discusses the nature of our simulations. Chapter 4 gives our results when considering a static non-evolving Kuiper Belt. Chapter 5 gives our results when we consider an evolving Kuiper Belt and Chapter 6 does so when we take into account collisions with passing bodies. Chapter 7 summarizes our findings across all of our simulations.

Chapter 2

Methodology

In this chapter, we detail the process behind determining the number of encounters a CCB binary would experience over time as well as the parameters of each encounter. An encountering body will have a specified mass, velocity, and direction, each contributing to its overall influence. In some simulations, we factor in the modification of these parameters as the Kuiper Belt evolves (Diachronic Kuiper Belt) as opposed to simulations where they are held static (Monochronic Kuiper Belt).

While we mostly simulate gravitational encounters between binaries and passing bodies, we do begin simulating impacts with passing bodies. The differences between generating a series of gravitational perturbations and collisional perturbations are addressed here.

2.1 Relevant Populations of the Kuiper Belt

In this work, we consider the influence that close encounters with other TNOs have on the dynamical evolution of Ultra-Wide TNBs. To do this, first we must determine which Kuiper Belt populations have the most influential interactions with CCB binary

systems and are thus important to include in our simulations. However, the priorities for determining which populations have the most influence in purely gravitational encounters are different than those of collisional encounters. For instance, the most significant collisional encounters are those with very high collisional velocities, while the opposite is true for gravitational encounters. The significance of a population in a gravitational sense generally boils down to two criteria. First, this population must have a high number of encounters with the CCB. This factor is determined by the size of each population and both populations' collisional probability with each other, where collisional probability is simply the number of collisions that can occur in a given encounter radius over a set time. Second, the velocities of these encounters must be low for the effects of the perturbing gravity to be maximized.

In judging a modern Kuiper Belt population on the basis of these two criteria, we turn to the work of Abedin et al. (2021). They have determined the collision probability, population size, and average encounter velocity of several Kuiper Belt populations with the CCB based on the orbits of TNOs detected in the outer Solar System (Bannister et al., 2018).

The first population to consider is the Resonant Population. Abedin et al. (2021) examines three different such populations: inner (4:3, 3:2), main (5:3, 7:4), and outer (2:1, 7:3, 5:2). Of these three, the inner and main resonances provide a mixture of high encounter rates and low encounter velocities. The outer population, however, has almost half the collision probability of the other two while still having a comparable population size. Thus, we incorporate both the inner and main resonance populations but not the outer one.

The Scattering Population is composed of bodies with large eccentricities and perihelia near Neptune's orbit (Gladman et al., 2008). These bodies have had a close encounter with Neptune which put them into their current orbit, and likely will do so

again in the future. Due to their wide orbit and high eccentricity, bodies from the Scattering Population do not provide a significant portion of encounters with CCB binaries, failing our first criteria. Additionally, any scattering bodies that by chance encounter a CCB binary will likely have very high relative velocities (Abedin et al., 2021); failing our second criteria. However, we will revisit this population in Section 2.7 when we consider an evolving Kuiper Belt and when we incorporate collisional interactions.

From the Classical Population, the self-interaction of the CCB is the most influential component of our study. In addition to the average velocity between encountering bodies being very low, the collision probability is very high (Abedin et al., 2021). This is simply because CCB bodies share both the same location in the Kuiper Belt and the same mild orbital properties. The CCB interaction with HCB is also significant for similar reasons. Though, because of its more extended inclination distribution, its encounter rate is lower than that of the CCB self-interaction and its encounter velocity is a bit higher (Abedin et al., 2021). Nevertheless, the many encounters stemming from this interaction are slow enough for us to consider them significant.

Naturally, when it comes to an evolving Kuiper Belt, our evaluation must extend beyond the results of (Abedin et al., 2021). In this case, each population has very different relative sizes, so it becomes necessary to group the entire Kuiper Belt into the populations of CKB and KKB. This is discussed in more depth in Chapter 2.7.

In all, the Kuiper Belt populations whose encounters with the CCB we simulate for the modern Kuiper Belt are the HCB, the Inner Resonant Population, the Main Resonant Population, and the CCB itself.

2.2 TNO Size Distribution

The masses of encountering TNOs and the number of encounters a binary experiences depend on the TNO Size Frequency Distribution (SFD). As the Kuiper Belt's formation is shaped by collisions in its early history, an SFD in the rough form of a power law is to be expected (Dohnanyi, 1969). However, given the two different formation paths of the CCB and the rest of our relevant populations, it seems prudent to examine their SFDs separately. It should be noted that since the majority of the Kuiper Belt is unresolved, any population's distribution will be expressed in magnitude, rather than in radius or mass. The assumptions we make about a KBO population's albedo and mass are discussed. These magnitude distributions are generally represented by one or more power laws joined together abruptly or gradually (Lawler et al., 2018).

Observations suggest that the size distribution of the Kuiper Belt is likely not consistent across all radii or magnitudes. For much brighter KBOs, a very steep SFD is observed where the number of bodies drops precipitously with decreasing magnitude (and thus increasing size) (Gladman et al., 2001; Fraser et al., 2008). This likely indicates a very short formation period for bodies of large size before being disrupted by the eventual instability of the giant planets (Morbidelli et al., 2008). However, at larger magnitudes, the SFD seems to become far shallower. This has been suggested by observations early on (Gladman et al., 2001; Bernstein et al., 2004; Fraser et al., 2014) and affirmed by analyzing the craters observed on Pluto and Charon during the New Horizon's passage of the dwarf planet (Greenstreet et al., 2019; Abedin et al., 2021). Pluto spending more of its orbit within reach of HCB bodies than in the reach of CCB gives a direct indication that the HCB distribution may be more complicated (Stern et al., 2015; Moore et al., 2016). It even appears possible that this shallowing increases more dramatically towards the lower end of KBO sizes that can be gleaned from crater data (Singer et al., 2019), though this is disputed by later analyses of

Arrokoth's cratering record (Morbidelli et al., 2021). With the exact shape of the Kuiper Belt SFD in doubt, we turn to the best approximations available.

For the dynamically hot populations (the HCB and Inner and Main Resonance), we utilize the "Knee" model distribution as described by Lawler et al. (2018). This is an absolute magnitude (H) distribution that consists of two power laws joined together at a sharp but continuous division, dubbed the knee, or the break magnitude (H_b). The power law at either end of the knee is expressed by $\frac{dN}{dH} \propto 10^{\alpha H}$, equivalently expressed in diameter space by $\frac{dN}{dD} \propto D^{-(5\alpha+1)}$, where $q = 5\alpha + 1$. The power law governing smaller bodies (the faint end) is defined with $\alpha_f = 0.4$ and likewise, the law governing larger bodies (the bright end) is defined with $\alpha_b = 0.9$. While Lawler et al. (2018) are able to fit the H distribution well with a knee power law, due to observational uncertainty, the exact break magnitude is somewhat unconstrained, and to probe the possible parameter space, we use break magnitudes of 9.1 and 7.9.

The H distribution of the CCB, however, may follow a different curve. The slope of the CCB's SFD towards smaller magnitudes appears to be a bit larger than that of the other populations (Petit et al., 2011). While initially we had modeled the CCB with a split power law like that of the dynamically hot populations, only with a bright end slope of 1.2, we eventually choose to follow the model proposed by Kavelaars et al. (2021). They have determined it to be an exponentially tapered power law. This power law nominally resembles that of our knee model, with a faint end slope of either 0.4 or 0.5. But at bright magnitudes lower than H < 9, the slope starts to increase, eventually arriving at an exponential distribution. We utilize this SFD along with their fit fixed faint power law slope of $\alpha_C = 0.4$. These two SFDs are how we model the two distinct Kuiper Belt populations, though more recent publications suggest that these two SFDs may not in fact be different (Petit et al., 2023). Thus, the SFDs described here and graphed in Figure 6 are used throughout the entirety of this thesis.
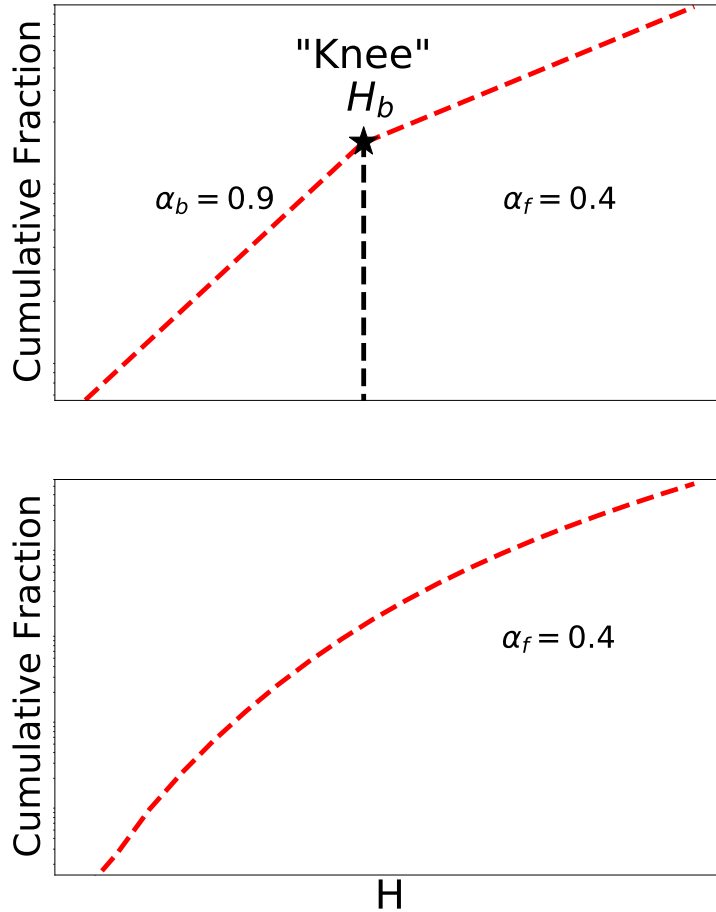
Figure 2.1: The Size Frequency Distribution of the KKB (top panel) and the CCB (bottom panel). The remaining populations' distribution consists of two power laws joined together at break magnitude or "knee". The CCB distribution is a tapered power law that becomes steeper towards smaller H.

Of course, a magnitude distribution does not translate directly into size. We do need to know or at least assume the albedo of the bodies we are modeling, though only a small minority of TNOs have had their albedo measured. For the dynamically hot population (the HCB and both resonance populations), we use an albedo value of 0.04, as this is the value used by Lawler et al. (2018) when they determine their split

power law distribution. With this albedo assumption, we can translate our two break magnitudes into radii of 50 km and 85 km, respectively. However, as explained in the previous section, the albedo of the CCB is greater than that of other populations. With this in mind, we assume a CCB albedo of 0.14 as determined by Vilenius et al. (2014). Additionally, albedo has been shown in practice to be a very influential parameter in binary survival lifetimes, so we also employ a CCB albedo of 0.12 as a lower extreme. A difference in assumption of even 0.01 has been shown to greatly alter a binary lifetime estimate (see Section 5.3) so employing a reasonable lower limit seems prudent to test the possible extremity of gravitational interactions. In all populations, we assume a density of 1.0 g cm^{-3} as this is a value used by Parker & Kavelaars (2011) and Nesvorný et al. (2021). Petit & Mousis (2004) also uses this density in addition to a comparatively less likely density of 2.0 g cm^{-3}.

The SFD that we sample from for our CCB tapers off at low H such that no bodies of $H < 4$ (r300 km) are generated. This is agreeable with present day observations (Nesvorný et al., 2021) setting a natural upper limit on the size of bodies generated in our simulation for this encounter type. For our HCB and resonant SFD, we set an artificial H limit of 4 ($r = 500$ km) as well.

In any collisional interaction regime, however, we must consider far lower KBO sizes than gravitational ones. Until now, we had been considering SFDs that extend down to radii of 20-30 km, but for collisional evolution, we must go much lower, as past works have shown even impacts with 5 km bodies are significant (Petit & Mousis, 2004; Parker & Kavelaars, 2011). But, as seen in cratering records on Charon, this SFD may not extend farther down than bodies of 1-2 km radius (Singer et al., 2019). Again, the SFD at lower radii may get shallower past this point. But as there is some disagreement as to whether or not this shallowing occurs here, we consider the new knee in the SFD carefully. This is discussed in more depth in Section 2.4, but Kuiper

Belt bodies at this size are irrelevant for gravitational perturbation consideration.

By varying our CCB albedo and our dynamically hot populations' break radius, we thus have 4 total Kuiper Belt combinations that we simulate.

2.3 Encounter Rate Velocities

To determine the rate of encounters between a CCB binary and each individual modern Kuiper Belt population, we again turn to the work of (Abedin et al., 2021). While they already provide us with encounter rates, we elected to take a detailed look at encounter velocities.

Previous studies have often assumed a single encounter velocity that is given to each one of their encountering bodies. The original study done by Petit & Mousis (2004) uses a set velocity of 1.5 km/s for collisions and 0.5 km/s for gravitational encounters. Parker & Kavelaars (2011) uses a velocity of 1 km/s. We felt that we could improve the accuracy of our simulations by instead assigning our encountering bodies velocities from a distribution.

To this end, we assume that the encounter velocity distribution is a Boltzmann distribution whose mean we assign to be the average velocity indicated in Abedin et al. (2021). These values are unique to each encounter and are assigned accordingly. By assuming a Boltzmann distribution, we are still able to reproduce the fifth and ninety fifth percentile velocities that they determine in Table 1 of their work.

Our combined velocity distributions are plotted in Figure 7, normalized to account for relative encounter frequency, which is the population size multiplied by the collision probability. The only further modification we make is setting a lower velocity limit at 20 m/s. Though incredibly rare (0.002% of all encounters), these events can cause integration errors as strong gravitational focusing leads to encounter timescales unresolvable with our integration step size. Any encounter speeds that would fall below 20 m/s are simply set to 20 m/s.

For our evolving Kuiper Belt simulations, we diverge from Abedin et al. (2021) and employ a dynamic simulation of the evolving Kuiper Belt to calculate encounter velocity at any given time. This is discussed in more depth in Section 2.7
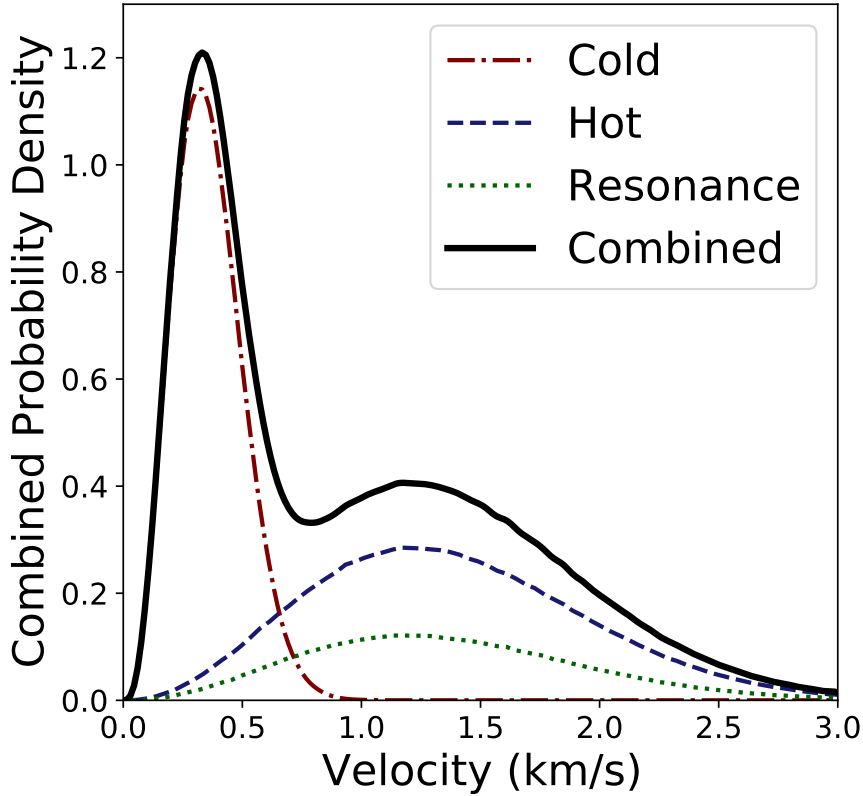
Figure 2.2: The combined probability density of encounter speeds for a CCB binary from each TNO population. Also plotted are the individual component population speeds, with the resonant populations merged into one.

2.4 Minimum Impactor Radius Cutoff

A consequence of using a mass distribution that is derived from one or two power laws is that as one models lower and lower mass bodies, the number of encounters approaches infinity. However, the effects of such low mass encounters diminish despite their increased frequency as their mass becomes increasingly small. Thus, we need to choose a minimum TNO size below which we can ignore encounters without significantly affecting their aggregate effects in our simulation.

For each of our different SFD shapes, we simulate 5 million encounters between each

of our previously established Kuiper Belt models and a stationary body. These shapes are the CCB tapered power law and the dynamically hot populations' split power law, with break radii of 50 km and 85 km. Encounter direction is sampled from a uniform sphere, reflecting random directions in 3D space (Henon, 1972). Though the masses of these passing TNOs reflect our established distributions, their velocities are fixed. For each encounter, we record the gravitational impulse imparted on the stationary body in three dimensions. Smaller bodies, though significantly more numerous, tend to evenly distribute their impulse in three-dimensional space, canceling each other out. They do not contribute much to the overall impulse outside of a random walk that is dwarfed by encounters with larger bodies.

Each encounter imparts an impulse onto the central body, which is recorded. To find the smallest radius of encountering bodies that contribute substantially to the evolution of a binary, we pair the radius of every encountering body with the impulse it provides. The total three-dimensional impulse imparted by all bodies in the simulation is recorded and compared to the individual impulses provided by each body. We arrange the encountering bodies by radius and incrementally add the impulse they provide until we reach 10% of the total impulse. The radius at which this boundary is reached is the smallest significant radius. One such simulation is shown in Figure 8. We run 300 such simulations, with the lower 5th percentile of results being our calculated minimum significant radius.

Of course, in order to begin sampling from these distributions, we need to assume a minimum radius to draw from, or else we run into the same problem described at the beginning of this section. The minimum radius we choose is 5 km. This radius is appropriate, as after some experimentation, using a lower radius does not influence the results of our minimum radius simulations.

Our resulting minimum significant radius from CCB self interaction is 36.3 km. In
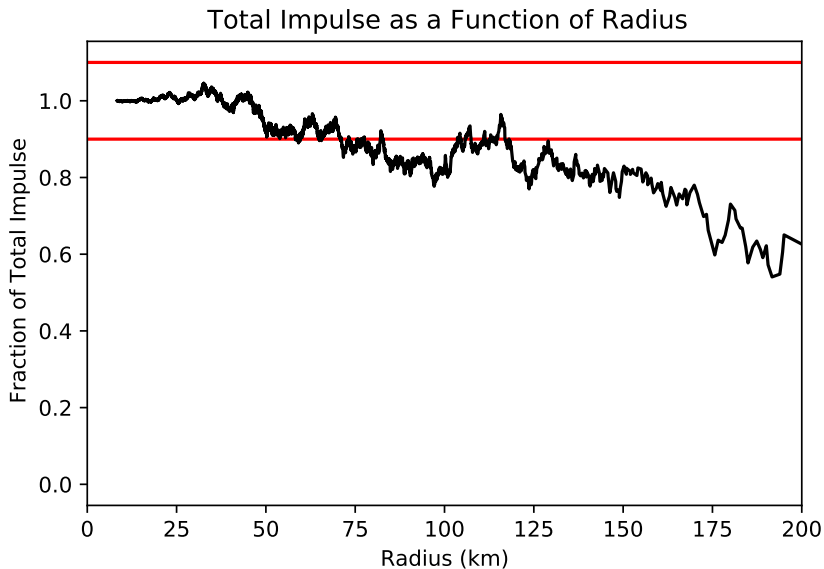
Figure 2.3: A reverse cumulative distribution of the impulse upon a test body in three dimensional space imparted by passing bodies as a function of their radius. The red lines represent where the cumulative impulse contribution is 10% of the total impulse contribution. Once the impulse contribution reaches here, we consider this to be the minimum significant radius of interacting TNOs.

our dynamically hot populations, it varied significantly based on our break radius. For break radii of 50 km and 85 km, our minimum encountering body radius is 34.0 km and 46.7 km respectively. Out of an abundance of caution, however, we elect to use a minimum significant encounter radius of 20 km for all of our SFDs.

When considering collisional encounters, however, a different approach must be taken. A gravitational encounter with a body 10 km in radius might not be significant, but a collision with one is likely to shake up the entire binary. Interactions are far less likely, but bodies of much smaller radii must now be considered. Again, as discussed in Section 2.2, the SFD of the HCB inferred from the craters of Pluto and Charon may become very shallow at radii smaller than 1 to 2 km. Assuming a very shallow slope in a similar minimum radius test leads to the conclusion that 1 km is a perfectly acceptable minimum radius. Assuming a steeper slope, however, does not. Though dwarfed by the effects of much more massive impacts, impacts from bodies less than 1

km in radius could play a role in the evolution of a binary if their SFD slope is steep. However, to avoid the ambiguity of this region of the KKB SFD, we choose to set the minimum radius to 1 km nonetheless. Our results here can thus be considered an estimate of the minimum effects of collisions on a binary system.

2.5 Total Number of Encounters

Our simulations are meant to span billions of years. The total number of encounters our binary system will have over that time can be calculated with,

$$N_E = \langle P_i \rangle N R^2 t \tag{2.1}$$

where N_E is the number of encounters, $\langle P_i \rangle$ is the mean intrinsic probability of encounter, N is the total number of bodies that may possibly be encountered, R is the maximum impact parameter over which we consider encounters, and t is the time over which an encounter can happen. Our intrinsic probability of encounter parameter is discussed in Section 2.1 but we have not yet talked about N and R.

In order to determine the total number of bodies that may be encountered by a modern CCB binary, we need a definitive number of known TNOs above a certain size to which we can anchor our SFDs. Each of our populations has its own anchor. For the HCB, we turn to Petit et al. (2011), who estimate the number of bodies brighter than $H < 8$ to be 4,100. For our various resonant populations, we turn to Gladman et al. (2012) who estimate the number of Inner Resonance and Main Resonance bodies brighter than $H < 8$ to be 1270 and 750 respectively. These values anchor and calibrate our SFDs, allowing us to generate the proper number of potential encounters down to an arbitrary minimum radius. The SFD of the CCB, as per Kavelaars et al. (2021) is already defined with an anchor and does not need further calibration. As for R, the maximum impact parameter, we use a value of 3.6×10^6 km, or 8 times the R_H of 2001 QW$_{322}$

However, such calculations produce a large number of encounters that are not especially significant. Passages of small TNOs that never get much closer than 4 R_H dominate such encounter generators. Thus, we discard TNOs whose mass is not large

enough to have a significant impact on our binary system during their flyby. The space around our binary is divided into three zones, as depicted in Figure 9. The first encompasses the inner 1 R_H, the second encompasses the space between 1 and 4 R_H and the last is the space between 4 and 8 R_H. TNOs whose encounter distance is further than 4 R_H would have to be very massive indeed to affect a binary at all, so only passing TNOs of mass greater than 1.1×10^{20} kg (R 300 km) are simulated; all others are discarded. In the second zone, only TNOs of mass greater than 2.6×10^{17} kg (R 40 km) are simulated. In the innermost zone, all encounters are simulated. With some testing, we find that simulating more expansive coverage of low mass encountering bodies has little impact on the results of a simulation.
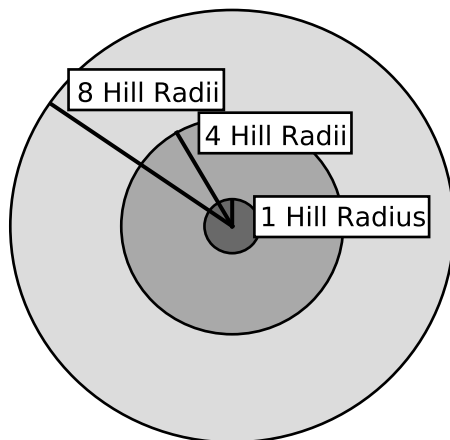

Figure 2.4: The three zones around the binary system. Bodies with an encounter separation between 4 and 8 R_H must have more mass than 1.1×10^{20} kg. Bodies with an encounter separation between 4 and 1 R_H must have more mass than 2.6×10^{17} kg. Bodies of any mass can pass closer than 1 R_H.

Naturally, in the case of collisions, a body must physically impact one of the binary components to affect it. The complex spheres of influence discussed earlier can be reduced to a simple question of whether the path of a passing body comes within the binary's physical radius. To this end, following closely the procedure of Parker

& Kavelaars (2011), we determine how many bodies come within 320 km of a binary component (5 times the radius of either 2001 QW$_{322}$ component). This number is then multiplied by 2 to account for any collisions that may befall the secondary component as well. Then, having been assigned a radius, we eliminate all bodies that do not meet the condition,

$$b < R_o + 0.9R_i \tag{2.2}$$

where b is the impact parameter of the encounter, R_o is the radius of the binary component, and R_i is the radius of the potential impactor. Only bodies that collide within 90% of the radius of the binary component are considered to eliminate any collisions that lead to bounces rather than a full transfer of momentum. In the end, this gives us a far smaller number of collisional encounters than gravitational ones, but each one is likely to be far more consequential than the average gravitational perturbation.

2.6   Fast Simulations

Ideally, each of our simulations would fully account for every single year of evolution, with each encounter time randomly distributed in that time span. However, in the interests of building a larger statistical sample of simulated systems, we can compress our simulated time without sacrificing the validity of our results.

In the simulation configuration described thus far, the amount of time that an interacting TNO is present in the system is very short compared to the overall simulation time where no encounters are happening. If it were not for the exterior gravitational force provided by the Sun, the test bodies would move in perfectly Keplerian orbits in this time between encounters. By not simulating all of this non-encounter time, our simulations can be much faster and require fewer resources to run.

This leaves only the Sun to be considered. Its gravity is the only force acting on the binary between encounters, so in compressing this time we must also simulate the Sun's influence on the system. In practice, the vast majority of the Sun's influence manifests in the form of Kozai cycles. While this does not have an effect on the mutual semimajor axes of the binary systems, it can cause their eccentricities and inclinations to oscillate (Kozai, 1962). As described in Section 1.5.3, this can play a big role in the instantaneous eccentricity of a binary, potentially affecting its stability. One significant consequence of this effect is that the two binary components may collide once their eccentricity becomes too high and their periapsis becomes too low. This can happen for binaries that attain a high inclination, especially if they have already attained a high eccentricity. These collisions very rarely happen in simulations that do not include the Sun. Thus, our metric for accurately accounting for billions of years of solar influence is comparing the number of binary collisions in them with those in simulations that fully account for billions of years of solar influence.

The savings from this time compression have varied quite a bit between monochronic

and diachronic simulations. In monochronic runs, through a series of trial runs, we empirically find that cutting inter-encounter time from a typical value of 700,000 days to 12,000 days still captures an adequate sampling of solar perturbations since collisions between both binary components happen just as often as in the uncompressed simulation runs. Because Kozai cycles are cyclical and, in our case, operate on timescales of tens of thousands of years, we do not need to simulate the entire billions of years of solar influence to account for them. This modest delay between encounters allows our simulations to run up to 50 times faster while fully reproducing the number of binary collisions that we see otherwise. Consequently, all simulations in this paper utilize this compression, though data and graphs are depicted assuming uncompressed time.

Prior simulations like those of Parker & Kavelaars (2011) and Nesvorný et al. (2021) do not account for Kozai Cycles induced by the Sun and thus have the freedom to not account for inter encounter time at all. They individually simulate each encounter and randomize the mean anomaly of their binary system for the next one. The simulations done by Brunini & Zanardi (2015) not only account for Kozai processes but also account for the tidal effects between each binary component. Such a process cannot be compressed in the same way ours is. Thus, we do not have prior work to compare our compression technique to. But our tests suggest this is a viable way to simulate the Kozai mechanism, so this is how we proceed.

2.7 Diachronic Simulations

When simulating a diachronic, time dependent Kuiper Belt, a number of our procedures must be done differently.

Our modeling of the Kuiper Belt throughout the history of the Solar System draws heavily from the simulations done by Anderson & Kaib (2021). They have simulated not just the primordial CCB that had formed in its current location, but migrations of the remainder of the belt into its present day configuration. Using their data on the relative size of each population at any given time in the history of the Solar System, as well as their orbital elements, we can approximate the evolving Kuiper Belt.

The previous discussion on the relevant populations of the Kuiper Belt is not a factor here. Despite the scattering population not having considerable influence on a CCB binary in the present Kuiper Belt, its population size is heavily inflated in the past. This along with the tendency for bodies to migrate from one population to another, makes it far more useful to again divide the Kuiper Belt into only two populations, the CKB and the KKB. For the purposes of this thesis, populations are defined such that the CKB formed in-situ and has not changed, and the non-CKB is anything simulated by Anderson & Kaib (2021) that started inside 30 au, whether it survives a long time or not.

As the encounter rate and velocity data provided by Abedin et al. (2021) is for the present Kuiper Belt, we must derive these things from the simulations of Anderson & Kaib (2021). To do this, a separate numerical simulation of the Kuiper Belt is run, stocked with the bodies from said work. Bodies from each population are allowed to interact with a population derived from the CCB (as defined by Petit et al. (2011)). This is because, as evidenced by Anderson & Kaib (2021), the orbital makeup of the CCB does not change substantially over time, so the present day CCB is an adequate stand in for the CCB across history. Each of the bodies in our constructed populations

is drifted along their orbit until 50 encounters occur, under the assumption that their movement is purely Keplerian. Any encounters within 1.5×10^6 km (about 4 R_H of 2001 QW$_{322}$) are recorded. With this value, as well as the total number of orbits integrated, the integration time, and the encounter threshold, we have an estimate for the collision probability between the CCB and each population. Collision velocities are directly sampled from this simulation as well. Because the population of CCB crossing bodies is constantly in flux in Anderson & Kaib (2021)'s simulations, this is done for every million year time interval over the 4 billion year time span of this study's simulations.

As in the monochronic procedure, this collision probability is multiplied by the total number of bodies in both populations and the area of collision to obtain the total number of encounters a CCB binary would have in a given stretch of time. This total number is again obtained from Abedin et al. (2021), but instead, every single population documented by them is counted among the KKB while their CCB population is taken to be our CKB population. In total, the present day number of KKB bodies with magnitudes under 8.66 is 249100, while the CKB number is taken to be the same as the CCB number noted in Section 2.2. These population sizes are inflated to account for the observed loss of Kuiper Belt bodies by Anderson & Kaib (2021) over time. Assuming the same SFDs described earlier and the same minimum radii described in Section 2.4, the exact number of encounters at any given time in the Solar System's history is derivable, though the same discarding process described in Section 2.5 is used to eliminate insignificant passages. The changing encounter rate and number are illustrated in Figure 10.

In total, a CCB binary in an evolving Kuiper Belt will experience about five times as many encounters as a binary in a static Kuiper Belt, though encounter velocities are generally double that. Even so, we expect binary evolution in a diachronic Kuiper
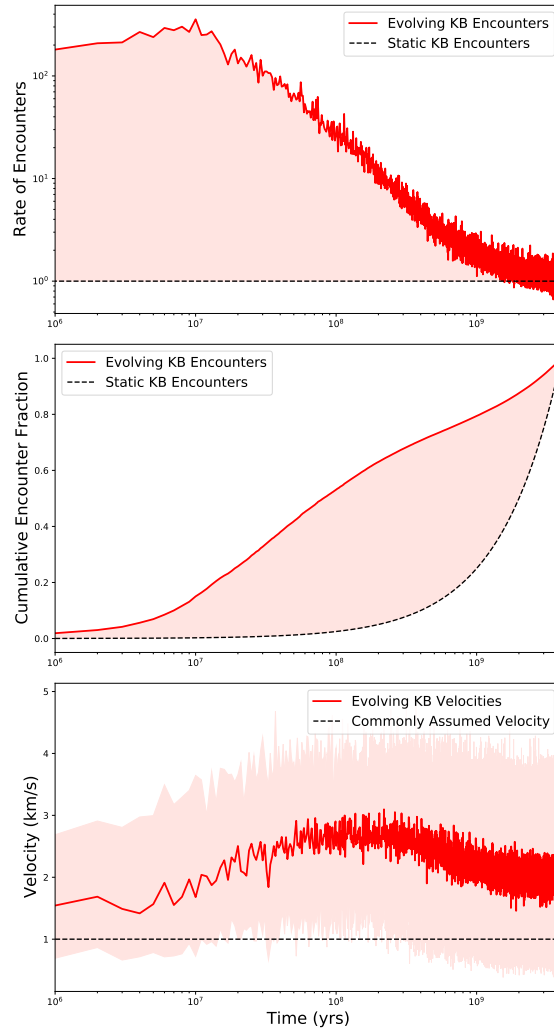
Figure 2.5: The total number of encounters between the KKB and a CCB binary in a diachronic Kuiper Belt versus in a Monochronic Kuiper Belt (top panel). A cumulative distribution of the number of encounters comparing both Kuiper Belt models (middle panel). The red fill represents excess encounters provided by a diachronic Kuiper Belt. Additionally, the evolving average velocity of encounters between the KKB and a CCB binary compared to the commonly employed velocity of 1km/s (bottom panel). Here, the red fill encompasses everything between the 5th and 95th percentile of velocities.

Belt model to happen considerably faster, especially in the early Kuiper Belt when the population of encountering bodies is much higher. It should be noted, however, that in keeping with the procedure discussed in Section 2.6, we still space each encounter by 12,000 simulated days of only solar gravity influencing our system. The Kozai Mechanism is likely to be as significant in a Diachronic model as it is in a Monochronic one. For the purposes of display and analysis, which require accurate timekeeping of a system, we correct these equally spaced encounters in data processing.

It must also be considered that as the velocity and encounter rate of a population change over time, so may its SFD. In the case of the CKB, its lack of catastrophic migration, as well as its low density, implies that its SFD has not changed significantly since the primordial Kuiper Belt. Its density and population size are additionally unlikely to have changed significantly, as indicated in the models of Anderson & Kaib (2021). However, even in the case of the KKB with a greatly changing population size and density, it is unlikely that collisional grinding can have altered its SFD within the magnitude ranges we sample (Greenstreet et al., 2019; McKinnon et al., 2020; Abedin et al., 2021).

All of these steps prepare our simulation with an accurate accounting of any passing TNO along with their velocities and masses, be they passing gravitational perturbers or impactors. The simulator itself and our modifications are described in the following chapter.

Chapter 3

Simulations

3.1 RMVS-SWIFT

All N-body simulations that we have done were performed using the SWIFT subroutine developed by Hal Levison and Martin Duncan (Levison & Duncan, 1994). The version we use simulates using the Regularized Mixed Variable Symplectic (RMVS) method. Designed to simulate a set of massive bodies alongside n number of massless test bodies whose orbits can be integrated accurately at arbitrarily high eccentricities, proved perfect for our simulations. The timestep used is dynamic and changes depending on the initial conditions of our binaries. When simulating any specific Ultra-Wide binary, we use a timestep of 50 days, a significantly shorter time than the period of any binary we simulate. All simulations of initially tight binaries use a time step at least 1/20th the period of the minimum starting semi major axis.

The binaries are set up such that one binary component bears the entire mass of the binary. Sitting at the center of our coordinate system, we place 10 massless orbiting test binaries. These bodies bear the semi major axis, eccentricity, and inclination of the system we simulate, and as they are massless, they do not interact with each

other. In all of our simulations, we randomize the arguments of perihelion, longitudes of ascending node and mean anomalies of these binaries, as these are undetermined for any known TNO binary and they serve as a way to meaningfully simulate different iterations of the same binary with the same set of encounters. An orbit's argument of perihelion defines an orbit's rotation relative to its periapsis and an arbitrary reference point. Longitude of ascending node is similar, but concerns an orbit's inclination. Mean anomaly denotes the position a body is in its orbit at any given time. Additionally, the gravity of the Sun is accounted for. Our Sun is drifted on a circular orbit 44 AU away, corresponding to the heliocentric semi major axis of the typical CCB binary.

A modification made to SWIFT by Dr. Nathan Kaib allows for the introduction of bodies bearing mass that pass through these binary systems. At their prescribed time, interacting TNOs are introduced to the simulation 8 R_H distant with velocities consistent with our established distributions from Sections 2.3 and 2.7 and random trajectories. After they pass through the system and reach 8 R_H again, they are removed.

A special case is taken into account when a passing body has a particularly high velocity and thus spends less time perturbing the binary. It becomes more convenient to treat this encounter as a single instantaneous impulse rather than fully simulating the gravity of a slowly passing body. We use the impulse approximation to perturb the primary and its swarm of test binary companions. The velocity of an incoming TNO is considered "high" when the encounter timescale (or closest approach over encounter velocity) is less than 50 days, or 10 times the shortest integration time-step we ever use.

There are two ways that a binary system can be considered disassociated. If the test particle comes within a radius set to the sum of the radii of the two tested binary components, it is lost. This represents a collision between the two binary components

and thus an end to the binary. The second scenario is if the test particle becomes unbound and drifts more than eight 2001 QW$_{322}$ Hill radii away from the central mass, representing a binary's gravitational binding energy being exceeded. Though a particle further than 1 Hill radius could be considered lost regardless, we choose a high value out of an abundance of caution. The exact time and nature of each binary dissociation is recorded, though as each test particle is massless, the loss of one does not affect the status of others in the same simulation.

3.2 Simulating Collisions

One final modification was made to SWIFT to allow for the simultaneous simulation of gravitational and collisional encounters. A separate file containing the mass, velocity, and direction of a set number of colliding bodies is now fed into each simulation. Collisions are simulated as a single instantaneous impulse onto each of the test bodies, such that,

$$\Delta V = 0.62 \frac{M_i}{M_t} V_i \tag{3.1}$$

Where M_i and V_i are the mass and velocity of an impacting body, while M_t is the mass of the struck test particle, which is set to be the same as half the system mass. While we do assign a mass to each test particle for the purposes of collisional simulation, the mass of the system is still borne by the central body. The change in velocity is multiplied by 0.62 as an average of all possible impact angles and the angle at which impulse is applied is the same as the entrance angle of the impactor.

Additionally, the resulting mass loss of an encounter is taken into account in our collisional regime. Following the same procedure as used by Parker & Kavelaars (2011), the resulting mass of any test particle following a collision is expressed by,

$$M = M_o - \frac{KE_i}{2Q_D^*} \tag{3.2}$$

Where M_o is the initial mass of the test particle (and thus the system), KE_i is the kinetic energy of the impactor, and Q_D^* is the energy required to disrupt half the mass of the struck binary component. This parameter is defined as,

$$Q_D^* = 7 \times 10^7 (R_o)^{-0.45} + 2.1\rho(R_o)^{1.19} erg\, g^{-1} \tag{3.3}$$

Where R_o is the radius of the struck test particle in cm, ρ is the mass density of the binary components in gm/cm^3. This procedure follows the results of Benz (1999) which apply to icy bodies colliding inelastically at velocities between 0.5 and 3 km s^{-1}. The mass deducted from a test particle is then deducted from the system. At the next collision, each test particle is again given half the mass of the system.

An additional process is accounted for by Parker & Kavelaars (2011) that we do not include. For larger collisions ($\gamma > 0.8$), a significant amount of momentum from any collision should be transferred into smaller fragments that are carried away. We do not account for this process and assume all collisions are perfectly inelastic. In testing, collisions of such size very often lead to the rapid disassociation of the system due to such a large loss of mass, regardless of the momentum transferred in that single impact. Thus, we do not feel the inclusion of this effect is necessary.

Another similar study assuming dynamic mass is Nesvorný et al. (2021). They utilize a program called Boulder (Morbidelli et al., 2009; Levison et al., 2009; Bottke et al., 2010) which accounts not only for mass loss following a collision but also the potential for mass accretion following a less energetic collision. Our modifications to SWIFT do not take these into account, nor do we consider the tidal effects that Brunini & Zanardi (2015) simulate in their study. Our modified SWIFT simply simulates gravitational impulses from passing bodies, collisional impulses from impacting bodies, Kozai effects provided by the Sun, and past loss in accordance to Benz (1999)'s pure inelastic collisions.

SWIFT is the only means by which we simulate Kuiper Belt binaries, and any modifications to this regime will be explicitly mentioned when they occur. It should be noted that collisions do not feature in any of our simulations until Chapter 6. Thus, mass loss is not taken into account until then.

Chapter 4

An Unevolving Kuiper Belt

In this chapter, the findings of my first project are discussed. Portions of this chapter also appear in the publication Campbell et al. (2022). Here, only an unevolving Kuiper Belt is simulated, and only the effects of gravitational perturbation from passing bodies are simulated. Physical impacts are not simulated. We subject known wide binaries to these processes as well as initially non-Ultra-Wide TNBs to examine how they might evolve over time. As such processes are limited to the effects of the Kuiper Belt as it exists today, the long term evolution of a binary in deep time is not directly simulated here. But the results of earlier studies, which similarly consider only an unevolving Kuiper Belt can be compared. And among the first things we wish to determine is the relevance of gravitational perturbations in binary evolution.

4.1 Significance of Iterative Perturbative Encounters

Perhaps the most important result, and the one that would ultimately predict the path of this project is just how significant gravitational interactions are to the evo-

lution of a Kuiper Belt binary. The initial result of Petit & Mousis (2004) indicated that perturbative encounters were significantly less impactful than physical impacts. Direct comparisons will be described in Chapter 6, but initially, the significance of gravitational perturbations is determined by comparing these results with those of similar monochronic simulations like those of Parker & Kavelaars (2011).

Specifically, as discussed in Chapter 3, there are two primary ways that a binary can become disassociated. The first of these binary loss mechanisms is collision between the two components of the binary themselves. This is caused primarily by Kozai oscillations driven by the Sun that dramatically raise the eccentricity of a mutually inclined binary system. Kozai oscillations are described in more detail in Section 1.5.3. Once this eccentricity approaches 1, the binary periapsis drops low enough that both components collide. Even initially less inclined binaries may succumb to this type of disassociation, as their inclinations can be altered by strong passages. This collision is not the result of any one TNO passage and, with an initial inclination close enough to 90°, can occur without any passages. It should be noted, however, that our model does not include the effects of tidal friction, which past work has found can tighten and circularize the orbits of eccentric binaries (Perets & Naoz, 2009; Porter & Grundy, 2012; Brunini & Zanardi, 2015). Thus, it is possible that destruction due to Kozai induced collisions may often be unphysical and simply be a consequence of neglecting this effect. Tidal friction is discussed in more detail again in Section 1.5.3.

The second mechanism of binary loss is ejection, or disassociation, resulting from a binary's gravitational binding energy being exceeded by the tidal potential of a passing TNO. This mechanism of binary loss is the focus of the analytical calculations done by Petit & Mousis (2004) and Parker & Kavelaars (2011). However, we find that such binary loss is often due to many encounters slowly widening the separation over time. This gradual widening of a binary's separation is very effective at making it more

CCB Albedo	$R_b = 50$ km	$R_b = 85$ km
$\alpha = 0.12$	0.82	0.77
$\alpha = 0.14$	0.77	0.72

Table 4.1: The fraction of lost 2001 QW$_{322}$-like binaries that become dissociated following an outward migration of at least 4.5% R$_H$. All such binaries begin with a separation of 22% R$_H$. α refers to our assumed CCB albedo, and R_b refers to the break radius of our split power law dynamically hot populations.

fragile. Eventually, the binary becomes fragile enough for a single encounter to break it.

When testing the long term stability of specific Ultra-Wide binaries, this increasing separation proved to be very influential. This is shown in Table 2 where in any Kuiper Belt SFD, between 72 and 82 percent of all lost binaries whose initial parameters are those of 2001 QW$_{322}$ become lost only after experiencing prior orbital widening of at least 4.5% R$_H$ or 20% of their initial separation.

The first of these loss mechanisms, collision between the two binary components, is far less likely to occur in simulations that do not account for Kozai mechanisms like those of Parker & Kavelaars (2011). The second mechanism, the ejection of a binary component, is a process greatly dependent on the gradual widening of a binary's separation. This gradual widening and eventual loss would not be included in Petit & Mousis (2004), possibly dulling an estimated impact of gravitational erosion.

4.2 Lifetimes of Wide Binaries

In this research, we consistently focus on the evolution of three specific Ultra-Wide TNBs. They are chosen for their diverse properties and their specific notice in many prior studies. The first is 2001 QW$_{322}$ (22.2% R$_H$ separation) (Kavelaars et al., 2001) as it is the widest known TNB and has been looked at specifically by Parker & Kavelaars (2011) and Petit & Mousis (2004). Our second is 2000 CF$_{105}$ (16.8% R$_H$ separation) (Noll et al., 2002) as it has shown to be the binary most sensitive to collisions (Parker & Kavelaars, 2011). Our third is 2004 JZ$_{81}$, representing an Ultra-Wide TNB with a comparatively low separation (9% R$_H$ separation) (Parker et al., 2011). Additionally, all three of these binaries have solar semi major axes close to 44 AU, and thus the location and period of our orbiting Sun in our simulations do not have to change.

The longevity of certain wide TNBs has been tested in the past assuming a collisionally active Kuiper Belt (Parker & Kavelaars, 2011; Nesvorný et al., 2021). To compare their results to our gravitationally active Kuiper Belt model, we tested this longevity as well. With these results, we can determine just how long one might expect these binaries to survive in the environment they now inhabit. Under the effects of many perturbative encounters with KBO bodies in an unevolving Kuiper Belt, binaries are disassociated at a rate greatly resembling that of exponential decay, as represented by,

$$N(t) = N_o e^{-t\,(a/\tau)} \tag{4.1}$$

Where τ is the mean lifetime of the binary system.

The resemblance is great enough that it starts to become convenient to express the decay rate of a given binary by the mean lifetime of a fitted exponential decay function. An example is shown in Figure 11, demonstrating the decay rate of the known Ultra-Wide TNB of 2000 CF$_{105}$ in all 4 Kuiper Belt models we simulate. Because the average

lifetimes of these binaries can at times be longer than the age of the Solar System, we subject them to 10 billion years of Kuiper Belt interactions rather than 4 billion. This assists us in fitting the exponential decay curve.
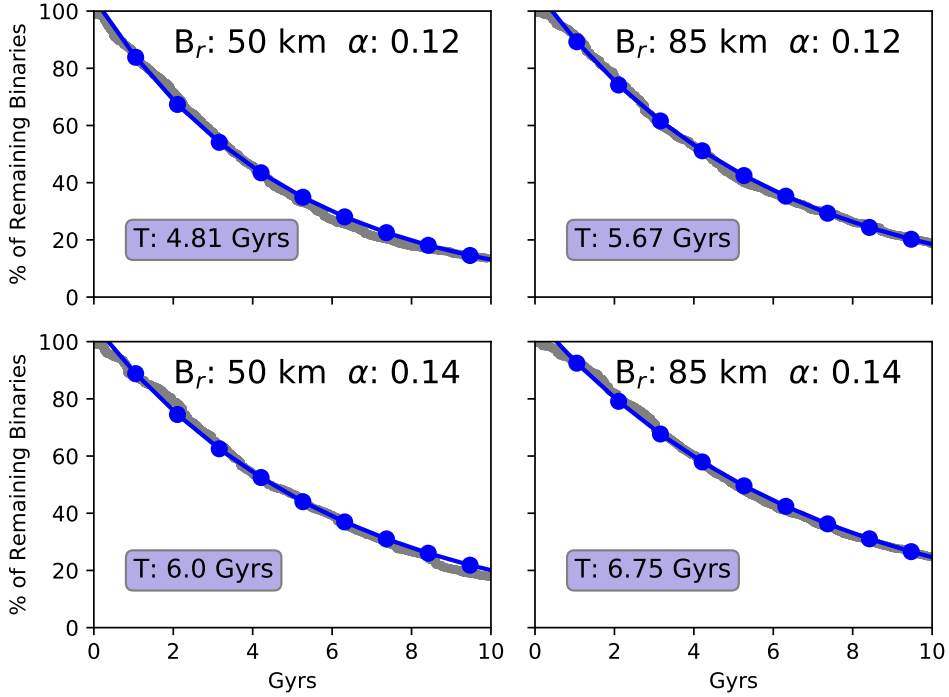

Figure 4.1: The dark gray points are the percentage of surviving binaries over time whose initial separation is that of 2000 CF$_{105}$ starting at 100. The blue dotted line represents a fitted exponential decay curve. Each panel represents the different Kuiper Belt parameters simulated and includes a box showing the average binary lifetime in that SFD. B$_r$ is break radius of the dynamically hot populations, and α is albedo of the CCB.

Assuming a reasonable CCB albedo of 0.14 (Lacerda et al., 2014; Vilenius et al., 2014) (see Section 1.4), a binary like 2000 CF$_{105}$ has a half life of between 6 and 6.75 billion years. This implies that the dissociation timescale of the binary is comparable to the age of the Solar System. Thus, if such binaries were formed in the early Kuiper Belt, we would expect 50-55% of an initial population of 2000 CF$_{105}$ like binaries to survive 4 billion years under the influence of gravitational encounters alone, given what we know of the modern Kuiper Belt. Doing such analysis on the other two binaries, we find that 2004 JZ$_{81}$ may be expected to survive into the modern day assuming

TNO Binary	CCB Albedo	$R_b = 50$ km	$R_b = 85$ km
2001 QW$_{322}$	$\alpha = 0.12$	5.81	6.15
	$\alpha = 0.14$	6.60	7.43
2000 CF$_{105}$	$\alpha = 0.12$	4.81	5.67
	$\alpha = 0.14$	6.0	6.75
2006 JZ$_{81}$	$\alpha = 0.12$	14.4	15.0
	$\alpha = 0.14$	15.1	19.2

Table 4.2: Our simulated average lifetime of 3 Kuiper Belt binaries in Gyrs under our 4 different Kuiper Belt SFDs. R$_b$ is break radius of the dynamically hot populations, and α is albedo of the CCB.

a stagnant Kuiper Belt but the survival of 2001 QW$_{322}$ is about as certain as 2000 CF$_{105}$'s. The exact average lifetimes of each binary under each Kuiper Belt SFD are listed in Table 3.

However, to say that a primordial ultra-wide binary survives ignores a key feature of our simulations. The separations of our systems are allowed to change. As noted in the prior section, binary separations tend to widen, rather than shrink. But among binaries that remain intact over a long period of time, binaries that instead lessen in separation are over represented. And if a QW$_{322}$-like binary manages to survive 4 billion years of encounters by reducing its separation considerably, it can hardly be considered a QW$_{322}$-like binary anymore. Thus, to gain an accurate ratio of initial to final populations of Ultra-Wide TNBs, we must consider binaries that reduce in separation as having been lost.

If we allow these binaries to evolve over 4 billion years and introduce the criterion that any surviving binary's final separation must not have decreased by more than 20% of its initial separation, then our initial binary populations must be higher. Under the same mass density and CCB SFD as before, we calculate that if subjected to 4 billion years of gravitational perturbations from the modern Kuiper Belt, a 2000 QW$_{322}$-like binary has a likelihood of between 43% and 45% of remaining both intact and of comparable separation to its origin. This assumes the albedo of the CCB is 0.14 and a break radius of 50 km and 85 km respectively. Table 4 lists the fraction of our previous

TNO Binary	CCB Albedo	$R_b = 50$ km	$R_b = 85$ km
2001 QW$_{322}$	$\alpha = 0.12$	0.38	0.40
	$\alpha = 0.14$	0.43	0.45
2000 CF$_{105}$	$\alpha = 0.12$	0.30	0.34
	$\alpha = 0.14$	0.37	0.44
2006 JZ$_{81}$	$\alpha = 0.12$	0.79	0.80
	$\alpha = 0.14$	0.81	0.84

Table 4.3: Fraction of binaries that both survive 4 billion years and do not migrate inward by more than 20% of their initial separation. B$_r$ is break radius of the dynamically hot populations, and α is albedo of the CCB.

three binaries that survive 4 billion years under our different Kuiper Belt SFDs.

This implies that for every binary resembling 2000 CF$_{105}$ in the modern Kuiper Belt, there must have been between 2 and 3 in the primordial Kuiper Belt. But naturally, this makes the very unreasonable assumption that the Kuiper Belt has been static and unchanging for the last 4 billion years. As discussed in Section 1.3, the Kuiper Belt has changed considerably over the course of its history. Thus, these figures are likely to be significantly underestimating the effect of gravitational encounters. Our analysis of binary lifetimes in an evolving Kuiper Belt is discussed in detail in the following chapter.

However, what we can conclude is that in the modern Kuiper Belt, the known Ultra-Wide CCB binaries are likely generally stable, including even the widest binary, 2001 QW$_{322}$. This result agrees with that of Parker & Kavelaars (2011), showing that even the inclusion of gravitational perturbative encounters cannot sufficiently disrupt the stability of these binaries assuming reasonable restrictions on the Kuiper Belt's SFD. The average lifetimes of these binaries can be comparable to the age of the Solar System. For 2000 CF$_{105}$ in particular, assuming a CCB albedo of 0.14, its estimated lifespan is between 6 and 7 billion years. Even accounting for a possible separation change over time, after 4 billion years of perturbations, it is not unreasonable for a binary like 2000 CF$_{105}$ to not only survive but to remain nearly as wide.

This separation change also plays an important part in the disassociation rate of

binary systems. A similar effect is observed by Parker & Kavelaars (2011) in the case of collisional interactions among TNBs. Such evolution is not accounted for in the original work of Petit & Mousis (2004) which may affect their determination of the relative importance of TNO encounter types in TNB disassociation rates.

One thing that becomes apparent is that the average lifespan of our tested Ultra-Wide binaries is very dependent on the albedo of the CCB. We assume an average CCB albedo of 0.14 as this is what is estimated by Vilenius et al. (2014). But the directly measured R-band geometric albedo of 486958 Arrokoth is 0.21 (Hofgartner et al., 2021), considerably higher than our assumption. If it should be the case that the average albedo of the CCB is higher than 0.14, the observed Ultra-Wide CCBs are likely to be more stable.

Additionally, our binary's lifetimes seem to be weakly dependent on our assumed break radius of the dynamically hot portion of the Kuiper Belt, with a larger break radius favoring slightly longer binary lifetimes. This relationship is weak though, and predictions on this break radius cannot be made here. But the larger relationship with varying Kuiper Belt SFD is likely to still be applicable. Differing SFD is very likely the main driving force causing differences between Petit & Mousis (2004) and Parker & Kavelaars (2011). Any greater understanding of the nature of the CCB and KKB Size Frequency Distribution, especially along radii ranging from 40 to 100 km, will likely affect this result. A steeper slope will result in reduced binary stability, while a shallower slope will do the opposite.

However, these preliminary results cannot be used to determine the likelihood of any specific binary surviving unscathed since the formation of the Kuiper Belt. These models only take into consideration the Kuiper Belt as it is currently observed. In the past, it had a much larger population than it does today. Thus, we cannot compare our results with those of Nesvorný et al. (2021) who considered a dynamically changing

Kuiper Belt. Because of the much greater number of perturbing bodies in the historical Kuiper Belt, these binary lifetimes are likely overestimates. However, the conclusions reached by Nesvorný et al. (2021) are that binary survival is decently assured, even up to 50% R_H. While we never simulate binaries this widely separated, binary survival for 2001 QW$_{322}$ at 22% R_H is not certain, even in a static unevolving Kuiper Belt. This may indicate that gravitational perturbations are, in some way, more significant than collisions in terms of binary disassociation. Chapter 5 discusses our results for an evolving Kuiper Belt that accounts for the far higher population density in the distant past.

4.3 Binary Widening

The possibility that binary separations can change over time in our simulations gives rise to another phenomenon that we wish to study: the gradual widening of binaries. As discussed in Section 4.1, binaries subject to gravitational encounters often widen rather than shrink, giving the impression that present day binaries are wider than their primordial forms.

When simulated, binaries of separations ranging from 7 to 23% R_H diffuse outward over time. While some decrease in separation, most of the separation change appears to be increasing. This general outward diffusion is illustrated in Figure 12. As noted in the previous section, however, initially wide binaries that survive are more likely to have decreased in separation. Here, we discuss our experimentation with this outward separation increase over time and its potential to leave a mark on the mutual separation distributions of Kuiper Belt systems.

While the results of the previous section show that the primordial survival of wide binaries may not be a certainty, this section concerns itself with the hypothesis that Ultra-Wide TNBs have a gradual formation mechanism even in the modern Kuiper Belt. Because binaries tend to widen over time, it is possible that modern day wide binaries may be the widened descendants of a formerly much tighter population. And if this is the case, we might then be able to determine how large the fraction of wide binaries that we presently observe would be given the present day conditions of the Kuiper Belt.

Here, we subject a population of binary systems with separations randomly distributed between 3% and 5% R_H to 4 billion years of gravitational Kuiper Belt interactions. The eccentricities and inclinations of these binaries are sampled from the known non-Ultra-Wide TNB sample in the modern Kuiper Belt (Grundy et al., 2019). For a good comparison to a known Ultra-Wide TNB, each of these binary systems is
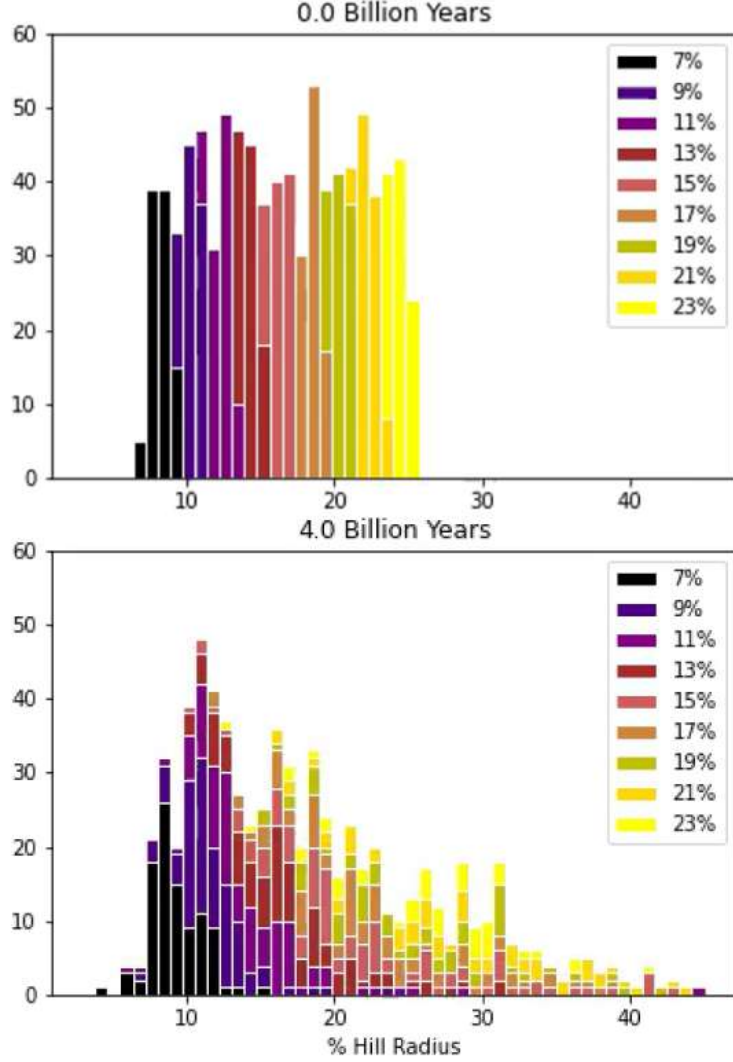
Figure 4.2: A mutual separation map of 1000 binaries, all initially separated by distances between 7 and 23% R_H. The upper panel illustrates the initial separation map, and the final panel is the separation map after 4 billion years of monochronic Kuiper Belt interactions. Darker colors indicate more initially tight binaries.

given a total mass equal to 2001 QW$_{322}$.

What we find is that binaries that initially have tight separations can in fact become Ultra-Wide due to gravitational perturbations. An example is shown in Figure 13, coming from one of our simulations with a SFD defined by $\alpha_{CCB} = 0.14$ and $R_B = 50$ km. Here, our binary begins with a separation around 5% of its Hill radius,

CCB Albedo	$R_b = 50$ km	$R_b = 85$ km
$\alpha = 0.12$	0.015	0.012
$\alpha = 0.14$	0.010	0.009

Table 4.4: Fraction of initial tight ($3\% < R < 5\%$ R_H) TNBs that are ultra-wide ($R > 0.07$ R_H) at any given time.

where it stably orbits until a large perturbation at around t = 0.4 Gyrs. After this perturbation, the binary maintains a separation comparable to 2001 QW$_{322}$ and 2000 CF$_{105}$, eventually surpassing them both. It then achieves a separation far higher than any observed today following a perturbation at t = 3.6 Gyrs. This binary's eccentricity and inclination are guided primarily by Kozai oscillations prior to its first major encounter. Following this, perturbations from passing bodies become the primary driver behind the changes in the binary's orbital properties.

In this example, the binary widens significantly but becomes disassociated before the end of the simulation. This possibility is to be expected, as wide binaries are more susceptible to perturbations than tight ones, but despite their eventual loss, they can be fairly long-lived. One could imagine observing a widened binary, noting that it is very weakly bound, and wondering how such a system could have survived so long had it been formed in the primordial Kuiper Belt. Thus, instead of measuring the fraction of wide binaries after 4 billion years of simulation, we instead measure the fraction of Ultra-Wide ($R > 0.07$ R_H) binaries at any given time between years 3 and 4 billion of our simulation. This data is shown in Table 4. Across all assumed CCB albedos and SFDs, we find that ∼1% of all binaries that were initialized at 3-5% R_H separations reside in Ultra-Wide configurations billions of years later.

However, binaries with separations between 3 and 5% R_H are already likely not the most common. Only about 30% of all known binaries have separations beyond 3% R_H (Grundy et al., 2019) and this sample is already likely to over represent wider binaries. In trying to evolve binaries with starting separations of 1-2% R_H, we find that
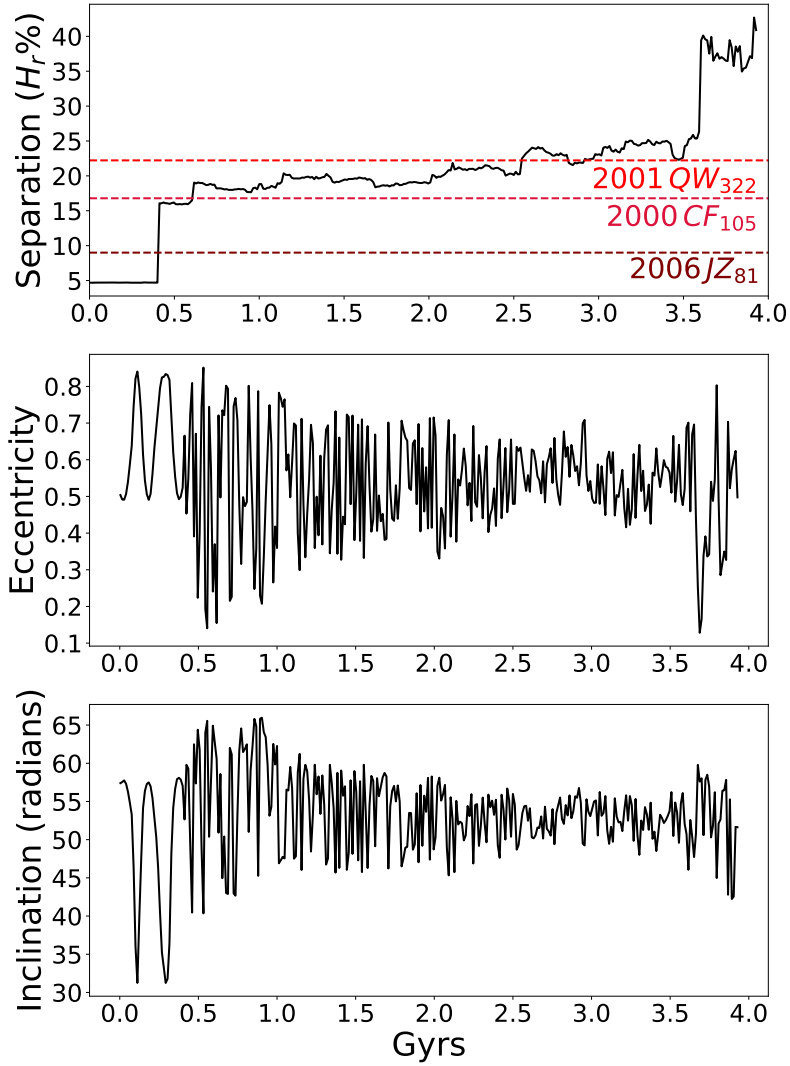
Figure 4.3: Separation (R_H percentage) vs. time (millions of years) of a simulated binary. This is an example of a binary starting with a separation under 5% R_H but eventually widens to beyond that of 2001 QW$_{322}$. For comparison are the current separations (in relative Hill radii) of the binaries 2001 QW$_{322}$ (22%H_R), 2000 CF$_{105}$ (17%H_R), and 2006 JZ$_{81}$ (9%H_R). This wide separation does not last as the binary is lost at around 3.8 Gyrs.

they are generally immobile. With no Kuiper Belt SFDs do any significant quantity of binaries ($<$ .2%) become Ultra-Wide, indicating that in the modern Kuiper Belt, these binaries are quite resistant to gravitational perturbations and may not be a plausible source for modern Ultra-Wide binaries. The exact distribution of binaries in the primordial Kuiper Belt is a mystery, but it is unlikely to be entirely composed of 3-5% R_H separated binaries.

One thing we can conclude here is that while Ultra-Wide TNBs readily form from a population of initially tight binaries subjected to gravitational perturbations, we do not ever produce a population size consistent with observations. Even in our most optimistic scenarios, our Ultra-Wide ($a > 7\%R_H$) binary fraction is never greater than 1.6%. In contrast, we would expect this ratio to be at least 5% (Lin et al., 2010). The degree of widening of our binaries is shown in Figure 5. Our population of binaries is sampled in each simulation, every 5 million years from 3-4 Gyrs in our 4 Gyr simulations. We can reliably produce Ultra-Wide binaries in excess of 14% Hill radius separation, but our quantity of Ultra-Wide binaries consistently falls short of predictions.

Additionally, we begin with a population of binaries that, while not Ultra-Wide, are wider on average than the typical Kuiper Belt binary. 64% of known Kuiper Belt binaries have less separation than 2% of their own Hill radius (Grundy et al., 2019) and these binaries generally do not widen. The actual fraction of $> 2\%$ R_H binaries is also likely to be even higher given their increased difficulty of detection. We also make the assumption that tight precursor binaries have very similar orbital makeups to the tight binaries we currently observe in the Kuiper Belt. It is of course possible that these precursor binaries have properties unique to an earlier era of the Kuiper Belt and thus are not seen today.

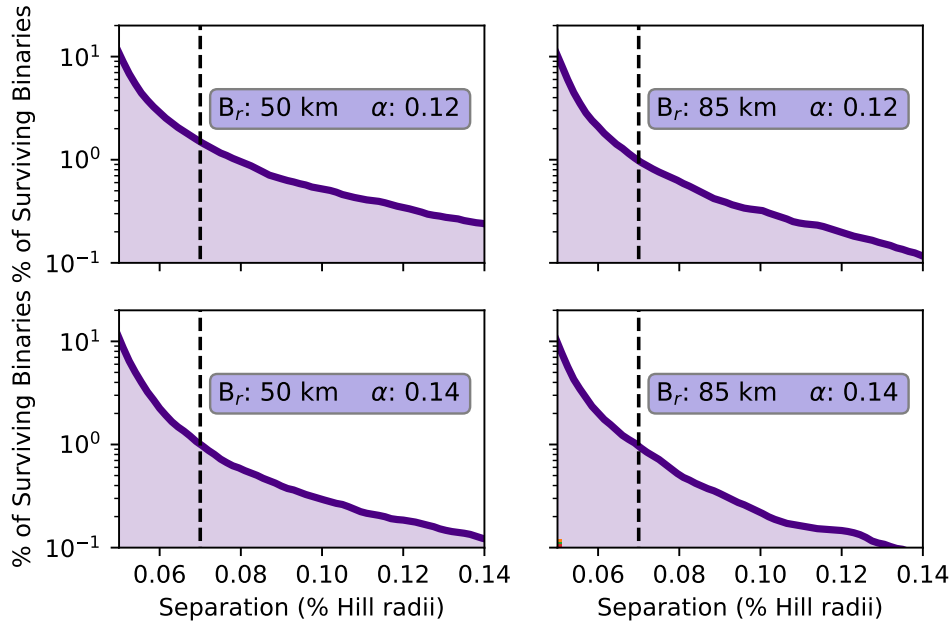However, it should be noted again that the models of the Kuiper Belt used here

Figure 4.4: A cumulative distribution of the separations of each sampled binary. A line is drawn at 7% Hill radius, as this marks where a binary becomes Ultra-Wide. Each panel represents a Kuiper Belt SFD we have modeled; in none of them does the fraction of Ultra-Wide binaries rise over 2%.

have not been diachronic. We had only been simulating the Kuiper Belt as it currently is. In the more crowded era of the early Kuiper Belt, the larger number of perturbers magnifies this effect and can create a larger population of Ultra-Wide binaries.

4.4 Evolving Orbital Properties

A goal of this work was to not only determine if Ultra-Wide binaries can be produced through gradual widening, but also if their emergent orbital properties are consistent with those of the wide binaries we observe. As explained in Sections 1.5 and 1.5.3 Ultra-Wide TNBs have been shown to have different mutual orbital properties than tight (R < 7% R_H) binaries. Their orbital separations are, of course, higher, but they also seem to have different eccentricity and inclination distributions. Among our simulated binaries that become Ultra-Wide over the course of our simulations, we observe similar orbital properties. These widened binaries are similarly sampled from 3–4 billion years into our simulation, as described in the previous section.

The mutual eccentricities of Ultra-Wide TNBs tend to be, on average, larger than those of tighter binaries. The average eccentricity of Ultra-Wide CCB binaries is 0.53, compared to the average value for tight binaries of 0.34 (Grundy et al., 2019). With many perturbations over long periods of time, one might expect the eccentricity distribution of a set of binaries to be thermalized. This occurs if the relative velocities between each binary component are randomized in direction and magnitude from 0 to escape velocity. Such an eccentricity distribution takes the form of $N \propto e^2$. The observed distribution of Wide binaries is more eccentric than tight binaries, but it remains distinct from a thermalized distribution.

We initialize such simulations with tight binaries possessing eccentricities sampled from our known tight binary sample. As before, some of them gradually widen and become Ultra-Wide TNBs. As they do, their eccentricity distribution actually changes and starts to greatly resemble that of the known Ultra-Wide binary sample, as shown in Figure 15. It remains more extended than the known tight binary eccentricity sample while still not resembling a thermalized distribution. Figure 15 depicts a widened population from our Kuiper Belt SFD defined by $\alpha_{CCB} = 0.14$ and $R_B = 50$ km but

the resemblance holds true with every SFD that we simulated.

This particular eccentricity distribution is so stable that even our binaries that are not quite Ultra-Wide assume it. Amongst the known data, it appears that the majority of the low mutual eccentricity binaries have less than a percent Hill radius separation (Grundy et al., 2019). Any binary wider than this is likely to have a much more eccentric orbit. As we do not simulate any binaries tighter than 1% R_H, it is difficult to ascertain whether widening from this separation will yield an eccentricity distribution like this. It's likely that in these monochronic simulations, such binaries would not significantly widen anyway. Such consistent distributions across a wide range of separations from 3% R_H onward demonstrate that the observed distribution is likely to occur naturally in any binaries subject to perturbative encounters.

As explained in Section 1.5.3, the inclination differences between the observed tight and Ultra-Wide components of the CCB are more complex. Tight CCB binaries are very heavily biased towards prograde orbits but have a strong tendency towards higher mutual orbital inclination. In contrast, a third of all known Ultra-Wide TNBs are retrograde. In addition, these orbits prefer a more planar inclination orientation, with a dearth of binaries having mutual inclinations between 55° and 125° (Grundy et al., 2019).

This discrepancy between our observed tight and wide binaries has a similar eccentricity discrepancy. Most unplanar binaries have lower separation than 3% R_H, meaning that our relatively tight binaries are not quite representative of the known binary sample here. The substantially unplanar inclination distribution of very tight binaries is likely more stable due to its low separation.

Among our monochronic gravitationally widened binaries, we are unable to replicate this inclination distribution as well as we do with eccentricity. As pictured in Figure 16, our binaries begin with an inclination distribution sampled from the known tight
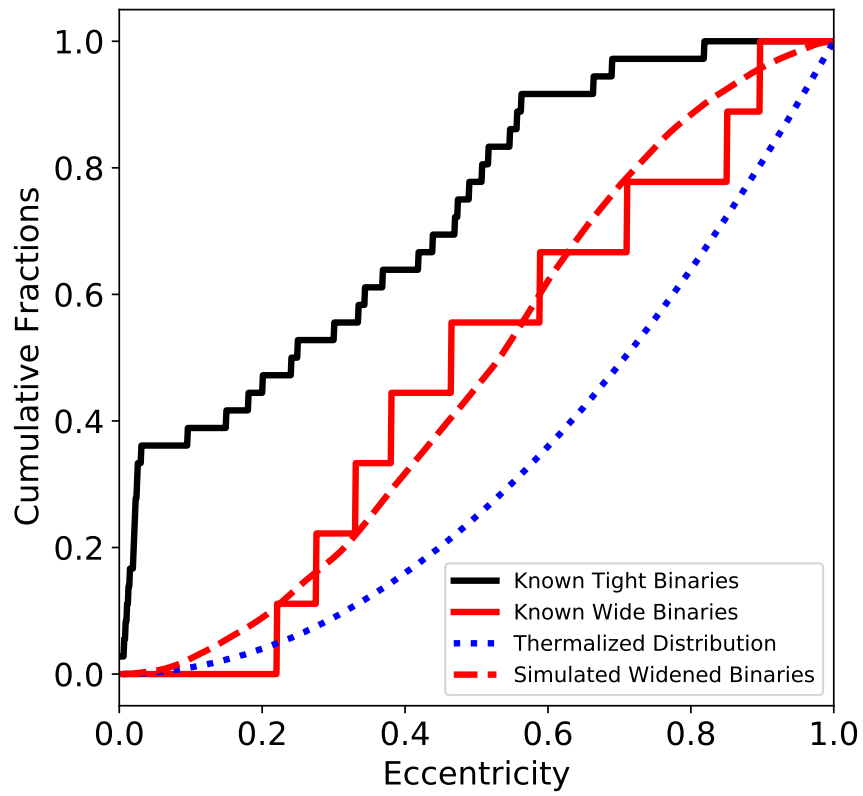
Figure 4.5: The eccentricity distribution of our widened binaries compared to the known distribution of both tight and Ultra-Wide binaries. Also plotted for comparison is a thermalized eccentricity distribution.

binary population and eventually assume a slightly more planar distribution. What is pictured is again taken from our simulation, whose Kuiper Belt SFD is defined by $\alpha_{CCB} = 0.14$ and $R_B = 50$km. But again, this result is common to all of the SFDs tested. This result tends to agree with that of Parker & Kavelaars (2011) who concluded that binary widening does not sufficiently change the inclination distribution to account for the discrepancy between tight and wide populations.
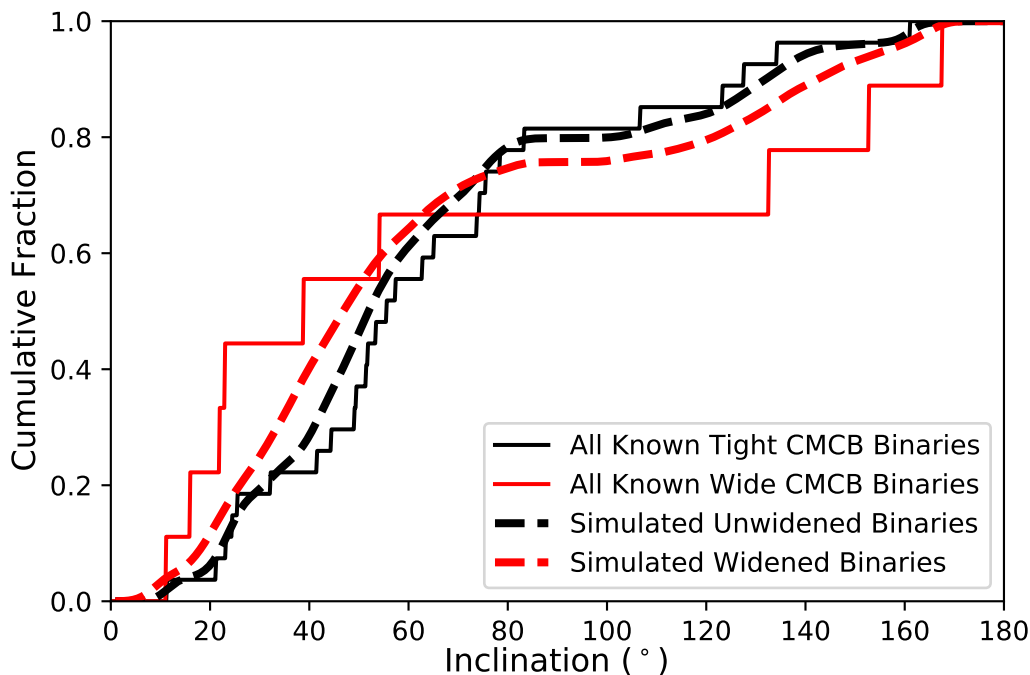

Figure 4.6: The inclinations of our simulated binaries that have become Ultra-Wide vs. those that have not, compared to the inclinations of observed Ultra-Wide binaries and tight binaries.

With all of these SFDs, a Kolmogorov–Smirnov (K-S) statistic cannot rule out the possibility that the known Ultra-Wide TNB inclination distribution is drawn from our gravitationally evolved Ultra-Wide TNBs to within 95% confidence. No K-S test p-values are ever below 0.2. This statistic is the standard for ruling out one sample's capability of being drawn from another. However, with the low number of Ultra-Wide TNBs known at present, a K-S test similarly cannot even rule out the possibility of

the known wide inclination sample being underivable from the known tight sample within the same confidence. This p-value is 0.3, much higher than 0.05, which would be needed to conclusively rule out this possibility. This means that while our widened inclination distribution does not conflict with the observed sample, its similarity is scarcely more significant than that of the tight binary sample. But this can also mean that the known tight and wide distributions cannot with certainty be considered distinct, despite their apparent differences. So, our largely unchanging inclinations do not preclude gravitational perturbation based widening from being an Ultra-Wide TNB formation mechanism.

Our final result differs from that of Parker & Kavelaars (2011), even though the inclination distributions of our widened binaries do look similar. Their application of a K-S test gave the answer that their Ultra-Wide TNB inclination distribution could not be drawn from the known sample. We believe that this occurs because they only consider the planarness of their inclinations, lumping in all inclinations greater than 90° with binaries less than that. The only measurement of an inclination is the deviation from a planar orbit, regardless of whether it is prograde or retrograde. We have elected to compare inclinations as they are, and doing this seems to yield a different ultimate result. But this is a difference in methodology philosophy rather than a more similar inclination distribution. This difference is slightly exacerbated by the discovery of three new Ultra-Wide TNBs discovered since the publication of Parker & Kavelaars (2011), all of which are prograde. With this new approach, a K-S test yields a p-value of 0.28 for ruling out sampling the known Ultra-Wide TNB inclinations from the combined TNB inclination distribution.

While we have been unable to replicate the number of Ultra-Wide TNBs that we presently see, it seems that binaries widened through gravitational perturbations have orbital properties similar to those observed. Our widened eccentricity distribution

greatly resembles the observed sample, while our inclination distribution is not in conflict with it. Accounting for an evolving Kuiper Belt, however, may have a large effect on these evolved distributions. While the eccentricity distribution of widened binaries seems very stable, the larger number of encounters conferred by the diachronic Kuiper Belt may cause it to evolve more towards a thermal distribution, unlike what we observe. The changes to our widened inclination distribution may be more favorable towards reproducing what we see.

With the numerous possible effects that an evolving Kuiper Belt may have on our current results, it would make sense to add it to our simulations. The following chapter talks about our results assuming this far more dense and active Kuiper Belt.

Chapter 5

An Evolving Kuiper Belt

In this chapter, the results of our simulations employing an evolving diachronic model of the Kuiper Belt are discussed. These simulations again only account for gravitationally perturbative interactions and not impacts. Nevertheless, these results can be used to predict the evolution of binaries in deep time across the whole history of the Kuiper Belt. Like in the last chapter, specific Ultra-Wide TNBs are simulated, as well as tighter binaries that are not Ultra-Wide at first. Here, the results of the previous chapter are expanded upon, and predictions made are tested.

Simulations here are done similarly to those in the previous chapter. We subject a series of binaries with specific initial conditions to a number of flyby encounters approximating what would have been experienced across the history of the Solar System. In this chapter, rather than drawing encounters from the 4 most influential modern day populations of TNOs, we draw from the entire Kuiper Belt, dividing them into two main populations. These are the Cold Kuiper Belt (CKB) and the Kinetic Kuiper Belt (KKB), described in more detail in Section 1.3. As these populations evolve over time, their differing population size, distribution, and average encounter velocities are calculated from the simulations of Anderson & Kaib (2021). This is discussed in more detail in Section 2.7. Here, the KKB whose modern components in the prior chapter

are dwarfed by those of the CCB in influence, now dominate due to their far larger population sizes in the Kuiper Belt's early history. Thus, the CCB albedo is no longer a parameter we vary. Encounter masses are sampled from one of two SFDs corresponding to the CKB and KKB described in Section 2.2. It is from these simulations, where binaries are subject to gravitational encounters over the history of the Solar System that our data is derived.

The SFDs we use however, are unchanged from the previous chapter. As discussed more in Section 2.2, we utilize a split power law to approximate the SFD of the KKB and a tapered power law to approximate that of the CKB. Like in the previous chapter, the point where the KKB's split power laws connect, the break radius, is not completely constrained. Thus, we use break radii of 50 km and 85 km.

5.1 Binary Survival

Like in the unevolving Kuiper Belt models, we determine the rate at which binaries of varying initial properties decay. For the same reasons outlined in the previous chapter, we follow the lifetimes of three binaries in particular: 2001 QW_{322} (Kavelaars et al., 2001) as it is the widest known, 2000 CF_{105} (Noll et al., 2002) for being wide and more susceptible to perturbations, and 2006 JZ_{81} (Parker et al., 2011) for being a relatively tight but still Ultra-Wide TNB.

Like in the previous section, these binaries are given the initial separations, eccentricities, and inclinations of specific Ultra-Wide TNBs. The system mass is similarly set to be that of the binary they represent. It is their arguments of perihelia, longitudes of ascending node, and mean anomalies that are randomized such that test binaries influenced by the same encounters are not influenced identically. Unlike the previous chapter, however, we need only simulate these binaries for the 4 billion years of Solar System history to determine their probable survival likelihoods.

Unfortunately, unlike the loss rates of binaries in an unevolving Kuiper Belt, these binaries do not decay at a rate resembling an exponential decay curve. Indeed, with the number of encounters a binary experiences changing so rapidly, it does not seem useful to fit the decay rate to any curve in particular, exponential or otherwise. Additionally, simply calculating an average survival time would greatly bias the losses that happen very early on due to the much denser Kuiper Belt environment. Accordingly, in any images depicting the decay rate of these binaries, the vast majority will occur prior to 500 Myrs. Thus, we only make note of the fraction and nature of binaries that survive the 4 billion years of encounters generated from the Kuiper Belt.

What is clear, though, is that is that all our three Kuiper Belt binaries tested now have considerably lower chances of surviving 4 billion years of encounters compared to the previous chapter with an unevolving Kuiper Belt. This is not particularly

TNO Binary	CCB Albedo	$R_b = 50$ km	$R_b = 85$ km
2001 QW$_{322}$	Surviving	0.051	0.079
	Wide	0.017	0.025
2000 CF$_{105}$	Surviving	0.068	0.079
	Wide	0.019	0.023
2006 JZ$_{81}$	Surviving	0.245	0.343
	Wide	0.187	0.264

Table 5.1: Fraction of binaries that remain undisassociated (Surviving) and fraction of those that have not decreased in separation by more than 20% of their original mutual orbits. Each system is given the initial conditions of a specific Ultra-Wide TNB.

surprising, as almost five times as many encounters now occur in this evolving model. As listed in Table 6, only 5-8% of all 2001 QW$_{322}$-like binaries survive the whole of the Solar System's history, depending on the assumed Kuiper Belt model. 2000 CF$_{105}$ has a similar survival likelihood of 6-8%. Even the initially stable 2006 JZ$_{81}$ system now only survives between 26 and 34% of the time.

The plausibility of these binaries' proposed primordial history seems to be far reduced from the previous chapter. Despite the efficient rate at which such binaries may form in the early Kuiper Belt (Nesvorný et al., 2010), a vast population indeed must have been formed to account for the continued presence of such Ultra-Wide TNBs in the modern Kuiper Belt. The fraction of remaining binaries from each of our tested samples is shown in Table 6. Compared to the results of the previous chapter in Table 4, the fractions have decreased dramatically.

But again, simply examining the survival of wide binaries ignores the fact that many survivors may only escape dissociation because they evolve into more stable arrangements. The preferential survival of binaries that tighten or evolve into a smaller semimajor axis, ceasing to have their unusual properties, must be taken into account. If we account for a binary's possible lessening of separation, it's clear again that most surviving 2001 QW$_{322}$-like binaries have done so by tightening considerably. If we introduce a criterion that any surviving binary's separation must not have decreased by more than 20% of its initial separation, then our initial Ultra-Wide TNB populations

must be far higher. Of the starting sample, only 1.7 to 2.5% of all initial 2001 QW_{322}-like binaries both survive and maintain a separation of at least 80% of their initial semi major axis. The rapid loss of these wide binaries is shown in the red curve in Figure 17. 2000 CF_{105} has a similar persistence rate of 1.9-2.3%, depending on the break radius employed.
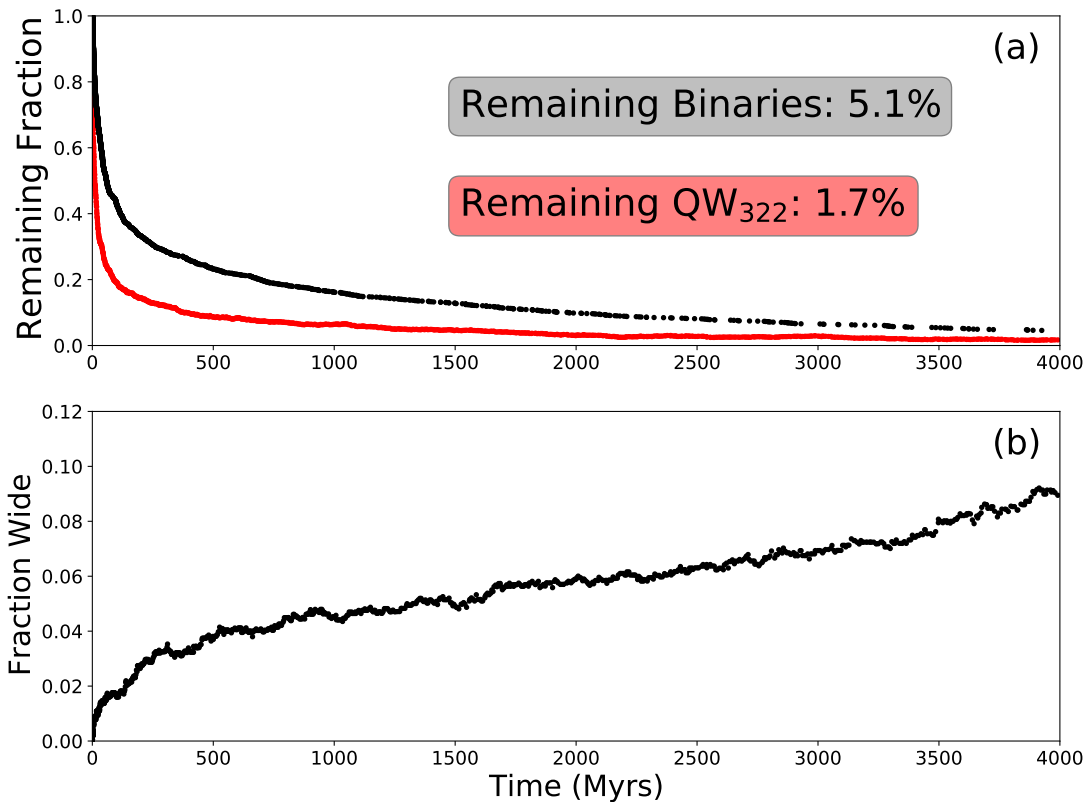

Figure 5.1: Panel (a) depicts the decay of initially 2001 QW_{322}-like binaries. The black points depict the fraction of binaries that have not been disassociated, while the red line depicts this as well as all surviving binaries that have not migrated inward by more than 20% of their initial separation. Panel (b) depicts that fraction of binaries that initially start with separations of 3-5% R_H becoming ultra-wide over the same timescale with the same encounters.

In tracking the rate of binary separation reduction, we determine the percentage of binaries that remain wide at any given time. But, as a binary may increase in

separation, it may also decrease in separation. This effect gives the impression that wide binaries decay and then reform in Figure 17, but this is simply the population of binaries widening and shrinking individually. Overall, the Ultra-Wide TNB population decreases in separation. These results, shown in Table 6, again are samples of each binary's separation between 3 and 4 billion years into the simulation every 20 million years.

Plotted under these loss rates in Figure 17 is a slowly building population of wide binaries with a different set of initial conditions. Like in the previous chapter, these binaries begin as less than Ultra-Wide and become so over time. This population widening largely mirrors the population loss of initially 2001 QW$_{322}$-like binaries. Such binary widening is discussed in more detail in the next section.

With the survival likelihood of wide binaries being this low, the present day population may not be dependent on their formation rates in the early Kuiper Belt. It may be that formation happens not in the primordial Kuiper Belt but in the intervening years due to gravitational widening. With such a large change in the survival rates of specific binaries with the inclusion of a diachronic Kuiper Belt model, the gradual widening described in the prior chapter may also happen more efficiently.

CCB Albedo	$R_b = 50$ km	$R_b = 85$ km
Ultra-Wide	0.094	0.086
2001 QW$_{322}$-like	0.0051	0.0046

Table 5.2: Fraction of initial tight ($3\% < $ R $ < 5\%$ R$_H$) TNBs that are ultra-wide (R > 0.07 R$_H$) or resemble 2001 QW$_{322}$ (R > 0.18 R$_H$) at any given time.

5.2 Binary Widening

Like in our monochronic simulations, Ultra-Wide TNBs are capable of forming from tighter binaries in a diachronic Kuiper Belt regime. Just as was done in the previous chapter, we begin with a population of less than Ultra-Wide TNBs with initial separations randomly distributed between 3 and 5% R$_H$ and the system mass of 2001 QW$_{322}$. Their initial conditions, aside from their separations, are drawn directly from the known sample of tight Kuiper Belt binaries. The initial inclination and eccentricity distributions are drawn from this, while argument of periapsis, longitude of ascending node, and mean anomaly are randomized. These binaries are allowed to evolve over 4 billion years of gravitational perturbations from the Kuiper Belt, potentially forming a population of Ultra-Wide TNBs with separations in excess of 7% R$_H$. But just as perturbations cause binaries to widen, they may also cause them to become disassociated. Thus, we measure the fraction of this emerging population at any given time in a Kuiper Belt of advanced age, this being every 20 million years between 3 and 4 billion years into the simulation.

In fact, as predicted, accounting for the greater number of encounters increases the size of the Ultra-Wide population that we generate. In our prior monochronic simulations, the fraction of Ultra-Wide TNBs in any remaining binary sample was less than 2%. With our current diachronic regime, we consistently produce an Ultra-Wide fraction in excess of 5%. Our widened separation distributions are shown in Figure 18.

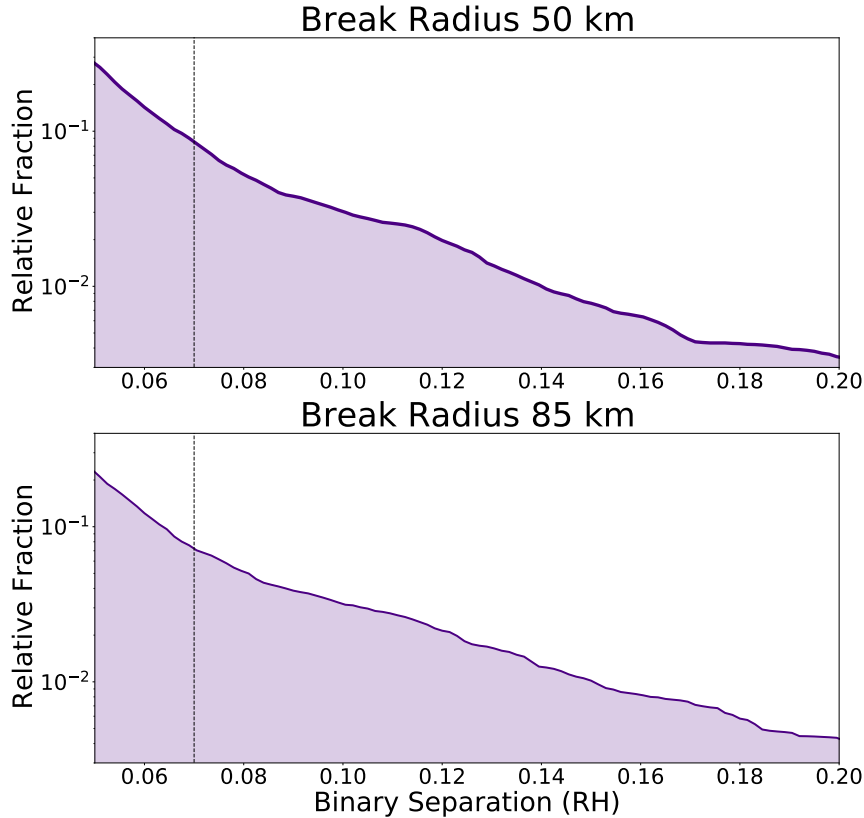With either KKB break radius, 8% of the surviving binary sample becomes Ultra-

Figure 5.2: A cumulative distribution of the separations of each simulated binary with an initial separation of 3-5% R_H. A line is drawn at 7% Hill radius as this marks where a binary becomes Ultra-Wide. The top panel represents a KKB SFD defined by a break radius of 50 km, and the bottom panel represents this SFD defined with a break radius of 85 km.

Wide and this fraction is maintained over the last 3 billion years of the Kuiper Belt's history. This is far in excess of the 5% Ultra-Wide binary fraction observed in the present Kuiper Belt. As stated in the prior section, many Ultra-Wide TNBs are quite unstable over time. Even the relatively tight 2006 JZ_{81} will retain its wide separation without disassociating only 25% of the time. If these binaries are not primordial, then they require a later and perhaps continuous source of formation, and widening via gravitational perturbation is a viable mechanism behind this.

An additional population we test for now is binaries that have not only become Ultra-Wide but have reached a separation comparable to 2001 QW$_{322}$. This binary, being the widest known, is quite extreme compared even to the other Ultra-Wide TNBs. Despite this, of the 9 known Ultra-Wide binaries, one of them is 2001 QW$_{322}$. Thus, of the fraction of wide binaries that our binary-widening simulations form and maintain, we should see a roughly similar fraction of 2001 QW322-like binaries (even if the known sample is one) if our binary widening mechanism is a viable explanation for UWBs. We define this population as having a separation of at least 80% that of 2001 QW$_{322}$ or 0.18 R$_H$. We produce a 2001 QW$_{322}$ to Ultra-Wide fraction of approximately 5.4% in both of our Kuiper Belt SFDs. This is lower than the observed fraction of 11%. This separation distribution is plotted in panel (a) of Figure 19.

When looked at as a whole, however, the separation distribution of our widened population does not disagree with the observed sample. A K-S test examining the probability that the nine known Ultra-Wide TNBs can be sampled from our widened population gives a p-value of 8.8% and 9.1% assuming an SFD break radius of 50 and 85 km, respectively. This implies potential agreement; the separation distribution that we observe in the Kuiper Belt can be the result of binary widening via gravitational perturbations, assuming an initial separation of between 3 and 5% R$_H$.

Continuing from the last chapter, the eccentricities of widened binaries continue to be very consistent with the known sample. The increased number of encounters that occur does not disrupt this distribution. Despite the increased number of encounters, the widened eccentricity distribution does not become thermalized as it might otherwise be expected to assume (see Section 1.5.3) (Jeans, 1919). This distribution, plotted in panel (b) of Figure 19, additionally still holds across a wide range of separations from 3% to past 7% R$_H$. Its consistency, even when employing more encounters, suggests that the observed distribution occurs quite naturally, without requiring excessive fine
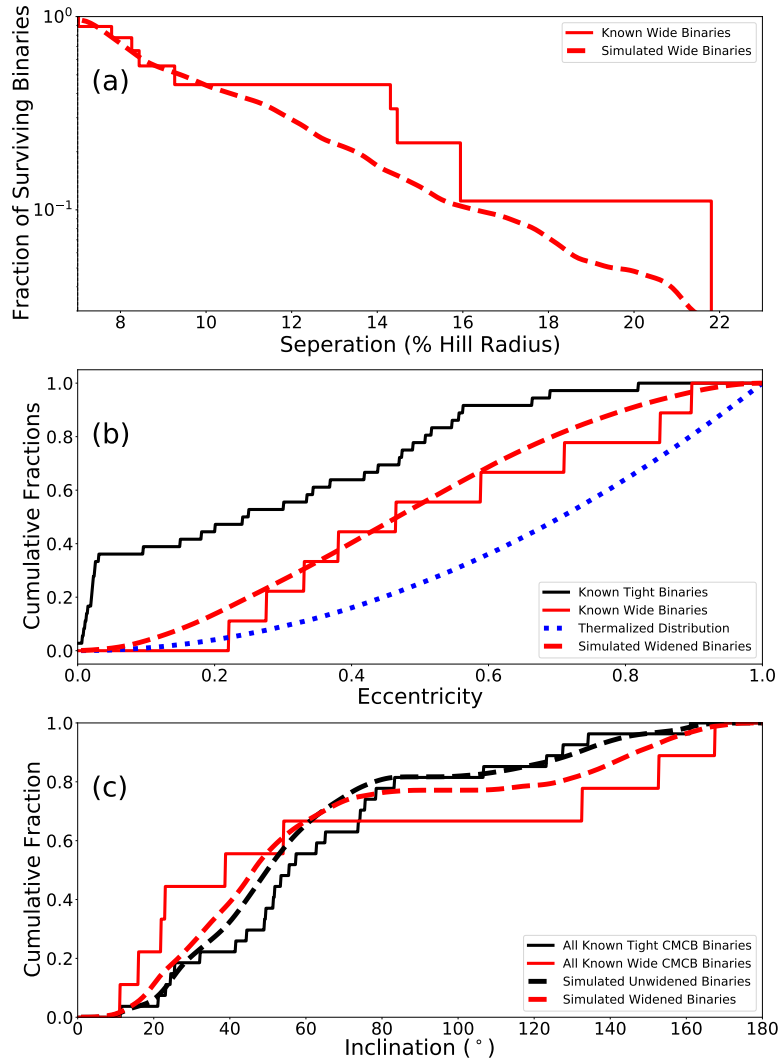
Figure 5.3: Panel a plots the cumulative distribution of the separations of our widened binaries compared to the known sample of Ultra-Wide TNBs. Panel b plots the eccentricity distribution of widened binaries compared to the known sample of tight, Ultra-Wide, and a thermalized distribution. Panel c plots inclination distribution. The dotted lines represent our simulated binaries, black and red representing tight and widened binaries respectively. The solid line represents known binaries, with black and red meaning non-Ultra-Wide and Ultra-Wide, respectively.

tuning of Kuiper Belt conditions. A thermal distribution indeed seems to be rather unnatural for eccentricities in an environment like this. A possible explanation may come back to the Kozai mechanism, wherein a large eccentricity may oscillate with inclination.

Inclination seems to also follow a similar trend to that seen in the previous chapter. Widened orbits tend to become more planar, but not nearly to the same extent as the known wide binary sample. Retrograde orbits, though, do not become more preferred than prograde orbits, and the general shape of this distribution does not change substantially. The only small difference that occurs is that the tight binary sample seems to evolve closer to a planar distribution that it had previously. Our widened and unwidened distributions are plotted in panel (c) of Figure 19. K-S tests give p-values of 0.18 and 0.34 for rejecting the observed Ultra-Wide TNB distribution being sampled from our unwidened and widened binaries, respectively. That binary inclinations become more planar is due to Kozai oscillations. This causes such tight orbits to become more eccentric, making them either more susceptible to the larger number of interactions that occur under the new regime or more likely for the two binary components to collide.

The fact that this distribution does not yield K-S p-values substantially higher than in the monochronic model implies that the number of encounters does not affect the final inclinations. It's possible that gravitationally perturbative encounters simply do not change the binary inclination distribution even as they widen their orbits. It seems doubtful that a decrease in albedo or an increase in the number of encounters will change this. It may be necessary for another process we haven't accounted for to occur.

Thus, we are unable to quite replicate the apparent distinction of Ultra-Wide TNB inclinations. But like in the previous chapter, a p-value of 0.34 cannot rule out the

possibility that the known Ultra-Wide TNB inclination distribution is drawn from our gravitationally evolved Ultra-Wide TNBs. And, as mentioned in Section 4.3, the possibility that the nine known Ultra-Wide inclinations are merely sampled from the known tight inclinations cannot be ruled out. Therefore, it cannot be said with certainty that such an inclination distinction exists, despite the apparently planar appearance of the wide binary distribution. However, if the distinction proves to be real, gravitational perturbation driven widening is not able to replicate it.

Thus far, the binaries widened through gravitational encounters do have orbital elements consistent with the known sample. The wide eccentricity distinction can be reproduced through perturbation, though the inclination distinction cannot. But this still leaves out the effects of impacts. While comparing the lifetimes of specific wide binaries with Nesvorný et al. (2021) indicates that impacts may not be as substantial in influencing binary evolution, they may still leave their mark on these orbital elements.

One noteworthy caveat here is that among tighter binaries, the outward migration of mutual separation is still present but is smaller. Starting with an initial sample of binaries at 2-3% R_H starting separations, less than 2% become Ultra-Wide after 4 billion years. Their final mutual orbital properties match those of their initially wider counterparts, but this final population size is much less than the known fraction of 5%. Though greater population sizes of Ultra-Wide binaries can be formed from initially 3-5% R_H separated origins, they do not seem to be the most common variety. As noted in the prior section concerning a monochronic Kuiper Belt, only 15 of the resolved 45 TNBs have separations greater than 3% (Grundy et al., 2019).

What can be concluded here then is that if Ultra-Wide TNBs aren't primordial as Section 5.1 proposes, and are instead evolved initially tight binaries, then the binary population of the primordial Kuiper Belt must have been different than today. Though it is possible for there to have been an incredibly high binary fraction in the

early Kuiper Belt (Nesvorný et al., 2010; Fraser et al., 2017; Nesvorny et al., 2019), a large fine tuned population of binaries with greater separation than 3% R_H would be required to reproduce the observed binary fraction. Additionally, though the fraction of Ultra-Wide TNBs we produce is quite high, the fraction of binaries that become as wide as 2001 QW_{322} is consistently lower than observed. This may be explained as observational bias, as wider binaries are easier to spot and catalog than tighter ones. Had we done this analysis in the same year as Parker & Kavelaars (2011), 2001 QW_{322} would be one of six known Ultra-Wide TNBs as opposed to one of nine today. Even nine known binaries is still a small sample size with which to draw conclusions about an optimal separation distribution. Nonetheless, unless the presence of 2001 QW_{322} is an anomaly, there may be more physical processes our simulation does not capture.

However, in terms of the Ultra-Wide TNB population generated, the Kuiper Belt models employing a 50 km break radius seem to be more efficient, like in the previous chapter. The break radius used does not have any significant effect on the final eccentricity or inclination distributions of this widened population. Thus, to best explain the ratio of Ultra-Wide TNBs to tighter TNBs favored by observations, assuming the primordial Kuiper Belt did not have a 3-5% R_H of 100%, a break radius of 50km is a more likely SFD parameter than 85 km.

5.3 Sensitivity of Albedo

As we had observed in the previous chapter, the evolution of these binaries is greatly dependent on the assumed albedo of the Kuiper Belt. Lower albedo implies that the bodies we see are larger and more massive, meaning stronger gravitational effects for flybys. For all other diachronic evolution simulations described to this point, we use an assumed KKB albedo of 0.04 (Lawler et al., 2018), but there is some uncertainty in this value (see Section 1.4). Here, we repeat the simulation setup as in the previous section, with an initial population of binaries with separations between 3 and 5% R_H, but instead of a consistent KKB albedo, we vary it to a wide range of plausible and implausible albedos. Thus, we determine the fraction of widened binaries like before as a function of KKB albedo.

In the previous chapter, to test different possible Kuiper belt parameters, we had carried the albedo of the CCB. In a monochronic un-evolving Kuiper Belt, the CCB due to its high encounter rate and low velocity, plays more of a role in the evolution of our binaries. But in this diachronic evolving model, the KKB plays a much larger role due to its far greater encounter rate. While the CCB (now the CKB, see Section 1.3) is still a significant contribution to binary evolution, the KKB now dominates, and thus to test the relation between albedo and the properties of widened binaries, we vary the KKB albedo.

This function of wide binary abundance is plotted in Figure 20. While we had initially hypothesized that higher albedo Kuiper Belt models might be much better at preserving wide binaries, enabling a greater abundance, this did not turn out to be the case. Wide binary production is the dominant factor in determining the fraction of Ultra-Wide TNBs among unwidened ones, and this is inversely related to albedo. In log-linear space, there seems to be a linear relation between the two; these linear fits are plotted as well. It should be noted that despite its apparent importance in our

monochronic Kuiper Belt simulations, the albedo of the CKB no longer significantly affects the evolution of these binaries as KKB encounters now dominate.
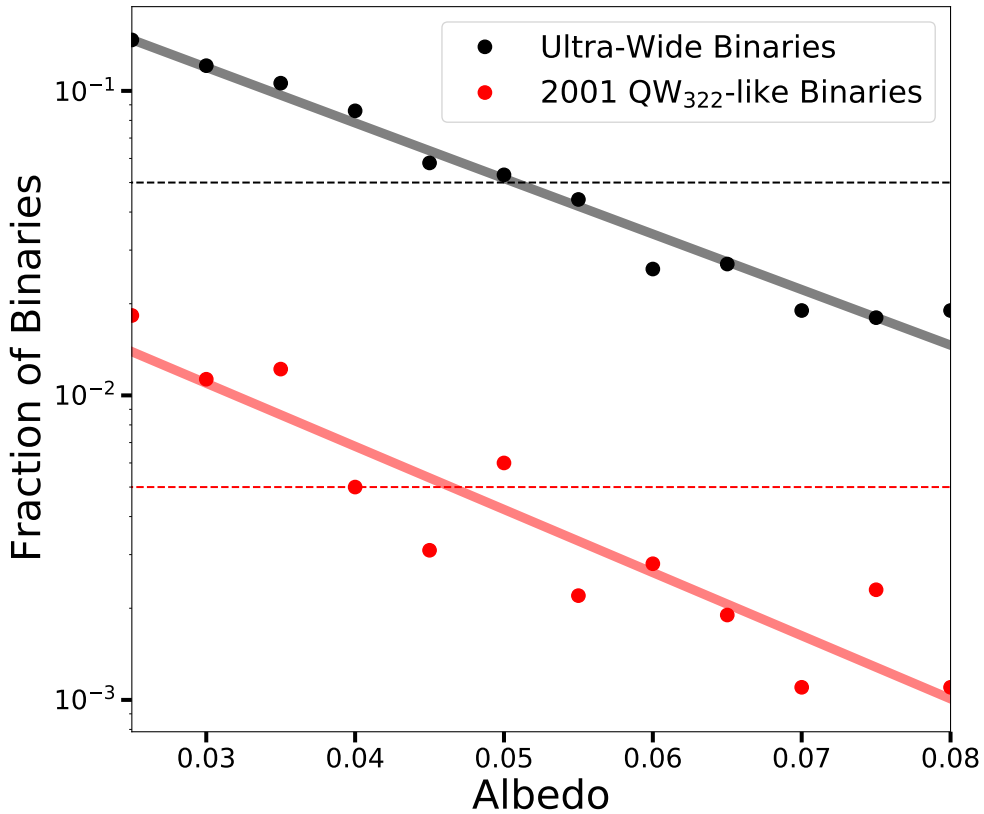

Figure 5.4: Fraction of surviving binaries that are Ultra-Wide as a function of KKB albedo. Black points are the fractions of binaries at any given time that are beyond 7% R_H (Ultra-Wide) with the black line representing an exponential fit. Red points are the fractions of binaries at any given time that are beyond 18% R_H (80% of 2001 QW_{322}) with the red line representing an exponential fit. The black and red dotted lines represent the predicted fraction of Ultra-Wide binaries and 2001 QW_{322}-like binaries respectively (Lin et al., 2010).

The great sensitivity to albedo indicates that base assumptions made by any future studies about the albedo of the Kuiper Belt will play a substantial role in any conclusions they reach. Assuming a KKB albedo of 0.05 rather than 0.04 will equate to a 30% lower wide binary fraction and a 50% drop in the number of 2001 QW_{322}-like

binaries. This mirrors the results of our monochronic Kuiper Belt models, which show the sensitivity of binary widening and disassociation to the CCB albedo. With such immense dependence on a parameter that is not known for certain, it is hard to draw definitive conclusions about the state of the primordial Kuiper Belt or how efficient gravitational perturbations are at widening binaries. Assuming an initial binary fraction near 100% and an initial population of binaries with average separations of 3-5% R_H, then the albedo of the KKB must be approximately 0.05 or less to produce wide binary fractions consistent with observations assuming our SFD.

A binary fraction of this nature being 100% is very unlikely, indicating that albedo may be lower than 0.05. An albedo of 0.04 would lead to a required initial 3-5% R_H binary fraction of 63%. What we can conclude is that either the albedo of the KKB is lower even than 0.04, the initial 3-5% R_H must have been comparable to 63%, or that there may be more forces at play in widening binaries. In neither this chapter nor the previous one have we accounted for the likely significant effect of impacts in our simulations. While its effect on Ultra-Wide binary stability is almost certainly to lower it, it's possible that such a process may lead to wide binaries decaying faster than they can form. The next chapter discusses our results assuming not just a gravitationally interactive Kuiper Belt, but a collisionally active one as well.

Chapter 6

A Collisionally Active Kuiper Belt

In this chapter, we finally incorporate a collisionally interactive Kuiper Belt in addition to a gravitationally interactive one. Much like the previous chapter, this modeled Kuiper Belt is also evolving with time, with the number of encounters and their relative velocities varying over time, though we now include the possibility of collisions from the larger Kuiper Belt. The SFDs we employ for our two evolving Kuiper Belt populations remain the same as in the prior chapter, described in far greater detail in Section 2.2. In this chapter, the most accurate and predictive models of binary evolution can be employed, and collisions and gravitational perturbations can be directly compared.

6.1 Survivability

In the previous two chapters, we determine the likelihood that particular Ultra-Wide TNBs survive into the present day Solar System, assuming that they had formed in the primordial Kuiper Belt. These binaries are again 2001 QW_{322}, 2000 CF_{105}, and 2006

JZ_{81} for being representative of the diversity of wide binaries, as well as 2001 QW_{322} and 2000 CF_{105} having been examined by prior studies. 2001 QW_{322} in particular is the widest known of Kuiper Belt binaries, and 2000 CF_{105} has been shown to be the least stable under collisional perturbations (Parker & Kavelaars, 2011).

Much like in the previous chapter, the decay rates of these binaries do not fit well into an exponential decay curve as they do in Chapter 4. Because of the rapidly changing number of encounters across time, the decay rate does not fit well into any curve in particular, so we evaluate these binary's stability by determining what fraction survives by the end of the 4 billion year simulation time. 2001 QW_{322} in particular now survives between 2.5 and 3.5% of the time, assuming a KKB break radius of 50 and 85 km respectively, but collisions throw in one further complication. Just as the addition of an evolving Kuiper Belt decreased the stability of the known Ultra-Wide TNBs, the inclusion of collisions decreases it even further. This was not particularly surprising, but the extent of the reduced stability now means that of our very wide Ultra-Wide TNBs, 2001 QW_{322} and 2000 CF_{105}, less than 4% survive with either KKB break radius.

A new noteworthy quality to our simulated collisions is defined by Petit & Mousis (2004) regarding the required impact energy to completely unbind a binary. Assuming an impact speed of 1.5 km/s, the minimum size of an impactor required to disassociate 2001 QW_{322} is 9.5 km, and our impact velocities are often higher (see Section 2.7). 2000 CF_{105} only requires a 5.7 km radius impactor to be disassociated due to its mass being roughly one tenth that of 2001 QW_{322} (Grundy et al., 2019), though a collision like this with 2000 CF_{105} would occur less often than it would with 2001 QW_{322} due to the former's smaller radius.

By factoring collisions into our simulations, 2000 CF_{105} now only survives approximately 2% of the time, regardless of the assumed break radii. This implies that for

TNO Binary	CCB Albedo	$R_b = 50$ km	$R_b = 85$ km
2001 QW$_{322}$	Surviving	0.025	0.035
	Wide	0.008	0.010
2000 CF$_{105}$	Surviving	0.018	0.023
	Wide	0.006	0.007
2006 JZ$_{81}$	Surviving	0.164	0.181
	Wide	0.107	0.123

Table 6.1: Fraction of binaries that remain undisassociated (Surviving) and fraction of those that have not decreased in separation by more than 20% of their original mutual orbits. Each system is given the initial conditions of a specific Ultra-Wide TNB.

every modern Kuiper Belt binary that had initially been as wide and massive as 2000 CF$_{105}$, there must have been 50 in the primordial Kuiper Belt. With the addition of collisions, it seems that system mass becomes a more influential component of a binary's stability. 2000 CF$_{105}$ and 2001 QW$_{322}$ have comparable stability in the previous chapter, which assumes only gravitational perturbations; now 2000 CF$_{105}$ is 50% more likely to become disassociated before the modern day than 2001 QW$_{322}$. These results and those of our third binary, 2006 JZ$_{81}$ are shown in Table 8.

But, as stated in the previous two chapters, binaries that shrink rather than widen are overrepresented in our surviving sample. Introducing the criterion that a binary must not have decreased in separation by more than 20% gives a very similar result as before, as shown in Figure 21. With this criterion added, only 1% of all initially 2001 QW$_{322}$-like binaries survive while still remaining nearly as wide as they once were. But more significantly, nearly all surviving 2000 CF$_{105}$-like binaries have reduced in separation considerably. Of every system that starts with the orbital parameters of that binary, a little more than half a percent remains intact and of comparable separation. To account for a single primordial 2000 CF$_{105}$-like system to persist into the present day at comparable separation, there must have been between 140 and 170 in the early Solar System. The survival rate of our three binaries is also shown in Table 8.

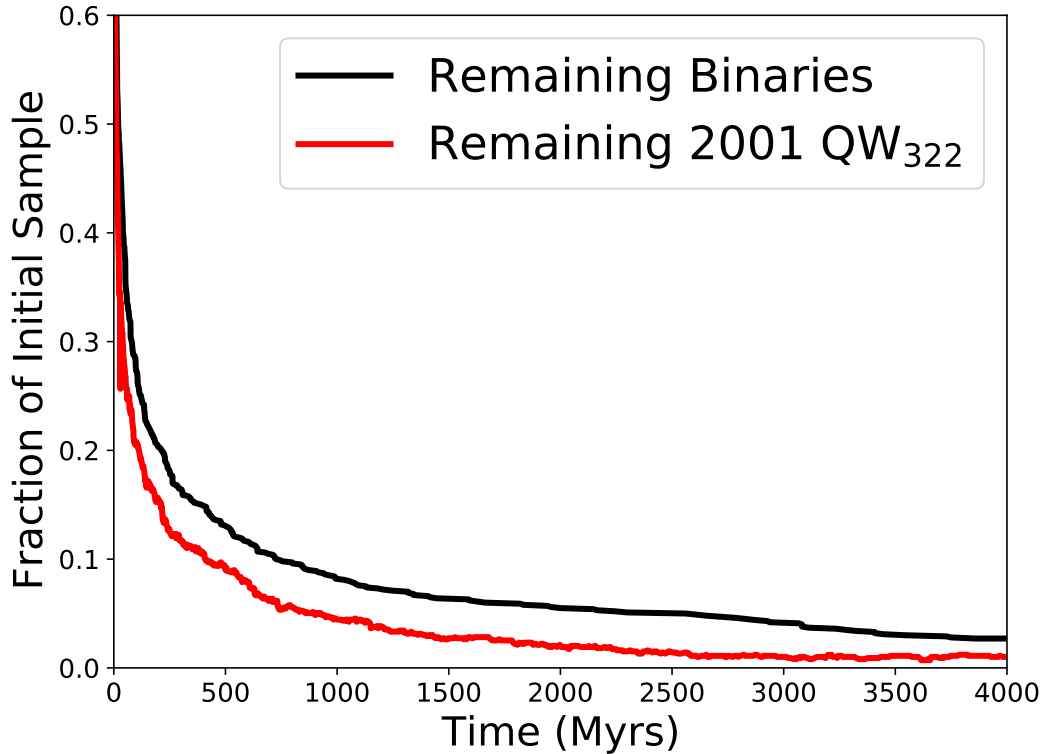What can be concluded here is that the binaries 2001 QW$_{322}$ and especially 2000

Figure 6.1: The decay of initially 2001-QW$_{322}$-like binaries over the lifetime of the Kuiper Belt. The black line depicts the fraction of binaries that have not been disassociated, while the red line depicts this as well as all surviving binaries that have not migrated inward by more than 20% of their initial separation.

CF$_{105}$ are very unlikely to be primordial. Though they can form efficiently in the early Kuiper Belt (Nesvorný et al., 2010), their destruction in the intervening years is highly likely. If they are primordial, then they represent a very small surviving component of a much larger Ultra-Wide binary population. This directly conflicts with the results of Parker & Kavelaars (2011) and especially Nesvorný et al. (2021) which indicate that these binaries are generally stable, even in an evolving Kuiper Belt.

By including collisions in our simulations, the initial mass of the binary also becomes a more significant factor in its stability. While 2001 QW$_{322}$ now remains both intact and comparably wide about half as often as in simulations without collisions, the

likelihood of 2000 CF$_{105}$ doing the same has dropped almost threefold. 2000 CF$_{105}$, having only about one tenth the mass of the other, has a lower stability despite its smaller collision cross section. This result agrees with the conclusion reached by Parker & Kavelaars (2011), that 2000 CF$_{105}$ was the least stable of the known Ultra-Wide TNBs, a result we had not observed in the prior two chapters that did not feature collisions.

6.2 Binary Widening

Like in the previous chapters, we test the hypothesis that the Ultra-Wide TNB sample can be produced by widening an initially tight binary sample. We again start with a sample of less-than-Ultra-Wide binaries with initial separations distributed randomly between 3-5% R_H. As shown in the previous section, a binary that becomes wide may remain so for a time but may disassociate eventually. Thus, even in a stable widened population, any one Ultra-Wide binary may be fleeting. To account for this, we sample our surviving simulated binaries every 20 Myrs between 3 and 4 Gyrs into our simulation. The fraction of Ultra-Wide TNBs among all other binaries is recorded.

As expected, the inclusion of collisions only accelerates the rate at which binaries increase their separation. Without collisions, we know, assuming every initial TNO binary has an initial 3-5% R_H separation, that between 9.4 and 8.6% of observed binaries will be Ultra-Wide at any given time, as seen in the previous chapter. This shows that gradual widening is a viable pathway towards forming the present day observed population, as the expected Ultra-Wide TNB fraction is only 5% (Lin et al., 2010; Parker et al., 2011), .

In testing, it is clear that collisions tend to raise the number of initially tight binaries that are disassociated before 4 billion years have passed. But against our expectations, the maintained population of Ultra-Wide TNBs in our simulations at any given time has only increased. With collisions, a population greater than 10% can be widened and maintained using either KKB break radius. These separation distributions are shown in Figure 22, and the exact fraction of binaries that these populations take up is shown in Table 9. This larger generated population indicates that collisions ensure that this process is more efficient, not less. A fraction so much higher than the 5% observed today may be an indication that the primordial binary population was not entirely composed of systems separated by 3-5% R_H, but perhaps by binaries of smaller

separations.

Such tighter binaries do not widen to nearly the same degree. Among binaries with initial separations of 2-3% R_H, the emerging fraction of wide binaries does not exceed 2.5% with either KKB break radius. Among binaries with starting separations of 1-2% R_H, the fraction does not exceed 1%. Binaries starting with 3-5% R_H separations are capable of widening to form Ultra-Wide fractions greater than 5% but tighter ones do not seem to.
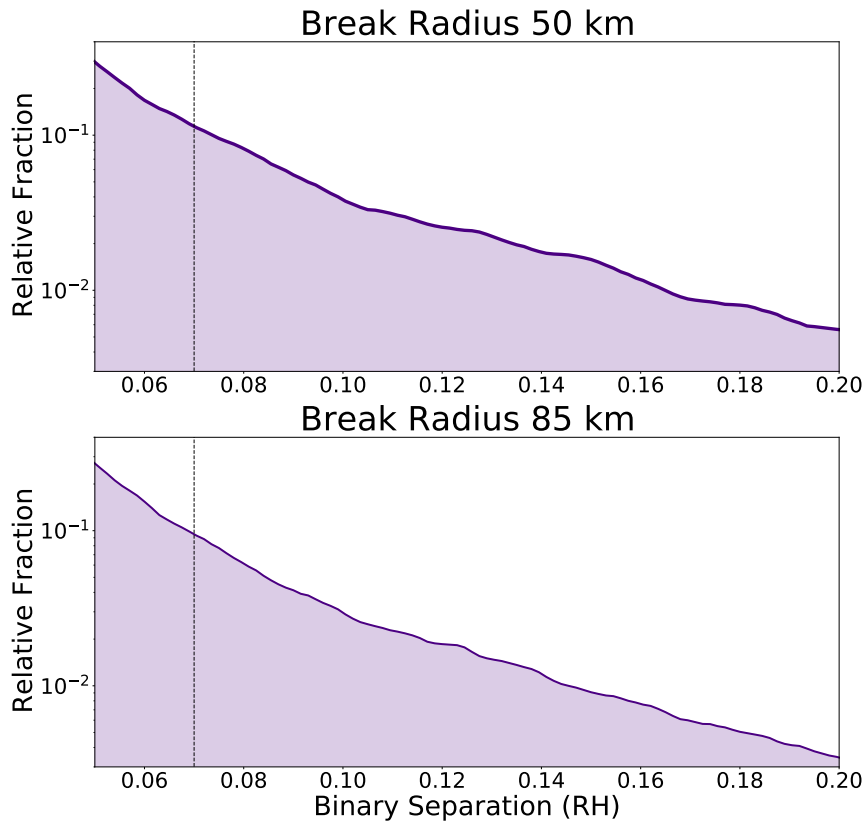

Figure 6.2: A cumulative distribution of the separations of each simulated binary with an initial separation of 3-5% R_H. A line is drawn at 7% Hill radius, as this marks where a binary becomes Ultra-Wide. The top panel represents a KKB SFD defined by a break radius of 50 km, and the bottom panel represents this SFD defined with a break radius of 85 km.

Like the last chapter, we also wish to see the quantity of widened binaries that achieve the extreme separation of 2001 QW_{322}. At 22.2% R_H separation, 2001 QW_{322} is the only binary nearly as separated as this among the 9 known Ultra-Wide TNBs, with 2000 CF_{105} being the runner up at 16.5% R_H. Even with a sample size of 1, we still should see a similar fraction of 2001 QW_{322} among our widened Ultra-Wide sample. The fraction we find in our simulations is 7.1% and 6.4% for KKB break radii of 50 and 85 km respectively, against an observed fraction of 11% or 1 in 9. The fraction of 2001 QW_{322}-like binaries amongst the entire surviving binary sample is also shown in Table 9, while the overall widened separation distribution is plotted in panel (a) of Figure 23.

One other apparent result of these simulations is the large number of binaries that become disassociated at even these small initial separations. For a break radius of 50 and 85 km, we see that 30% and 20%, respectively, of initial binaries do not survive intact by the end of the simulation. Assuming each lost binary then produces two isolated bodies (termed singles), then for every Ultra-Wide TNB, we would expect to see 6 and 4 singles for each break radius, respectively.

As explained in Section 1.5, this blue singles population (Fraser et al., 2021) makes up a mere 2% of CCB bodies with known color. If a large population of blue binaries of 3-5% R_H are implanted into the CCB and are then subject to the widening effects of passing bodies, a large reservoir of blue singlets would be expected; especially if the formation of a single Ultra-Wide TNB implies the formation of 4-6 blue singles. Blue bodies, however, have lower albedos than the red bodies more typical of the CCB (Lacerda et al., 2014; Farkas-Takács et al., 2020). Thus, there is an observational bias toward detecting red bodies. Binaries are also inherently easier to detect, so a blue Ultra-Wide TNB binary like 2001 QW_{322} (Fraser et al., 2017) is more likely to be found than the many more produced blue singles that formed as well. However,

CCB Albedo	$R_b = 50$ km	$R_b = 85$ km
Ultra-Wide	0.112	0.101
2001 QW$_{322}$-like	0.0080	0.0065

Table 6.2: Fraction of initial tight ($3\% <$ R $< 5\%$ R$_{\text{H}}$) TNBs that are ultra-wide (R > 0.07 R$_{\text{H}}$) or resemble 2001 QW$_{322}$ (R > 0.18 R$_{\text{H}}$) at any given time.

if a blue binary like 2001 QW$_{322}$ is primordial, and is one of only 2.5-3.5% of similar binaries that survive intact into the modern Solar System, then for every such 2001 QW$_{322}$-like binary, we would expect to see between 60 and 80 blue singles.

Collisions do not seem to significantly change the orbital elements of binaries that they help widen. The eccentricity distribution, plotted in panel (b) of Figure 23, seems to be almost identical to that of the purely gravitationally interactive Kuiper Belt model used in the last chapter. This distribution is again assumed even by bodies that are less than Ultra-Wide in separation, as is consistent with observations of binaries wider than 1% R$_{\text{H}}$. The continued stability across collisionally inactive and collisionally active models implies that any pressures on the eccentricity of widened binaries that collisions provide are not sufficient to overcome the pressures applied by Kozai Oscillations.

The widened inclination distribution seems to tell the same story as in the prior chapters as well. This distribution does seem to become more planar in a similar way to that observed in the purely gravitationally interactive Kuiper Belt model. Widened Ultra-Wide TNBs seem to be more planar than ones that have not widened, but this result does not compare to the stark difference observed between the two. Neither is the widened population more biased towards retrograde orbits than the unwidened one. Ultimately, collisions seem to have had little effect on this distribution, as it looks nearly identical to that of the prior chapter. A K-S test again cannot rule out the observed distribution coming from a collisionally and gravitationally widened population, but the distinction we produce between tight and Ultra-Wide TNBs is not
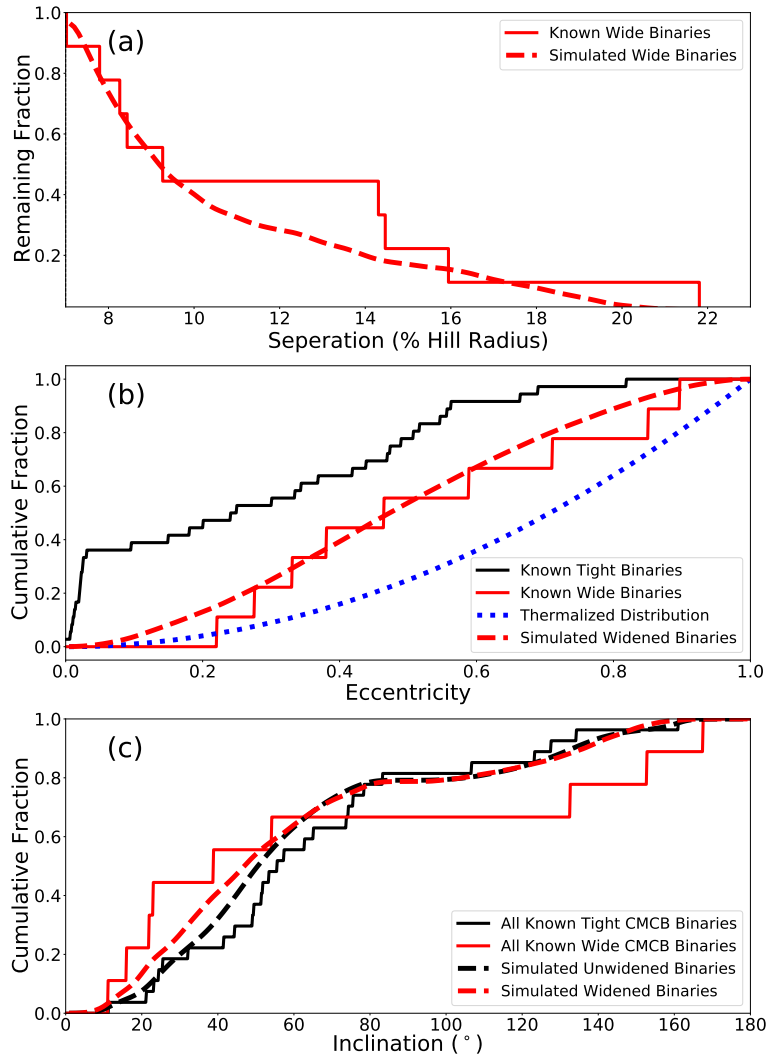
Figure 6.3: Panel a plots the cumulative distribution of the separations of our widened binaries compared to the known sample of Ultra-Wide TNBs. Panel b plots the eccentricity distribution of widened binaries compared to the known sample of tight, Ultra-Wide, and a thermalized distribution. Panel c plots the inclination distribution. The dotted lines represent our simulated binaries, black and red representing tight and widened binaries, respectively. The solid line represents known binaries, with black and red meaning non-Ultra-Wide and Ultra-Wide respectively.

as strong as that observed. The p-values of such tests are 0.21 and 0.33 for rejecting the observed Ultra-Wide TNB distribution being sampled from our unwidened and widened binaries, respectively. The widened and unwidened distributions are plotted in panel (c) of Figure 23.

What can be concluded here is that the presently observed Ultra-Wide TNBs do not have to be primordial. Their rapid disassociation rate discussed in the previous section is not necessarily in conflict with their present day existence. A population of initially tight binaries can be widened gradually through a combination of many gravitational perturbations and collisions with passing KBOs. Within a range of initial binary fractions and separations, this population of emerging Ultra-Wide TNBs can be as large as we now observe. In addition to this, the distinct mutual orbital properties of the known Ultra-Wide TNBs can be reproduced via a combination of these interactions and the Kozai mechanism.

If Ultra-Wide TNBs are primarily formed from an initial binary population via these mechanisms, a number of conclusions can be drawn about the conditions of the primordial Kuiper Belt. This widening is most effective on binaries that are already fairly wide, such as those between 3 and 5% R_H. But as stated in Chapter 4, only 15 of the 45 resolved TNBs have separations greater than 3%. And due to more widely separated systems being easier to detect, it's unlikely that additional discoveries of new binaries will increase this fraction. Thus, the mutual separation distribution of the primordial Kuiper Belt must have been different than it is today. Additionally, we would expect a very high binary fraction in the primordial Kuiper Belt. Though this is a plausible assumption (Nesvorný et al., 2010; Fraser et al., 2017; Nesvorny et al., 2019), it is very different from what we currently observe.

Initial binary orbital elements, on the other hand, do not need to be any different than what we currently observe in tight binaries. An initial sample with an inclination

distribution resembling that of modern tight binaries can reproduce the inclinations that we see among Ultra-Wide TNBs. The initial eccentricity distribution so reliably evolves into what we observe among Ultra-Wide TNBs that no fine tuning is necessary.

6.3 Collisions vs. Gravitational Perturbations

With the inclusion of collisions into our simulations, we are now able to directly compare the two perturbation mechanisms and see which one is more significant in terms of driving binary evolution. In terms of binary disruption, gravitational perturbations are definitively more influential. Though we had been initially doubtful about reproducing the results of Nesvorný et al. (2021), it would seem that binaries like 2001 QW_{322} are indeed fairly stable even in an evolving Kuiper Belt. This stability may not quite extend out to 50% R_H as suggested in their study, but their general result that 2001 QW_{322} is likely to survive into the modern Kuiper Belt under a purely collisional regime seems correct. A comparison of 2001 QW_{322}'s disassociation rate under gravitational perturbations and collisions is shown in Figure 24.
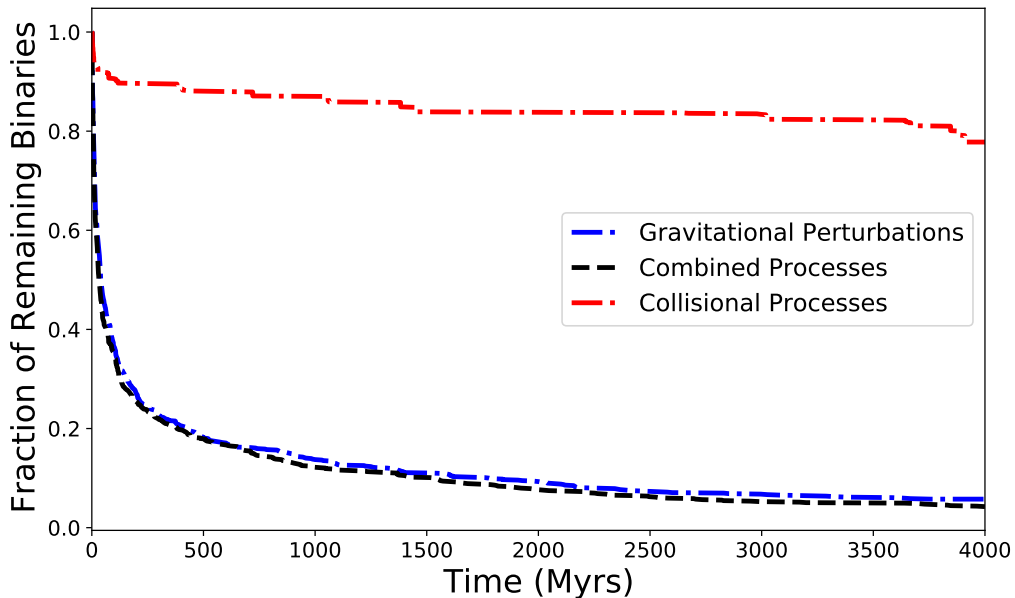

Figure 6.4: Loss rate of 2001 QW_{322} under the influence of gravitational perturbative encounters, collisional encounters, and both, assuming a KKB Break Radius of 85 km.

However, the stability of a binary system under the influence of collisions seems to

be very dependent on the mass of the system, perhaps even more so than its separation in Hill radii. 2000 CF$_{105}$ is less stable in a collisionally active Kuiper Belt than the far more widely separated 2001 QW$_{322}$. This may be due to the much smaller required radius of an impactor to completely disassociate the binary in a single strike. Most of our simulations include a body of at least 5.7 km, and as discussed in Section 6.1, regardless of any previous unbinding, an impact of this scale at 1.5 km/s is certain to break it. 2000 CF$_{105}$'s decay rate in a collisionally and gravitationally active Kuiper Belt is graphed in Figure 25.
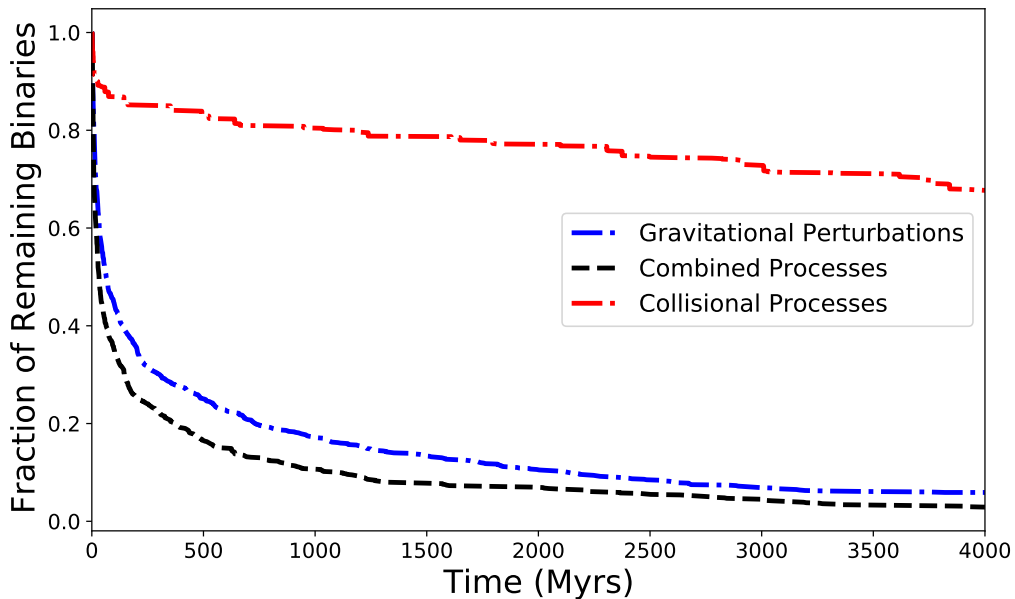

Figure 6.5: Loss rate of 2001 QW$_{322}$ under the influence of gravitational perturbative encounters, collisional encounters, and both, assuming a KKB Break Radius of 85 km.

While lower mass binaries like 2000 CF$_{105}$ have lower collisional stability than 2001 QW$_{322}$ regardless of Hill radii separation, it is clear that collisions are not as effective a destroyer of binaries as gravitational perturbation.

In terms of binary widening, it seems clear that gravitational perturbations are more efficient at forming Ultra-Wide TNBs. Pure gravitational interactions produce

more than twice as many wide binaries compared to purely impact-based interactions. The disparity is noticeable, though not nearly to the same extent as observed in higher mass binary disassociation timescales.

However, this disparity in wide binary production lessens significantly and potentially reverses for widened separations greater than 15% R_H. For binaries of separations comparable to 2001 QW_{322}, impact-only interactions are more efficient. Gravitational perturbative interactions are capable of producing a population of wide binaries that agrees with observations but are consistently unable to produce sufficient amounts of 2001 QW_{322}-like binaries. The inclusion of both effects not only increases the number of Ultra-Wide TNBs but even maintains a larger population of binaries wider than 15% R_H. The populations of wide binaries produced with each interaction type are shown in Figure 26.

In the context of the earlier results in binary disassociation, it may be that collisions are less able to produce wide binaries but may be less able to disassociate them as well, allowing for the maintenance of a wide population. It would appear that in forming a population of newly widened Ultra-Wide TNBs, both processes play a significant role and largely complement each other, though gravitational perturbations still rank as the more significant contribution in terms of the Ultra-Wide binary fraction.

This may be due to the separation dependent nature of gravitational perturbations. An impact imparts a specific impulse onto the struck binary component, regardless of its separation from the other. A gravitational perturbation, however, imparts an impulse to both binary components. The net effect on the binary system is the difference between these two impulses, which is dependent on the separation of the two components. Thus, in effect, binaries that are already fairly separated will decay faster and faster. Therefore, gravitational evolution, which seems comparable to that of impact for tight binaries, may be far stronger in comparison for large ones. And while

impacts may not be as efficient at producing 2001 QW$_{322}$ like binaries, they are far better at preserving them, leading to a large generated population of extremely widely separated binaries.

It should be noted, however, that we had not accounted for the possible effect of collisions with sub kilometer radius bodies. Though it is collisions with bodies greater than 1 kilometer that have the most influence and indeed are the most likely to disassociate a binary (Parker & Kavelaars, 2011), their significance cannot be entirely ruled out. Sub-kilometer bodies, if they are to be significant in binary disassociation or widening, will likely bring about their widening gradually, much in the way that smaller gravitational perturbations do. Their influence on the disassociation timescales and final orbital properties of widened binaries, especially eccentricity and inclination, cannot be discounted. But given that larger collisions seem to not greatly modify these properties that arise similarly in purely gravitational perturbative simulations, we do not find this likely. Their influence is also much less likely to influence binary disassociation.

The parameter determined by Parker & Kavelaars (2011) as mentioned in Section 1.5.3 (Equation 2) becomes useful here, where τ_{sim} is the simulated lifetime of a binary under a series of iterative impacts and τ_a is the estimated time between individual collisions large enough to disassociate the binary in a single hit. q here represents the slope of the radii based SFD of the assumed Kuiper Belt model. Their simulations assume a far smaller lower limit on impactor radius of 0.2 km as opposed to our limit of 1 km. A q value of 3 will only yield a ratio of 1.3. Our inclusion of collisional bodies down to 1 km radii likely already accounts for most of this ratio, but even if it had not, this would not greatly decrease the collisional lifetimes of binary systems. Gravitational perturbations would still greatly dominate binary disassociation.

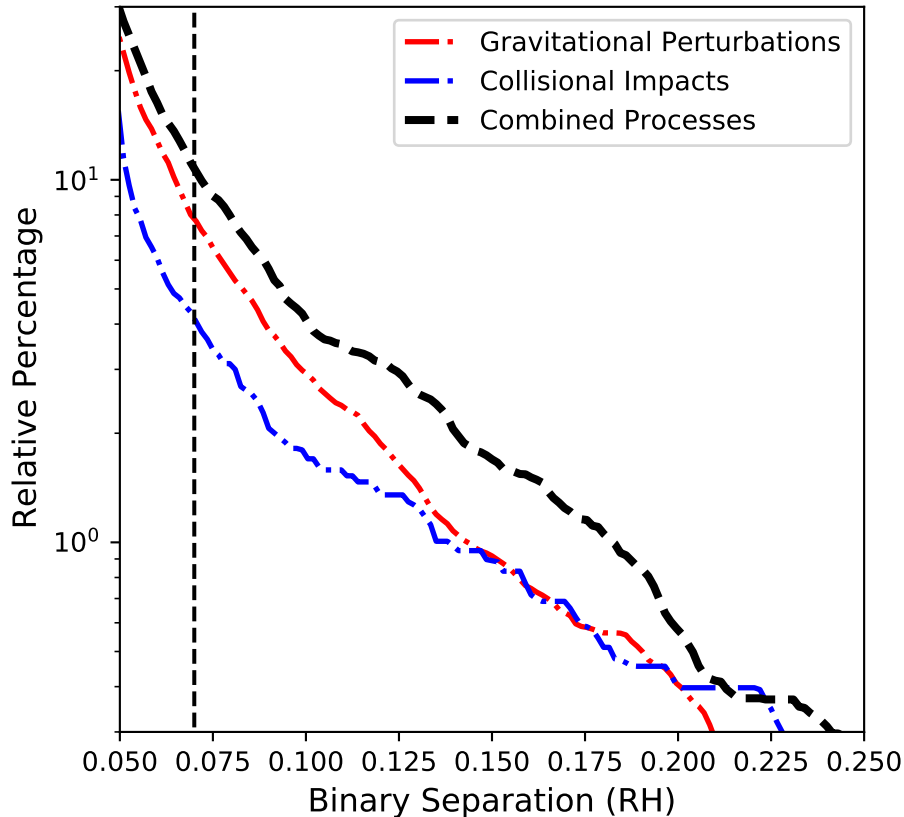It is harder to compare the results here with those of prior studies because of

Figure 6.6: Relative cumulative distribution of binary separations for different simulated Kuiper Belt interactions. The blue dot dash line represents impact only interactions, and the red dot dash line represents gravitation only interactions. The black dashed line represents binaries widened with both. These binaries begin with separations between 3 and 5% R_H becoming ultra-wide over the same timescale with the same encounters.

the different assumptions we make about various aspects of the Kuiper Belt. The first comparison done between the interaction types was conducted by Petit & Mousis (2004) who not only do not account for any gradual evolution a binary might experience over time but also use a very different SFD for the Kuiper Belt. Parker & Kavelaars (2011) similarly uses a different SFD.

The study conducted by Nesvorný et al. (2021) does attempt to determine the approximate lifetimes of Ultra-Wide TNBs in an evolving Kuiper Belt. They, like the

others examined, only allow for collisional interaction between their binaries and the wider Kuiper Belt. They predict binary CCB binary stability up into the staggeringly high separation of 0.5 R_H while we predict that even a binary like 2000 CF_{105} with a separation under 0.18 R_H is unstable. Though their SFD is similar to ours, it has some key differences in not only form but also the exact population size of the Kuiper Belt (Nesvorný & Vokrouhlický, 2016). With nearly an order of magnitude fewer bodies with radii greater than 1 km, this would greatly increase the stability of their simulated binary systems. We believe this is part of why they predict that Kuiper Belt binaries are so stable, though it may also be an anomalously low velocity assumption, as evidenced by a sample velocity given (Nesvorny et al., 2019). Either can be the reason why our results differ so significantly from Nesvorný et al. (2021).

Chapter 7

Conclusions

Over the 3 projects done here, we are able to draw novel results and applications for future research. We have relied on parameters of the Kuiper Belt determined by the army of giants before us whose shoulders we now stand on. As our knowledge about these parameters and properties change, so too will conclusions reached by research in the future. In this last chapter, we discuss our general conclusions and the future avenues that may come from our research.

7.1 Primordial Ultra-Wide TNBs

Based on the results of all three chapters, we do not believe it is likely that the binaries 2001 QW_{322} or 2000 CF_{105} are primordial. If binaries like these are primordial, then the initial population of Ultra-Wide TNBs must have been substantially higher than it is today. For every one 2001 QW_{322}-like binary in the Solar System today, we would expect an initial population of 100-125.

Though these binaries are stable in the modern Kuiper Belt, and likely to stay intact over comparable timescales to the age of the Solar System, the same does not

hold true when accounting for the much higher belt density of the past. Additionally, many initially Ultra-Wide TNBs that do remain intact only do so through evolving to tighter separations. Among our population of initially 2000 CF$_{105}$-like binaries, around 2% remain intact but only 0.7% do so without lessening in separation by more than 20%.

The inclusion of collisions does significantly affect the survival probability of more massive binaries like 2001 QW$_{322}$, reducing its survival likelihood to roughly 50% as without them. But 2000 CF$_{105}$, a binary at one tenth the mass of the former, is more significantly affected; having its survival likelihood reduced to roughly 30% as without collisions. Thus, 2000 CF$_{105}$, despite not being the most widely separated Ultra-Wide TNB in Hill radii, is still the most susceptible to outside perturbations. But with both collisional and gravitational perturbations, the low survival likelihood of both 2001 QW$_{322}$ and 2000 CF$_{105}$ over the history of the Solar System suggests that neither of these binaries formed in the primordial Kuiper Belt.

Prior studies such as that of Parker & Kavelaars (2011) sought to use the continued presence of Ultra-Wide TNBs to constrain the SFD of the Kuiper Belt. Indeed, assuming a Kuiper Belt that only acts through collisions, the Kuiper Belt's SFD can be reasonably constrained (Parker & Kavelaars, 2011; Nesvorný et al., 2021). However, if gravitational perturbations are accounted for, constraining the SFD further cannot justify their present existence of the binaries, because the most significant encounters are drawn from a portion of the SFD already reasonably well known (Lawler et al., 2018; Kavelaars et al., 2021; Petit et al., 2023). Additionally, the presence of these binaries has been one justification for the in situ formation of the CCB as close encounters with Neptune would disrupt Ultra-Wide TNBs (Parker & Kavelaars, 2010). These methods, however, assume that Ultra-Wide TNBs can only be formed in the primordial Kuiper Belt. If such binaries can be formed in the intervening years be-

tween the beginning of the Solar System and now, then their continued presence can be explained without needing to constrain the SFD.

7.2 Forming Ultra-Wide Binaries

On forming Ultra-Wide TBNs, Parker & Kavelaars (2011) had claimed that even as they widen binaries through collisions, they are unable to produce widened binaries with inclination distributions consistent with the known sample. While their conclusions that a simulated binary's inclinations do not change substantially as they widen, we believe this is due to how they analyze their data. As seen in Figure 5, they merge retrograde and prograde orbits and consider inclination only in how much each orbit diverges from planar. This approach works if one views deviation from the plane as the main difference between the two distributions, but if their inclinations are compared as is, then the incompatibility disappears. This is especially true now as the formerly 7 strong wide binary sample has since been expanded to 9, the 2 newcomers all having prograde orbits, shifting the balance considerably. Running a K-S test on the known wide and tight inclination distribution shows that the wide sample being drawn from the tight one cannot be ruled out at $> 95\%$ confidence.

Amongst our initial population of binaries, a 20-30% portion become disassociated before the end of the 4 billion year simulation runtime. This indicates that in addition to blue Ultra-Wide TNBs like 2001 QW_{322}, we would also expect to see a population of blue single bodies. Though the observed blue single population is smaller than would be expected, there are a number of observational biases to explain this (see Section 6.2). Additionally, given the low survival likelihood of a binary like 2001 QW_{322}, had the binary been primordial rather than widened, we should expect a far larger population of blue singles.

However, it is also clear that gravitational perturbations, even with the help of collisional encounters cannot cause widened binaries' orbits to become more planar, nor cause them to become retrograde preferentially. The mutual inclination distribution distinction between our widened and tight binaries is not as substantial as that

observed. Binary widening also fails to flip prograde orbits into retrograde orbits with the preference proposed by Grundy et al. (2019).

It is possible that our failure to observe wide binary orbits become planar is a product of not accounting for the tidal effects that can occur between binary components as they orbit each other. As discussed in Section 1.5.3, the Kozai oscillations that excite a binary's eccentricity from an already excited inclination affect wide binaries more so than tight ones. In this study, Kozai oscillations are entirely cyclic but when tidal friction is accounted for like in some prior studies (Perets & Naoz, 2009; Porter & Grundy, 2012; Brunini & Zanardi, 2015), high eccentricity can be reduced. Eccentricity reduction thus leads to inclination reduction, leading to more planar orbits among wide binaries. Inclusion of tidal friction may be a factor that leads to this inclination difference.

Eccentricity on the other hand requires no additional explanations. It would appear that gravitational and collisionally induced widening is perfectly able to produce the eccentricity difference between wide and tight binaries. Widened binaries not only tend to have higher eccentricities, but the resulting distribution is also not thermalized. This distribution is consistent for any binary of separation wider than even 3% R_H. Our widened separation distributions as well is consistent with the separation distribution of observed Ultra-Wide TNBs.

But as both inclination, eccentricity, and separation distributions are consistent between our widened sample and observations, we can conclude that gravitational perturbative and collisional widening are plausible mechanisms for forming Ultra-Wide TNBs. The modern day population of Ultra-Wide binaries can additionally be used to predict the conditions of the primordial Kuiper Belt. Assuming a KKB albedo of 0.14, this modern day population can be formed if half of the primordial belt binaries had separations of 3% R_H or wider. If we assume a higher albedo, a larger fraction

of 3% R_H or wider binaries would be required. Such a Kuiper Belt does not resemble the one we currently observe, but we see no reason to preclude the possibility of it. Constraints can also be placed upon the evolutionary parameters of the Kuiper Belt as well as its initial mass at the beginning of the Solar System.

One interesting question that may arise from this is that if Ultra-Wide TNBs are not primordial, then why are they much rarer in the HCB. Ultra-Wide TNBs that we see are all mostly consigned to the CCB (Parker et al., 2011). If these binaries are primordial, then their paucity in the HCB would make sense as the HCB was likely cast into its present day position by the early Solar System migrations of the outer planets (Nesvorný, 2018). Such encounters tend to disrupt even relatively tight binaries (Parker & Kavelaars, 2010; Stone & Kaib, 2021). But if Ultra-Wide TNBs can be formed by widening tight binaries in the intervening millennia, why do we not see any in the KKB?

We suspect that this may be due to both the decreased number of even tight binaries after the HCB was inserted into the Kuiper Belt, and the fact that TNO encounters in the KKB are less frequent and occur at higher velocities than in the CCB. In our simulations, the self-interaction of the CCB is by far the most significant encounter type as they are far more frequent and much slower than most others. The self interaction of the HCB on the other hand would consist of many high velocity encounters due to their more excited inclinations (Gladman et al., 2008; Gulbis et al., 2010). Because of this, it is likely that Ultra-Wide TNBs cannot form in the HCB through our proposed mechanism in the same numbers that they may form in the CCB, reflecting current observations.

7.3 Future Work

One trend observed at every step of the research presented here is the immense sensitivity of TNB evolution to the albedo of the Kuiper Belt. As most Kuiper Belt bodies are unresolved, assuming an albedo is necessary to make assumptions about a body's radius and mass. Because of the current uncertainty of Kuiper Belt albedo, including albedo's relation to size, different studies may come away with very different results depending on which value they assume. In the future, any continued study into Kuiper Belt evolution must consider the evolving knowledge about the distribution of these albedos and may come away with different conclusions than we do.

Our uncertainty in the exact albedo distribution of the Kuiper Belt is matched by some of our uncertainty in its SFD. It is becoming clear that the SFDs of the CCB and HCB are very similar at medium sizes and can be defined with tapered power laws (Kavelaars et al., 2021; Petit et al., 2023), but at smaller sizes, this is less certain. Simulating gravitational perturbations does not require considering bodies much smaller than 20 km in radius (see Section 2.4) but simulating collisions does. Accurately simulating collisions may require consideration of bodies less than 0.5 km in diameter, the exact size distribution of which is uncertain (Singer et al., 2019; Morbidelli et al., 2021). Our increasing understanding of the various SFDs of the Kuiper Belt is precisely the reason why Petit & Mousis (2004) and Parker & Kavelaars (2011) have such different results regarding the survival of binaries like 2001 QW_{322}.

Additionally, the different SFD used by Nesvorný et al. (2021) is likely the cause of the large differences between our results. Their SFD, and possibly their assumed encounter velocities may have allowed them to assume the long-term stability of binaries as wide as 50% R_H. This wide separation would not be stable at all given the assumptions we make. Separations of even 17% are not stable, though this depends in part on the mass of the binary system. The study done by Nesvorný et al. (2021)

is the most similar to ours in terms of accounting for an evolving Kuiper Belt, though they do not account for the Kozai effect, nor gravitational perturbations. Despite its similarity, its differently assumed SFD allows it to yield very different results. Further refinements in our knowledge of these SFDs will surely increase the accuracy of these simulations.

Future work may also consider accounting for collisions between a CCB and bodies of radii less than 1 km. As stated in Section 2.4, we set 1 km as the lower limit for impacting bodies we generate. If we assume the rapidly shallowing SFD proposed by Singer et al. (2019), we can safely assume that bodies below this radius have no significant effect on an evolving binary. If we do not assume this shallowing, or if the shallowing happens at smaller radii, then we cannot. It is unlikely that accounting for this will substantially change the outcome of these simulations, but they may yet play a role in binary evolution that we did not see here.

While our simulations do take into account Kozai oscillations, they do not take into account the tidal friction that Brunini & Zanardi (2015) has demonstrated the importance of. Tidal friction has the capability of reducing the eccentricity of a non-circular binary orbit. As a consequence of the oscillation of inclination and eccentricity through Kozai oscillations on wider binaries, this can cause wide binary orbits to become more planar. While future work taking this effect into account may be more successful in reproducing the distinction between tight and wide binary inclinations, this may result in a different eccentricity distribution as well.

Additionally, if the sample of Ultra-Wide TNBs is expanded, this may change not only the direction of future research but also the results of this one. During the time of Parker & Kavelaars (2011), only seven Ultra-Wide TNBs were known. Of those seven, three have retrograde mutual orbits, implying a near equal fraction of retrograde and prograde orbits among wide binaries. Thus, a goal of that study was to determine

if collisional widening was capable of flipping a significant number of binary orbits retrograde. In the time since that study, two more Ultra-Wide TNBs were discovered, all with prograde orbits, shifting this balance. Nine binaries, however, is still a small sample. As more are discovered, some of their observed distinguishing properties may be reinforced, undermined, or perhaps new properties we have not yet observed will be seen.

In using Kuiper Belt binaries as an indicator for the structure of our Kuiper Belt in the past and present, we can compare it to belts of similar structure in other star systems. It is becoming increasingly clear that analogues to the Kuiper Belt exist around other stars (Wyatt, 2020). Indeed, from limited observations of them, it would seem that some have orbital structures similar to our own such as a clumps resembling resonant populations and a Hot Classical Belt and Cold Classical Belt distinction seen in edge-on disks. Knowledge about the origin, evolution, and structure of our Kuiper Belt is doubtlessly transferable to these analogues.

Bibliography

Abedin, A. Y., Kavelaars, J. J., Greenstreet, S., et al. 2021, The Astronomical Journal, 161, 195, doi: 10.3847/1538-3881/abe418

Agnor, C. B., & Hamilton, D. P. 2006, Nature, 441, 192, doi: 10.1038/nature04792

Alexander, R. D., Armitage, P. J., & Cuadra, J. 2008, , 389, 1655, doi: 10.1111/j.1365-2966.2008.13706.x

Anderson, K. E., & Kaib, N. A. 2021, The Astrophysical Journal Letters, 920, L9, doi: 10.3847/2041-8213/ac26ca

Astakhov, S. A., Lee, E. A., & Farrelly, D. 2005, , 360, 401, doi: 10.1111/j.1365-2966.2005.09072.x

Bannister, M. T., Gladman, B. J., Kavelaars, J. J., et al. 2018, , 236, 18, doi: 10.3847/1538-4365/aab77a

Barucci, M. A. 2015, Kuiper Belt, ed. M. Gargaud, W. M. Irvine, R. Amils, H. J. J. Cleaves, D. L. Pinti, J. C. Quintanilla, D. Rouan, T. Spohn, S. Tirard, & M. Viso (Berlin, Heidelberg: Springer Berlin Heidelberg), 1341–1353, doi: 10.1007/978-3-662-44185-5_854

Benecchi, S., Noll, K., Grundy, W., et al. 2009, Icarus, 200, 292, doi: https://doi.org/10.1016/j.icarus.2008.10.025

Benz, W. 1999, Icarus, 142, 5, doi: 10.1006/icar.1999.6204

Bernstein, G. M., Trilling, D. E., Allen, R. L., et al. 2004, The Astronomical Journal, 128, 1364, doi: 10.1086/422919

Bottke, W. F., Nesvorný, D., Vokrouhlický, D., & Morbidelli, A. 2010, The Astronomical Journal, 139, 994, doi: 10.1088/0004-6256/139/3/994

Brown, M. E., Barkume, K. M., Ragozzine, D., & Schaller, E. L. 2007, Nature, 446, 294, doi: 10.1038/nature05619

Brown, M. E., Trujillo, C., & Rabinowitz, D. 2004, The Astrophysical Journal, 617, 645, doi: 10.1086/422095

Brunini, A., & Zanardi, M. 2015, Monthly Notices of the Royal Astronomical Society, 455, 4487, doi: 10.1093/mnras/stv2602

Campbell, H. M., Stone, L. R., & Kaib, N. A. 2022, The Astronomical Journal, 165, 19, doi: 10.3847/1538-3881/aca08e

Dohnanyi, J. S. 1969, Journal of Geophysical Research (1896-1977), 74, 2531, doi: https://doi.org/10.1029/JB074i010p02531

Doressoundiram, A., Peixinho, N., de Bergh, C., et al. 2002, The Astronomical Journal, 124, 2279, doi: 10.1086/342447

Farkas-Takács, A., Kiss, C., Vilenius, E., et al. 2020, Astronomy &amp Astrophysics, 638, A23, doi: 10.1051/0004-6361/201936183

Fernandez, J. A., & Ip, W. H. 1984, , 58, 109, doi: 10.1016/0019-1035(84)90101-5

Fraser, W. C., & Brown, M. E. 2012, The Astrophysical Journal, 749, 33, doi: 10.1088/0004-637X/749/1/33

Fraser, W. C., Brown, M. E., Morbidelli, A., Parker, A., & Batygin, K. 2014, The Astrophysical Journal, 782, 100, doi: `10.1088/0004-637x/782/2/100`

Fraser, W. C., Kavelaars, J., Holman, M., et al. 2008, Icarus, 195, 827, doi: `10.1016/j.icarus.2008.01.014`

Fraser, W. C., Bannister, M. T., Pike, R. E., et al. 2017, Nature Astronomy, 1, doi: `10.1038/s41550-017-0088`

Fraser, W. C., Benecchi, S. D., Kavelaars, J. J., et al. 2021, The Planetary Science Journal, 2, 90, doi: `10.3847/PSJ/abf04a`

Funato, Y., Makino, J., Hut, P., Kokubo, E., & Kinoshita, D. 2004, , 427, 518, doi: `10.1038/nature02323`

Gladman, B., Kavelaars, J. J., Petit, J.-M., et al. 2001, The Astronomical Journal, 122, 1051, doi: `10.1086/322080`

Gladman, B., Marsden, B., & Vanlaerhoven, C. 2008

Gladman, B., Lawler, S. M., Petit, J.-M., et al. 2012, The Astronomical Journal, 144, 23, doi: `10.1088/0004-6256/144/1/23`

Goldreich, P., Lithwick, Y., & Sari, R. 2002, , 420, 643, doi: `10.1038/nature01227`

Gomes, R., Levison, H. F., Tsiganis, K., & Morbidelli, A. 2005, Nature, 435, 466, doi: `10.1038/nature03676`

Greaves, J. S., Wyatt, M. C., Holland, W. S., & Dent, W. R. F. 2004, Monthly Notices of the Royal Astronomical Society, 351, L54, doi: `10.1111/j.1365-2966.2004.07957.x`

Greenstreet, S., Gladman, B., McKinnon, W. B., Kavelaars, J. J., & Singer, K. N. 2019, The Astrophysical Journal Letters, 872, L5, doi: `10.3847/2041-8213/ab01db`

Grundy, W., Noll, K., Roe, H., & Buie, M. 2019, Icarus, 334, 62, doi: `https://doi.org/10.1016/j.icarus.2019.03.035`

Gulbis, A. A. S., Elliot, J. L., Adams, E. R., et al. 2010, The Astronomical Journal, 140, 350, doi: `10.1088/0004-6256/140/2/350`

Henon, M. 1972, , 19, 488

Hofgartner, J. D., Buratti, B. J., Benecchi, S. D., et al. 2021, Icarus, 356, 113723, doi: `10.1016/j.icarus.2020.113723`

Jeans, J. H. 1919, Monthly Notices of the Royal Astronomical Society, 79, 408, doi: `10.1093/mnras/79.6.408`

Jewitt, D., & Luu, J. 1993, Nature, 362, 730, doi: `10.1038/362730a0`

Kalas, P., Graham, J. R., & Clampin, M. 2005, , 435, 1067, doi: `10.1038/nature03601`

Kavelaars, J., Jones, L., Gladman, B., Parker, J. W., & Petit, J. M. 2008, in The Solar System Beyond Neptune, ed. M. A. Barucci, H. Boehnhardt, D. P. Cruikshank, A. Morbidelli, & R. Dotson, 59

Kavelaars, J. J., Petit, J.-M., Gladman, B., et al. 2021, The Astrophysical Journal Letters, 920, L28, doi: `10.3847/2041-8213/ac2c72`

Kavelaars, J. J., Petit, J. M., Gladman, B., & Holman, M. 2001, , 7749, 1

Kozai, Y. 1962, The Astronomical Journal, 67, 591

Kratter, K. M., Matzner, C. D., & Krumholz, M. R. 2008, , 681, 375, doi: `10.1086/587543`

Lacerda, P., Fornasier, S., Lellouch, E., et al. 2014, The Astrophysical Journal, 793, L2, doi: `10.1088/2041-8205/793/1/l2`

Lawler, S. M., Shankman, C., Kavelaars, J. J., et al. 2018, The Astronomical Journal, 155, 197, doi: `10.3847/1538-3881/aab8ff`

Levison, H., Mordibelli, A., VANLAERHOVEN, C., GOMES, R., & TSIGANIS, K. 2008, Icarus, 196, 258, doi: `10.1016/j.icarus.2007.11.035`

Levison, H. F., Bottke, W. F., Gounelle, M., et al. 2009, Nature, 460, 364, doi: `10.1038/nature08094`

Levison, H. F., & Duncan, M. J. 1994, , 108, 18, doi: `10.1006/icar.1994.1039`

Li, R., Youdin, A. N., & Simon, J. B. 2019, The Astrophysical Journal, 885, 69, doi: `10.3847/1538-4357/ab480d`

Lin, H.-W., Kavelaars, J. J., Ip, W.-H., et al. 2010, Publications of the Astronomical Society of the Pacific, 122, 1030, doi: `10.1086/656358`

Love, A. E. H. 1909, Proceedings of the Royal Society of London Series A, 82, 73, doi: `10.1098/rspa.1909.0008`

Malhotra, R. 1993, , 365, 819, doi: `10.1038/365819a0`

Marsset, M., Fraser, W. C., Pike, R. E., et al. 2019, The Astronomical Journal, 157, 94, doi: `10.3847/1538-3881/aaf72e`

McKinnon, W. B., Richardson, D. C., Marohnic, J. C., et al. 2020, Science, 367, aay6620, doi: `10.1126/science.aay6620`

Moore, J. M., McKinnon, W. B., Spencer, J. R., et al. 2016, Science, 351, 1284, doi: `10.1126/science.aad7055`

Morbidelli, A., Bottke, W. F., Nesvorný, D., & Levison, H. F. 2009, Icarus, 204, 558, doi: `https://doi.org/10.1016/j.icarus.2009.07.011`

Morbidelli, A., & Crida, A. 2007, Icarus, 191, 158, doi: `https://doi.org/10.1016/j.icarus.2007.04.001`

Morbidelli, A., Levison, H. F., & Gomes, R. 2008, The Solar System Beyond Neptune, ed. M. A. Barucci, H. Boehnhardt, D. P. Cruikshank, & A. Mobidelli (Tucson, AZ: Univ. Arizona Press), 275

Morbidelli, A., Nesvorny, D., Bottke, W., & Marchi, S. 2021, Icarus, 356, 114256, doi: `https://doi.org/10.1016/j.icarus.2020.114256`

Morbidelli, A., & Nesvorný, D. 2020, in The Trans-Neptunian Solar System, ed. D. Prialnik, M. A. Barucci, & L. A. Young (Elsevier), 25–59, doi: `https://doi.org/10.1016/B978-0-12-816490-7.00002-3`

Nesvorný, D. 2011, The Astrophysical Journal, 742, L22, doi: `10.1088/2041-8205/742/2/l22`

Nesvorný, D., Li, R., Simon, J. B., et al. 2021, The Planetary Science Journal, 2, 27, doi: `10.3847/psj/abd858`

Nesvorny, D., Li, R., Youdin, A. N., Simon, J. B., & Grundy, W. M. 2019, Trans-Neptunian Binaries as Evidence for Planetesimal Formation by the Streaming Instability. `https://arxiv.org/abs/1906.11344`

Nesvorný, D., Youdin, A. N., & Richardson, D. C. 2010, The Astronomical Journal, 140, 785, doi: `10.1088/0004-6256/140/3/785`

Nesvorný, D. 2015, The Astronomical Journal, 150, 68, doi: `10.1088/0004-6256/150/3/68`

—. 2018, Annual Review of Astronomy and Astrophysics, 56, 137, doi: `10.1146/annurev-astro-081817-052028`

Nesvorný, D., & Morbidelli, A. 2012, The Astronomical Journal, 144, 117, doi: `10.1088/0004-6256/144/4/117`

Nesvorný, D., & Vokrouhlický, D. 2016, The Astrophysical Journal, 825, 94, doi: `10.3847/0004-637X/825/2/94`

—. 2019, Icarus, 331, 49, doi: `https://doi.org/10.1016/j.icarus.2019.04.030`

Noll, K., Stephens, D., Grundy, W., et al. 2002, , 7857, 1

Noll, K. S., Grundy, W. M., Nesvorný, D., & Thirouin, A. 2020, in The Trans-Neptunian Solar System, ed. D. Prialnik, M. A. Barucci, & L. A. Young (Elsevier), 205–224, doi: `https://doi.org/10.1016/B978-0-12-816490-7.00009-6`

Noll, K. S., Grundy, W. M., Stephens, D. C., Levison, H. F., & Kern, S. D. 2008, Icarus, 194, 758–768, doi: `10.1016/j.icarus.2007.10.022`

Parker, A., Kavelaars, J., Petit, J. M., et al. 2011, Minor Planet Electronic Circulars, 2011-N35

Parker, A. H., & Kavelaars, J. J. 2010, The Astrophysical Journal Letters, 722, L204, doi: `10.1088/2041-8205/722/2/L204`

—. 2011, The Astrophysical Journal, 744, 139, doi: `10.1088/0004-637x/744/2/139`

Parker, A. H., Kavelaars, J. J., Petit, J.-M., et al. 2011, The Astrophysical Journal, 743, 1, doi: `10.1088/0004-637x/743/1/1`

Perets, H. B., & Naoz, S. 2009, The Astrophysical Journal, 699, L17, doi: `10.1088/0004-637x/699/1/l17`

Petit, J.-M., Gladman, B., Kavelaars, J. J., et al. 2023, , 947, L4, doi: `10.3847/2041-8213/acc525`

Petit, J.-M., & Mousis, O. 2004, Icarus, 168, 409, doi: `https://doi.org/10.1016/j.icarus.2003.12.013`

Petit, J.-M., Kavelaars, J. J., Gladman, B. J., et al. 2008, Science, 322, 432, doi: `10.1126/science.1163148`

—. 2011, The Astronomical Journal, 142, 131, doi: `10.1088/0004-6256/142/4/131`

Porter, S. B., & Grundy, W. M. 2012, Icarus, 220, 947–957, doi: `10.1016/j.icarus.2012.06.034`

Schlichting, H. E., & Sari, R. 2008, , 686, 741, doi: `10.1086/591073`

Singer, K. N., McKinnon, W. B., Gladman, B., et al. 2019, Science, 363, 955, doi: `10.1126/science.aap8628`

Stern, S. A., Bagenal, F., Ennico, K., et al. 2015, Science, 350, doi: `10.1126/science.aad1815`

Stone, L. R., & Kaib, N. A. 2021, Monthly Notices of the Royal Astronomical Society: Letters, 505, L31, doi: `10.1093/mnrasl/slab044`

Tegler, S. C., Romanishin, W., & G. J. Consolmagno, S. J. 2016, The Astronomical Journal, 152, 210, doi: `10.3847/0004-6256/152/6/210`

Tsiganis, K., Gomes, R., Morbidelli, A., & Levison, H. F. 2005, Nature, 435, 459, doi: `10.1038/nature03539`

Veillet, C., Parker, J. W., Griffin, I., et al. 2002, , 416, 711, doi: `10.1038/416711a`

Vilenius, Kiss, C., Müller, T., et al. 2014, A&A, 564, A35, doi: `10.1051/0004-6361/201322416`

Wyatt, M. C. 2020, in The Trans-Neptunian Solar System (Elsevier), 351–376, doi: `10.1016/b978-0-12-816490-7.00016-3`

Youdin, A. N., & Goodman, J. 2005, The Astrophysical Journal, 620, 459, doi: 10.
1086/426895